January 2015

# Achieving Reliable Generation \& Delivery of Energy Through Robust Optimization

Anna Danandeh
*University of South Florida*, anna.danandeh@gmail.com

# Achieving Reliable Generation and Delivery of Energy Through Robust Optimization

by

Anna Danandeh

A dissertation submitted in partial fulfillment
of the requirements for the degree of
Doctor of Philosophy in Industrial Engineering
Department of Industrial and Management Systems Engineering
College of Engineering
University of South Florida

Major Professor: Bo Zeng, Ph.D.
Tapas K. Das, Ph.D.
Mark Daskin, Ph.D.
Lingling Fan, Ph.D.
Michael Fountain, Ph.D.
Shuai Huang, Ph.D.

Date of Approval:
June 28, 2015

Keywords: Integer Programming, Supply Chain Management, Power Systems, Dynamic Rating, Cutting Plane

## DEDICATION

To my two sets of parents who filled my life with love and ambition, and who taught me honesty and integrity.

And to my sister who kept my heart warm with her constant instant messages.

## ACKNOWLEDGMENT

I would like to express my sincere gratitude to my caring and knowledgable supervisor, Dr. Bo Zeng. During the past five years, you have constantly supported me in the way you thought helps me the best, and encouraged me to do not good but great.

I am grateful to my supervisory committee, Dr. Tapas Das, Dr. Mark Daskin, Dr. Lingling Fan, Dr. Michael Fountain, and Dr. Shuai Huang, for graciously sharing their knowledge and experience and supporting my academic endeavour. My special appreciation goes to Dr. Daskin for being a significant influencer in my professional life. I am also very appreciative to Dr. Das for his tremendous effort in the IMSE department to facilitate our study and research.

I would also like to thank my colleagues in Tampa Electric company, Gordon Gillette, Brent Caldwell, and Brian Buckley, for their collaboration and support of the research in chapter 2.

My deepest appreciation goes to my partner, Alireza Ghalebani, for flavoring my research with his business insights.

Lastly, I offer my regards to all whom I have learnt from in any context.

## TABLE OF CONTENTS

## LIST OF TABLES

## LIST OF FIGURES

## ABSTRACT

In this dissertation, we elaborate on the inherent risks and uncertainties in power systems and associated industries, and develop practical solution methods to eliminate their adverse effects. our research agenda consists of practice-driven problems in different stages of power generation as follows. (1) Affordable fuel procurement through developing a comprehensive fuel supply chain design and operations planning system for electricity generation companies, (2) reliable electricity generation through incorporating dynamic asset rating concept in the unit commitment problem, and (3) efficient demand management through proposing a job scheduling model for effective local generation consumption.

Since reliability cannot be compromised in energy sector, robust optimization has been adopted as a powerful method to model multiple sources of uncertainty, and to protect the performance of the systems against worst situations. Exact and heuristic methods are then developed and customized to solve these computationally challenging problems. In particular, inspired by the challenges in solving two-stage robust optimization problems, we developed a multi-scenario cutting plane generation algorithm, that considers all the realizations of the uncertainty set at once, and thus, alleviates the computational challenge.

# CHAPTER 1: INTRODUCTION

Electric energy is arguably the most critical component of our modern society, affecting its the economic growth and welfare. The common production and delivery of electric energy, in large scale, are real time processes. Therefore, it is important to maintain reliable and secure operations. In this regards, a key challenge for the decision makers, including systems operators and consumers, is handling various sources of uncertainty which are potential sources of disruptions and congestions. In order to address this challenge, this dissertation aims to investigate challenging problems in different phases of electricity supply and demand, and apply robust optimization to mitigate the impact of uncertainty on the performance of the whole system.

On the supply side, we studied the challenges in two main problems: The first one is the fuel procurement and supply chain management to support affordable electricity generation, and the second one is the unit commitment problem as a daily operation in power plants. On the demand side, we developed a scheduler for procumers, i.e. producers/ consumers, to organize their flexible load in order to maximize their utilisation of the local generation.

In a broad view, the reliable electricity generation is the fruit of dependable fuel supply chains. Among fuels, coal has been the primary energy source accounting for 36% of global and 42% of national power generation in 2013. Coal industry advisory board of International Energy Agency (IEA) reports that coal has a tangible role in setting the electricity price

in a range of regions from Europe with 15% to South Africa with 92% coal-fired units [4]. In regions where the electricity bill is proportional to the fuel cost, e.g., the United States, coal cost reduction directly benefits the end consumers. In other regions where the government controls the electricity price, e.g., China, possible cost reductions can prevent the power plants from possible loss. More importantly, considering the important role of energy production in national security, even in the regions that are not mainly relying on coal such as Europe, mid-merit coal plants set the price in 80% of the hours due to the expansion of renewable energy and their large cost differences from gas plants. Thus, constructing a reliable coal supply chain is an economic imperative, saving billions of dollars nationwide and globally.

This cost-effective, yet pollutant fuel, has a complex supply chain, including nonlinear logistics costs, quality issues, blending, and other operational challenges. Surveys rank coal blending and the associated logistics as the most pressing issue in power plants [5]. We have developed and implemented an elaborate design and management system, a mixed integer optimization model, for coal supply chain in collaboration with TECO Energy, a utility company in Tampa, Florida. The implementation of this system at TECO results in 2-3% annual saving in fuel cost, i.e., 10-12 million dollars. Moreover, this research can serve other industries such as chemical and pharmaceutical companies as well. In chapter 2, we describe the challenges in this problem and the novelties of our research approach.

One of the most challenging problem in power systems is the unit commitment problem. The Unit commitment problem is concerned with finding the less-expensive day-ahead

decisions on selecting power generating units and dispatching power given demand load. Electric utilities regularly use a combination of short and long start-up times. With the most of demand being satisfied via slower generators, it is important to determine the optimal unit commitment prior to the observation of the demand. However, power output of generating units and the capacity of overhead transmission network are inverse functions of ambient temperature. Since system capacity is mostly determined statically, weather changes can cause power outages and/or congestions. Moreover, actual data reveals load fluctuation with temperature change. To address these issues, we developed a two-stage robust security-constraint unit commitment formulation, which dynamically rates the assets and hedges against unpredicted efficiency drops. Leveraging the correlation between two sources of uncertainty, i.e., weather and load, yields a less conservative decision and a faster computation. In chapter 3, the two-stage robust mixed integer unit commitment problem that we have developed along with the necessity of considering such sources of uncertainty have been presented.

In addition, drastic rise in the electricity demand in certain periods requires frequently modifying the dispatched power, and may cause outages during peak times. Adopting time-of-use electricity prices and Demand Response programs, such as the Scheduled Load Reduction program, (SLRP) which incentives electricity reduction during pre-selected time periods. are methods to balance the load. Consumers can also respond by installing local generating units, such as solar panels, whose output is, however, uncertain. We consider a two-stage robust mixed integer scheduling problem where the prosumer (producer/ con-

sumer) schedules both less and more flexible jobs before and after realization of uncertainty in local generation, respectively. Presence of binary variable in both stages, especially the second, creates a challenging problem which could not be solved with typical solution algorithms such as Bender's Decomposition. Therefore, we implemented a nested Column and Constraint generation algorithm to solve it. The model and algorithm implementation are presented in chapter 4.

Over the course of two-stage model development and algorithm implementation, we noticed the computational burden is mainly related to addressing realizations of uncertainty in a stepwise manner. This observation led to rich theoretical investigations. As the result, we developed a dynamic programming approach to derive multi-scenario cutting planes through a robust lifting procedure. This procedure considers all realizations of the uncertainty set at once and reduces the computational challenge. This research is presented in chapter 5.

# CHAPTER 2: DESIGN AND OPERATIONS OF SUPPLY CHAIN FOR CLEANER FUELS

## 2.1 Background

Electric power, arguably the most critical component in our modern society, is mainly generated by either fossil fuels, like coal and natural gas or by renewable energy sources such as solar, nuclear or hydropower [6]. Among these energy sources, fossil fuels are more abundant and cost-effective, and thus they are currently the main input to traditional power plants. According to [4], coal provided 36% of the electric power in the world and 42% within the United States in 2013. Indeed, despite the ongoing efforts to retire coal-fired generators and replace them with cleaner fuels or renewable energy sources, as pointed out in 2013 Annual Energy Outlook of [7], coal will continue to dominate other sources for at least a few decades due to its relatively-low price, safety in stock, abundance in U.S. (being the largest domestic energy source), and other economic and energy-security considerations. See Figure 1(a) for a plot of the approximately 5000 coal-fired generators in the United States, where the radius of dots represents the amount of burned coal. As seen in this map, the density of coal-fired power plants is higher in the Eastern half of the country, which can be the result of abundance and acceptable quality of various coals in the Interior and Appalachian coal reserves. Moreover, Figure 1(b) demonstrates the billion KWh electricity generation by different energy sources in 2011, 2025, and 2040. Besides the demand increase,

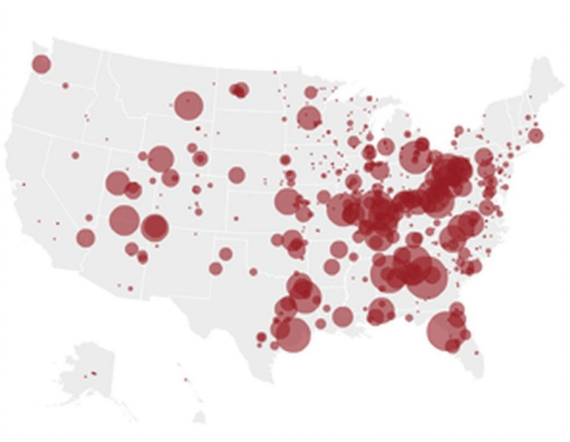

(a) The map of the coal-fired power stations in the U.S. (by [8])

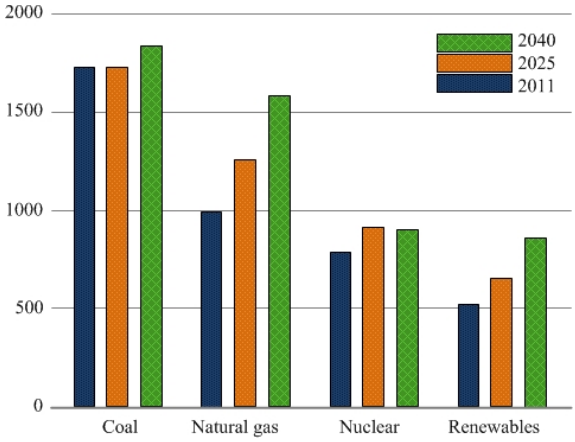


(b) The forecast of major energy sources' shares in electricity generation (by [7])

Figure 1: Coal consumption status in the United States

coal's affordable price and relatively more reliable accessability account for its consumption growth.

Although it is fairly cheap and plentiful, burning fossil fuels, especially coal, results in an extremely large volume of emissions of greenhouse gas and harmful pollutants [9]. Coal-fired power stations produced higher amounts of carbon dioxide per unit of energy, when compared to oil or natural gas [10]. With the growing concerns on global climate change and environmental issues, government regulations such as "The Clean Air Act Amendment of 1990" were introduced to control the emission from power stations [11]. In 2014, a new generation of regulations, i.e. "Clean Power Plan 2014", was proposed by EPA and discussed by various stakeholders, which emphasized on cutting carbon pollution, enhancing energy efficiency, and improving power plant operations.

The coal with high heat content often has high sulfur content which is a major pollutant gas. Therefore, in order to comply with emission regulations, coal blending is introduced

to mix coals with different qualities to satisfy the emission limit on $SO_2$. Later on, considerations of other coal quality measurements, such as chlorine and ash contents, were included in designing blending recipe. In addition to the emission reduction, blending enables power plant operators to diversify the sources in order to reduce the risk of shortage and single-supplier-dependency. It also has been argued that an appropriate blending recipe can result in a more efficient boiler performance with diversified coal supply [12]. Accordingly, the blending concept is extended to mix coal with other type of fuels, like biomass and petroleum coke, a dry residue of the refining process to achieve further improvements.

Clearly, if blending is not necessary, the fuel supply chain only needs to deal with a single supplier, a single transportation mode and a simple inventory model. However, the supply chain built for blending is significantly complicated: Each type of coal has its own quality attributes, each supplier is accessible through certain types of transportation modes with different cost structures. Therefore, designing a blending recipe that can meet the environmental requirements and satisfy the generators' demand as well as its logistics plan becomes a perplexing undertaking. According to [5], coal blending and the associated logistics is ranked as the most pressing issue in the whole power generation industry.

Managing such fuel supply chain involves coordinating many strategic and operational decisions, including long-term decisions such as procurement and transportation contract designs, as well as monthly or weekly decisions such as determining the blending recipes based on the inventory availability. To address these challenges, we collaborated with Tampa Electric Company (TECO), and developed a fuel supply chain support system, aptly named

Fuelsupport, which integrates a mixed integer programming (MIP) model with an Access database and Excel user interfaces. This platform analytically supports TECO's efforts to build a cost-effective, reliable, and emission-restricted fuel supply chain by handling its major considerations in purchase, logistics, material handling, and environmental aspects. Since TECO represents a sophisticated situation among coal-fired power plants, the whole platform, with minor customizations if necessary, is widely applicable to many other power plants.

Because of the importance of fuel supply chain for power plants, some aspects of this supply chain problem have been investigated in the literature for many years. Nevertheless, a comprehensive study considering both sophisticated blending requirements and complicated logistics challenges is largely missed. [13] and [14] are probably the first two quantitative studies on the coal blending and related problems. In the first paper, an MIP model is developed to determine optimal locations of blending facilities. The latter one analyzes the advantages and challenges of coal blending for power plants. Several single-objective or multi-objective optimization models on the (single-period) basic blending problem have been developed. [15] develops three separate but sequential models to determine potential mine sites, coal purchasing strategies, and blending recipes. However, due to the weak connections among these models the solution optimality cannot be guaranteed. [16] addresses long-term contracts in coal acquisition and develop a linear programming (LP) model accordingly. [17] applies Markov decision process (MDP) technique to simulate the quality of blend over time for a small-sized problem. [18] focuses more on the error of sampling and the rejection cost

for the supplier, and proposes a stochastic model to capture sampling error. [19] applies a goal programming (GP) model to balance coal stockpiles. In short, the main drawback of these studies is that they overlook transportation complications.

Multi-period models with consideration of inventory and holding costs are developed in [20] and [21]. [20] considers the problem from a coal producer's point of view. Thus, the resulting model is not applicable to power plants that must manage multiple supplier and transportation providers. [21] assumes that the purchase and transportation costs are hidden in the unit cost of each coal and proposes a nonlinear programming (NLP) formulation which is approximately solved using successive linear programming (SLP) method.

Extended models with logistics considerations and chance constraints are developed in [22] to minimize the blending cost as well as sulfur emission volume and its variation over time. [23] considers detailed coal quality constraints as well as shipload utilization restrictions and proposes an MIP-based heuristic approach to compute decisions. In [24], greater focus is placed on modeling environmental requirements with transportation availability consideration for each coal supplier. Basically, these studies deal with simplified logistical considerations and cost structures.

Note that the aforementioned research efforts do not consider major factors in an integrated way. For example, while widely neglected in the previous studies, according to [25], when delivering Powder River Basin coal from Wyoming to the Eastern coast of the U.S., the transportation cost is much higher than the mine-mouth selling price (5-7 times higher). Indeed, as we observed in TECO's situation, that cost structure could be nonlinear.

Also, uncontrollable weather disruptions such as severe winter storms or floods can halt or cause long delays in coal delivery, which necessitates safety stock arrangements and other reliability-assurance mechanisms. In response to the practical considerations and real needs of TECO's power plants, we developed the Fuelsupport system which considers all major aspects in the fuel supply chain and, to the best of our knowledge, constructs the most comprehensive analytical model.

In this chapter, we describe our investigation on TECO's fuel supply chain and the development and implementation of Fuelsupport system. A background of the fuel supply chain of TECO is provided in Section 2.2. We go over the Fuelsupport platform and implementation considerations and present the underlying mixed integer optimization model in Section 2.3. Some of the outcomes and analysis are provided in Section 2.4 to illustrate the usage of our system. Finally, the Section 2.5 concludes the chapter.

## 2.2 An Overview of TECO's Fuel Supply Chain

As is typical of utility companies, Tampa Electric Company (TECO) heavily depends on coal-fired generators to serve the electricity demand of its more than 687,000 customers spreading over 2,000 square miles in West Central Florida. Among TECO's 16 generators, there are five coal-fired units, i.e. generators, where four units are in Big Bend power station, Apollo Beach, FL, and one is in Polk power station, Bartow, FL. These coal-fired generators are basically must-run base-load units that account for 60% of TECO's electricity generation. The remaining gas-fired generators and oil-fired generators are dispatched upon demand to produce 39% and less than 1% of TECO's electricity, respectively. Currently, the coal-fired

generators demand for roughly 4.7 million tons of various coals and petroleum cokes every year. In 2013, 83% of these fuels were purchased under long-term contracts, and the rest were purchased in the spot market. As shown in Figure 2, the strategic location of TECO enables it to access these sources via railroads, ocean barges, and a two-leg Mississippi-river-Gulf-of-Mexico option. This two-leg transportation option allows TECO to first transport the coals from mines in Illinois Basin, Northern and Central Appalachia down over the Mississippi river, and then bring them to Big Bend power station over the Gulf of Mexico. This method relies on the presence of an intermediate depot in Louisiana, i.e. Davant Dock operated by United Bulk Terminal. At Davant, coal shipments over the river are received, sampled, temporarily stored, blended if needed, and then transported to Big Bend power station. The presence of the intermediate depot offers two main advantages. First, convenient transportation methods enable TECO to sell the excess inventory in the spot market. Second, coal handling and blending operations in Davant are safer and relatively less expensive, whereas Big Bend power station that is close to a few cities and the Everglade National Park. A schematic diagram of this fuel supply chain is presented in Figure 3. The involved decisions and operations generally fall into the categories of procurement, transportation, stockpiling and material handling, and blending and burn quality control.

### 2.2.1 Coal Procurement

Typically, there are many types of coals in the market. They have different quality attributes, accessabilities, and prices. Their quality attributes, especially heat, sulfur, and chlorine contents, directly affect the burn quality. Besides, the accessability of coal associ-

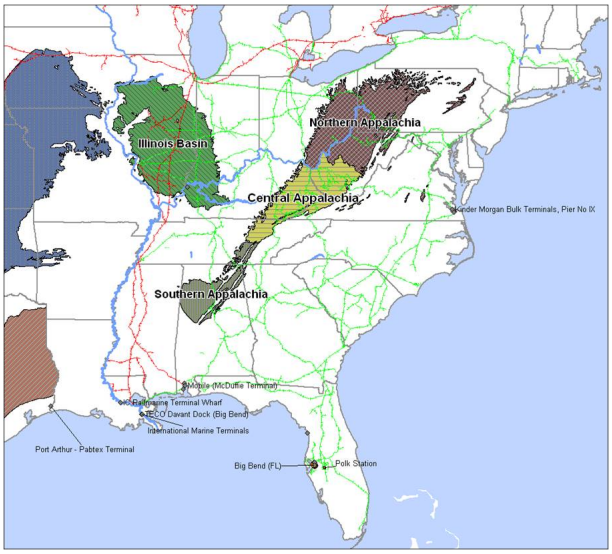


Figure 2: TECO's avenues for coal delivery (green and red lines represent railroad, and the blue line is the water transportation avenue)

ated with different transportation options, such as railroads and river barges, and different rates is another critical factor, which forces TECO to jointly consider coal suppliers and transportation carriers. In addition, long-term coal purchase contracts generally have their own complexities, including annual shipment commitments and the lower and upper bounds on monthly takes, which are requested by the coal suppliers to ensure a balanced operation. If such bounds are not satisfied, TECO may be penalized.

### 2.2.2 Commodity Transportation

Coals can be delivered by rail, barge, highway truck, coal slurry pipeline, or as in many cases a combination of those, i.e. a multi-leg transportation mode. Indeed, such multi-leg transportation modes have been overlooked in the majority of the previous studies. As shown in Figure 3, TECO has three distinct avenues to receive coal: coals from Illinois Basin, including those from the coal mines in Southern Illinois, Indiana, and Western Kentucky,

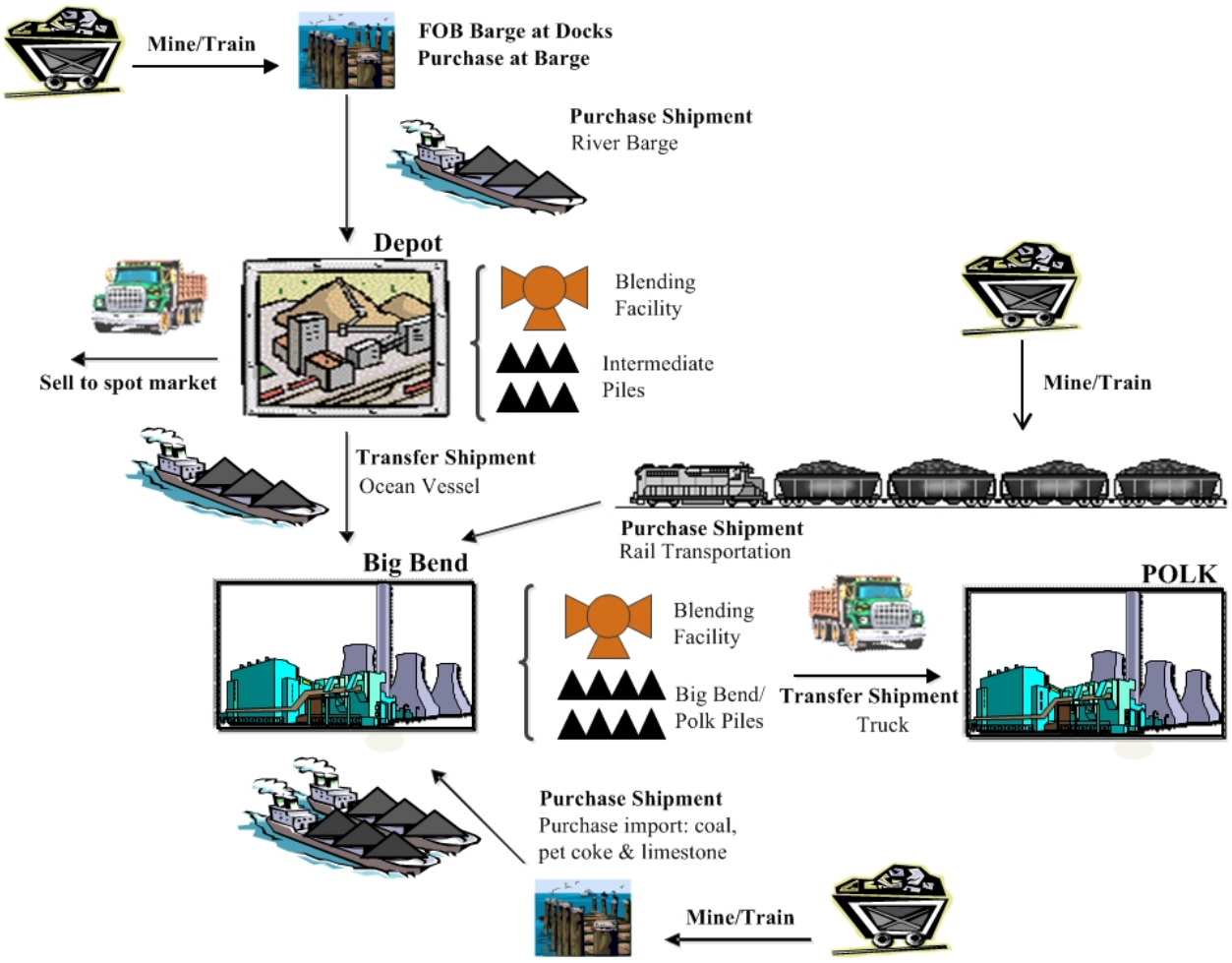


Figure 3: An overview to Tampa Electric's coal logistics

are transported through a two-leg mode, i.e. transported along the Mississippi river to Davant intermediate depot, blended if necessary, and then shipped to Big Bend station via ocean vessels over the Gulf of Mexico. Coals from Appalachian reserves, mainly produced by mines in West Virginia and Eastern Kentucky, can be transferred by railroads to Big Bend station. Finally, petroleum cokes from Texas and coals imported from other countries will be transported directly from suppliers to Big Bend station, again on the Gulf of Mexico. In addition to these three major transportation means to Big Bend station, there is a truck-

based transportation arrangement between Big Bend station and Polk station to transfer the generator-specific blend for Polk's single unit on a daily basis.

In many cases, transportation carriers propose a complex cost structure, often a piece-wise linear function which includes credit and/or dead freight charge. In Figure 4 we show a typical transportation cost structure of two transportation carriers. For each carrier, if the shipping quantity is less than $\alpha_i$, the deficit will be charged as dead freight. If this quantity is more than $\beta_i$, credit will be applied to the excess quantity. As can be seen, the choice of economically-desired carrier partially depends on the shipping volume. Very often, the unit rates and break points associated with credit and dead freight are open to negotiation between TECO and carriers. Therefore, a sensitivity analysis, which can be easily performed using our Fuelsupport system, can come to the aid of the fuel supply department to design the best contracts.

Furthermore, transportation rates are time-dependent. In fact, besides annual inflation, transportation rates can change seasonally. For example, according to [26], the railroad carrier may require a monthly mileage-based fuel adjustment if highway diesel fuel is higher than a threshold value. TECO typically predicts such adjustments for each carrier over the next few years, and incorporates the information into the Fuelsupport system. In addition, transportation carriers allow a variation-cap on the monthly takes, usually 10% of average monthly take, to help TECO hedge against possible variations from coal suppliers, which is also considered in Fuelsupport system.

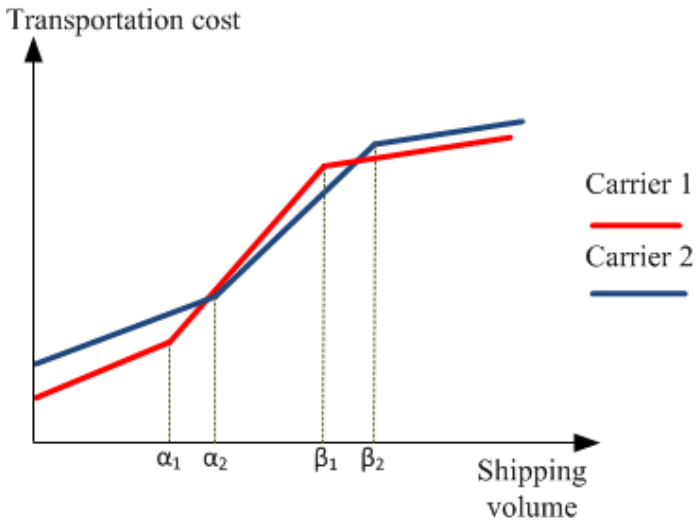


Figure 4: Nonlinear transportation cost structure

### 2.2.3 Coal Stockpiling, Material Handling, and Inventory Control

In order to ensure the reliability in electricity generation and to mitigate risk of late delivery, possibly caused by severe weather condition or railroad congestion, TECO must keep sufficient amount of coal in either one of its inventory sites: the backyard of Big Bend station and the depot site at Davant LA. In Big Bend station, the coal yard can hold up to 700,000 tons of coal and in Davant, TECO can store up to 500,000 tons of coal. In those sites, TECO stores coals into piles according to their origin, heat content, and sulfur content. Sometimes, due to the space limitation or handling convenience, coals of similar qualities are stored into the same piles.

In order to meet the environmental restrictions set by Florida local government, TECO has installed the coal pile runoff system in Big Bend station, which includes water sprays and filters, to handle runoff and dust suppression. Conveyor belt systems are used to transfer coals from piles to the blending facilities and then to pulverizer mills, which convert the mix

into a fine dust for subsequent combustion in the furnace. As two or three belts are often used to feed one blending facility in those sites, a cardinality restriction on the number of source coals follows naturally. This restriction also helps to track any quality issue airing in the combustion process.

### 2.2.4 Blending and Burn Quality Management

Based on the environmental regulations, TECO designs generator-specific blending recipes for its five coal-fired units and prepares the final burn in its blending facilities at either the deport site at Davant or Big Bend station. For a blended mix, quality measures include heat content (mmbtu/ton), sulfur content (lb/mmbtu), and chlorine content (% of the weight). The heat content is restricted within a range. On one hand, low heat content in the final burn certainly decreases the efficiency of combustion and thus is avoided. On the other hand, if the heat content in the final blend is too high, it will cause volatility and can be unsafe to handle. Besides using scrubbers to reduce the sulfur oxides of the burn, TECO limits the amount of sulfur in the blend. Similarly, high chlorine content is prohibited because it not only can cause pollution in the waste water, which is a serious issue in Florida, but also damages sulfur scrubbers. Other additive quality measures such as ash content and moisture content can be modeled in the same way.

We would like to highlight that blending recipes are not necessarily static. Within acceptable limits, they can change over time, according to coals' inventory levels, availabilities, and load situations. While such flexibility could be a source of cost saving, it is too cumbersome for practitioners to evaluate all possible blending combinations and their associated

costs. Therefore, power plant operators prefer to change the recipes only infrequently, which definitely narrows down their procurement options and results in an extra cost. Due to the powerful modeling and computational capacity of Fuelsupport system, such cumbersome issue can be easily addressed to achieve a superior flexibility in blending and consequently an improved system-wide performance.

### 2.3 Fuelsupport Platform Overview and the Mathematical Model

The goal of this project is providing an integrated and analytical decision making tool for the fuel supply department at TECO. Our collaboration has been conducted in four semi-parallel phases:

- System investigation and data collection
- Development, realization, and validation of the optimization engine, i.e. the MIP model and its GAMS implementation
- Development of data-support tools using Access and Excel
- Demonstration and training at TECO

We next, describe the mathematical model which is the heart of the Fuelsupport system. The nomenclature is presented in Table 2.

Table 1: Nomenclature used in chapter 2

| **Symbol** | **Meaning** |
|---|---|
| | **Index Sets** |
| $I$ | Generator, $i = 1, ..., \|I\|$ |
| $J$ | Supplier, $j = 1, ..., \|J\|$ |
| $K$ | Transportation mode/carrier, $k = 1, ..., \|K\|$ |
| $L$ | Stage level, $l = 1, 2$ |
| $T$ | Months in the planning horizon, $t = 1, ..., \|T\|$ |

Table 1 (continued)

| Symbol | Meaning |
|---|---|
| $N$ | Years in the planning horizon, $n = 1, ..., \|N\|$ |
| | **Parameters** |
| $B^l$ | Blending cost at stage $l$, "\$/ton" |
| $C_j^t$ | Purchase cost of supplier $j$ in month $t$, "\$/ton" |
| $E^l$ | Holding cost in stage $l$, "\$/ton" |
| $N'^k_{j,t}$ | Base transportation cost of carrier $k$ at time $t$, "\$/ton" |
| $N''^k$ | Dead freight of carrier $k$, "\$/ton" |
| $N'''^k$ | Credit of carrier $k$, "\$/ton" |
| $N''''$ | Truck transportation from Big Bend station to Polk station, "\$/ton" |
| $P_t^l$ | Profit from selling coal to spot market in stage $l$ at time $t$, "\$/ton" |
| $f_{t,j}^k$ | Binary indicator: 1 if supplier $j$ is accessible by carrier $k$, and 0 otherwise |
| $a'^k$ | Dead freight trigger for transportation carrier $k$, "tons" |
| $a''^k$ | Credit trigger for transportation carrier $k$, "tons" |
| $\kappa^k$ | Annual transportation upper bound of carrier $k$, "tons" |
| $\iota^k$ | Annual transportation lower bound of carrier $k$, "tons" |
| $\varepsilon_k$ | Allowed monthly shipment variation of carrier $k$, "%" |
| $u_j^s$ | The starting month of coal purchase contract of supplier $j$, |
| $u_j^e$ | The end month of coal purchase contract of supplier $j$, |
| $U_j$ | The purchase contract duration, i.e. $u_j^e - u_j^s + 1$, |
| $Q_{j,n}$ | Our purchase commitment to supplier $j$ in year $n$, "ton" |
| $\theta_j$ | Reciprocal heat content of coal from supplier $j$, "mmbtu/tons" |
| $\delta_j$ | Sulfur content of coal from supplier $j$, "lb/mmbtu" |
| $\omega_j$ | Chlorine content of coal from supplier $j$, " |
| $UB_{j,n}$ | Annual purchase upper bound of supplier $j$, "tons" |
| $LB_j$ | Annual purchase lower bound of supplier $j$, "tons" |
| $\epsilon_j$ | Allowed monthly purchase variation of supplier $j$, "%" |
| $\mu$ | Safety stock rate, " |
| $\underline{G^l}$ | Final inventory requirement at stage $l$, "ton" |
| $\overline{S^l}$ | Inventory capacity in stage $l$, "tons" |
| $\overline{B^l}$ | Blending facility's capacity in stage $l$, "tons" |
| $\overline{\beta^i}$ | Blending cardinality upper bound for generator $i$, "#" |
| $D_t^i$ | Demand of generator $i$ at time $t$, "tons" |
| $\nu_i$ | Demand variation of unit $i$, " |
| $\Theta_i$ | The minimum heat content required for generator $i$, "mmbtu/ton" |
| $\Delta_i$ | The maximum sulfur content allowed for generator $i$, "lb/mmbtu" |
| $\Omega_i$ | The maximum chlorine content allowed for generator $i$, "%" |
| $\gamma_\theta, \gamma_\delta, \gamma_\omega$ | Allowed variation of heat, sulfur, and chlorine contents, respectively, in the blend, "%" |
| | **Decision variables** |
| $s_{t,j}^l$ | Continuous; inventory level of coal from supplier $j$ in stage $l$ at time $t$, "tons" |

Table 1 (continued)

| Symbol | Meaning |
|---|---|
| $v_{t,j}^{l}$ | Continuous; sold amount from supplier $j$ to market at time $t$, "tons" |
| $x_{t,j}^{k}$ | Continuous; coal purchased from supplier $j$ at time $t$ and transported with carrier $k$, "tons" |
| $z_{t,j}$ | Continuous; transported coal of supplier $j$ from stage 1 to 2 at time $t$, "tons" |
| $\beta_{t,j}^{l,i}$ | Continuous; blended coal of supplier $j$ for generator $i$ at time $t$ at stage $l$, "tons" |
| $\rho_{n}^{k}$ | Continuous; amount of dead freight with carrier $k$, "tons" |
| $\upsilon_{n}^{k}$ | Continuous; transported amount with carrier $k$ above credit trigger, "tons" |
| $\chi_{j,n}$ | Binary; takes 1 if we purchase from supplier $j$ |
| $w_{n}^{k}$ | Binary; takes 1 if we transport more than credit trigger with carrier $k$ |
| $y^{k}$ | Binary; takes 1 if we use transportation carrier $k$ |
| $\varpi_{t,j}^{l,i}$ | Binary; takes 1 if we blend coal of supplier $j$ for generator $i$ at time $t$ at stage $l$ |

$$min \sum_{t=1}^{|T|}\sum_{j=1}^{|J|}[C_j^t\sum_{k=1}^{|K|}f_{t,j}^{k}x_{t,j}^{k}+\sum_{l=1}^{|L|}(E^{l}s_{t,j}^{l}-P_t^{l}v_{t,j}^{l}+N^{''''}\beta_{t,j}^{l,5}+B^{l}\sum_{i=1}^{|I|}\beta_{t,j}^{l,i})]+$$
$$\sum_{k=1}^{|K|}(N_{j,t}^{'k}\sum_{t>12(n-1)}^{12n}\sum_{j=1}^{|J|}x_{t,j}^{k}+N^{''k}\rho_{n}^{k}-N^{'''k}\upsilon_{n}^{k}) \tag{2.1}$$

$$\sum_{k=1}^{3}f_{t,j}^{k}x_{t,j}^{k}+s_{t-1,j}^{1}=v_{t,j}^{1}+s_{t,j}^{1}+x_{t,j}^{4}\quad\forall t\in T,j\in J \tag{2.2}$$

$$\sum_{k=5}^{6}f_{t,j}^{k}x_{t,j}^{k}+z_{t-1,j}+s_{t-1,j}^{2}=v_{t,j}^{2}+s_{t,j}^{2}+\sum_{i=1}^{|I|}\beta_{t,j}^{2,i}\quad\forall t\in T,j\in J \tag{2.3}$$

$$\sum_{t=1}^{|T|}\sum_{j=1}^{|J|}z_{t,j}+\sum_{i=1}^{|I|}\beta_{t,j}^{1,i}=x_{t,j}^{4}\quad\forall t\in T,j\in J \tag{2.4}$$

$$\sum_{t=1}^{|T|}\sum_{j=1}^{|J|}z_{t,j}+\sum_{i=1}^{|I|}\beta_{t,j}^{1,i}=x_{t,j}^{7}\quad\forall t\in T,j\in J \tag{2.5}$$

$$LB_j\ \chi_{j,n}\leq\sum_{t>12(n-1)}^{12n}\sum_{k=1}^{|K|}f_{t,j}^{k}x_{t,j}^{k}\leq UB_{j,n}\chi_{j,n}\quad\forall n\in N,j\in J \tag{2.6}$$

$$\sum_{k=1}^{|K|}f_{t,j}^{k}x_{t,j}^{k}\leq(1+\epsilon_j)\frac{\sum_{t>12(n-1)}^{12n}\sum_{k=1}^{|K|}f_{t,j}^{k}x_{t,j}^{k}}{U_{j,n}}\forall n\in N,t\in(12(n-1),12n],j\in J \tag{2.7}$$

$$(1-\epsilon_j)\sum_{k=1}^{|K|}f_{t,j}^{k}x_{t,j}^{k}\geq\frac{\sum_{t>12(n-1)}^{12n}\sum_{k=1}^{|K|}f_{t,j}^{k}x_{t,j}^{k}}{U_{j,n}}\forall n\in N,t\in(12(n-1),12n],j\in J \tag{2.8}$$

$$\sum_{t>12(n-1)}^{12n} \sum_{k=1}^{|K|} f_{t,j}^k x_{t,j}^k \geq Q_{j,n} \quad \forall n \in N, j \in J \tag{2.9}$$

$$y_n^k \leq y_{n-1}^k + y_{n+1}^k \quad \forall n \in N, k \in K \tag{2.10}$$

$$\iota^k y_n^k \leq \sum_{t>12(n-1)}^{12n} \sum_{j=1}^{|J|} x_{t,j}^k \leq \kappa^k y_n^k, \quad \forall n \in N, k \in K \tag{2.11}$$

$$\sum_{j=1}^{|J|} f_{t,j}^k x_{t,j}^k \leq (1+\varepsilon_k) \frac{\sum_{t>12(n-1)}^{12n} \sum_{j=1}^{|J|} x_{t,j}^k}{12} \forall n \in N, t \in (12(n-1), 12n], k \in K \tag{2.12}$$

$$\sum_{j=1}^{|J|} f_{t,j}^k x_{t,j}^k \geq (1-\varepsilon_k) \frac{\sum_{t>12(n-1)}^{12n} \sum_{j=1}^{|J|} x_{t,j}^k}{12} \forall n \in N, t \in (12(n-1), 12n], k \in K \tag{2.13}$$

$$\rho_n^k \geq \alpha^k y_n^k - \sum_{t>12(n-1)}^{12n} \sum_{j=1}^{|J|} x_{t,j}^k \quad \forall n \in N, k \in K \tag{2.14}$$

$$yt_{year}^k \geq a^k w_n^k \quad \forall n \in N, k \in K \tag{2.15}$$

$$\upsilon_n^k = w_n^k (yt_{year}^k - a^k) \quad \forall n \in N, k \in K \tag{2.16}$$

$$\sum_{j=1}^{|J|} s_{t,j}^l \leq \overline{S^l} \quad \forall t \in T \tag{2.17}$$

$$\sum_{j=1}^{|J|} \theta_j s_{t,j}^2 \geq \mu \sum_{i=1}^{|I|} (1+\nu_i) D_{t+1}^i \quad \forall t \in T \tag{2.18}$$

$$\sum_{j=1}^{|J|} s_{T,j}^l \geq G^l \quad \forall l \in L \tag{2.19}$$

$$\sum_{j=1}^{|J|} \theta_j (\beta_{t-1,j}^{1,i} + \beta_{t,j}^{2,i}) \geq (1+\nu_i) D_t^i \quad \forall t \in T, i \in I \tag{2.20}$$

$$\sum_{j=1}^{|J|} \theta_j (\beta_{t-1,j}^{1,i} + \beta_{t,j}^{2,i}) \leq \sum_{j=1}^{|J|} (\Theta_i + \gamma_\theta)(\beta_{t-1,j}^{1,i} + \beta_{t,j}^{2,i}) \quad \forall t \in T, i \in I \tag{2.21}$$

$$\sum_{j=1}^{|J|} \theta_j (\beta_{t-1,j}^{1,i} + \beta_{t,j}^{2,i}) \geq \sum_{j=1}^{|J|} (\Theta_i - \gamma_\theta)(\beta_{t-1,j}^{1,i} + \beta_{t,j}^{2,i}) \quad \forall t \in T, i \in I \tag{2.22}$$

$$\sum_{j=1}^{|J|} \theta_j \delta_j (\beta_{t-1,j}^{1,i} + \beta_{t,j}^{2,i}) \leq \sum_{j=1}^{|J|} \Theta_i (\Delta_i + \gamma_\delta)(\beta_{t-1,j}^{1,i} + \beta_{t,j}^{2,i}) \quad \forall t \in T, i \in I \tag{2.23}$$

$$\sum_{j=1}^{|J|} \omega_j(\beta_{t-1,j}^{1,i} + \beta_{t,j}^{2,i}) \leq \sum_{j=1}^{|J|} (\Omega_i + \gamma_\omega)(\beta_{t-1,j}^{1,i} + \beta_{t,j}^{2,i}) \quad \forall t \in T, i \in I \tag{2.24}$$

$$\beta_{t,j}^{l,i} \leq \overline{B^l} \varpi_{t,j}^{l,i} \quad \forall t \in T, j \in J, l \in L, i \in I \tag{2.25}$$

$$\sum_{j=1}^{|J|} \varpi_{t,j}^{l,i} \leq \overline{\beta^i} \quad \forall t \in T, l \in L, i \in I \tag{2.26}$$

$$s_{t,j}^l, v_{t,j}^l, x_{t,j}^k, z_{t,j}, \beta_{t,j}^{l,i}, \rho_n^k, \upsilon_n^k, \in \mathbb{R}^+; \chi_{j,n}, w_n^k, y_n^k, \varpi_{t,j}^{l,i} \in \mathbb{B} \quad \forall t \in T, j \in J, l \in L, k \in K \tag{2.27}$$

The objective function aims at minimizing the total fuel cost, which consists of procurement, transportation, handling, inventory, and blending cost terms. Coal procurement category of constraints consists of two main groups:

- Flow balance constraint sets (2.2)-(2.4) track each individual coal shipment from the time they are purchased to the time they are burned or stored in the inventory. Based on TECO's operation, one time period is defined to be one month, thus we ignore the transportation time from the mines to either the depot or directly to Big Bend station, because they are roughly one week long, but consider a one month lag for shipping coal from the depot to Big Bend power station to indicate the delay of transshipment by gulf barges.
- Purchase constraints (2.6–(2.8)) ensure the annual and monthly purchases from each vendor are within the agreed range. TECO has purchase commitments based on its previous contracts which is reflected in constraint (2.9).

Transportation contracts are usually long-term contracts. As shown by constraint set (2.10), we are obliged to a minimum of two-year commitment to a chosen carrier. Simi-

lar to procurement contracts, there are annual and monthly transportation range reflected in constraint sets (2.11)-(2.13). Constraint sets (2.14)-(2.16) capture the piecewise-linear transportation cost structure and calculate dead freight and credit.

Each type of coal has its own pile in either the intermediate depot or Big Bend station. We do not consider inventory at Polk station as the blended mix for this unit comes directly from Big Bend station on a daily basis. We start the planning horizon with a level of initial inventory that can be used with newly-purchased sources of coals. Constraint set (2.17) makes sure that the total inventory is below the capacity at each storage facility. Constraint set (2.18) guarantees there is always a certain ratio of future's demand, e.g., 45 days burn, in the inventory as a safety stock to cover emergency situations such as interruptions in coal delivery. Finally, by constraint set (2.19), a specified amount of coal must be available at the end of the planning horizon for the next planning period.

Constraint set (2.20) assures the demands of Big Bend and Polk stations are satisfied based on their specific recipes, which are dynamically determined with main additive quality attributes, i.e. heat content, sulfur content, and chlorine content. Since the generators are different in type, the blend fed to each generator must not only comply with EPA specifications, but also be in a range that the generator can handle. Therefore we have a range for the heat content which is presented in constraint sets (2.21) and (2.22). Upper bounds on sulfur and chlorine contents are presented in constraint sets (2.23) and (2.24), respectively. Finally, constraint sets (2.25)-(2.26) are to impose bounds on blending cardinalities.

## 2.4 Implementation, Analysis, and Discussion

In this section we describe how Fuelsupport system is utilized by TECO staff to facilitate the fuel supply chain design and operations. Numerical analysis and discussions are conducted based on TECO's historical and forecasted data, as well as its actual configuration. Based on the supply proposals, we considered 30 potential suppliers for long-term contracts and 9 spot market suppliers that offer high-quality high-cost coals. TECO considers spot market coals in case there is a disruption in coal deliveries either caused by lack of supplies or failure of one of the 6 transportation carriers over rail, river, and gulf. We consider a 4-year planning horizon with annual coal contracts and bi-annual transportation contracts. The resulting MIP model, populated with TECO's real data, includes almost 52,000 continuous variables, 23,600 binary variables, and about 54,000 constraints. Computing by CPLEX 12.5 through GAMS, the computational times are generally less than 15 minutes.

### 2.4.1 Decision Making and Rolling Horizon Planning

Usage of Fuelsupport is not limited to the first planning point. Actually, whenever a new supply or transportation option arises, the operator can update the database and run the MIP model to determine the (long-term) source coal portfolio, the appropriate transportation and logistics arrangements, as well as the detailed monthly operational decisions. In addition to fuel supplier and transportation carrier selections, a variety of operational decisions such as monthly shipment schedule, monthly generator-specific blending plan, monthly inventory status, transportation carrier's utilization status, and coal source utilization status are output by Fuelsupport.

The rolling-horizon run feature enables the decision maker to handle new fuel offers dynamically. Moreover, such a strategy is also effective when attempting to minimize the impact of possible deviations from the planned or expected situation. Specifically, we can fix all the commitment decisions on the selections of fuel suppliers and transportation carriers, as well as historical results/information on blending, inventory, and transportation, then re-run the system to minimize the overall cost. The new solution provides optimal monthly decisions in the remaining planning horizon.

TECO and the neighbouring utilities are located in a strategic location which accommodates affordable importation of South American fuels via international transportation carriers. TECO realized the strategic impact of adopting this transportation avenue as it would enable TECO to access petroleum coke and low-sulfur coals produced in South America, and consequently to reorganize its whole fuel supply chain. In this regard, a set of experiments were conducted to investigate the economical aspects of such adoption. The transportation proposal includes both delivery to TECO's Big Bend power station and to its intermediate depot. Our investigations showed that acquiring South American coal is beneficial. If the intermediate depot is chosen as the point of delivery, TECO could save about 0.1%- 0.3% annually, based on the negotiable transportation rates. If Big Bend power station is selected as the delivery point, that cost reduction could be increased to 0.7%. Further investigation on fuel source selection showed that South American low-sulfur coal is not cost-effective when it is delivered at the intermediate depot, while South American petroleum coke is selected in both aforementioned situations. This analysis provides a basis

for TECO administrators to evaluate this new opportunity within the context of the issues and challenges of importing foreign fuels.

### 2.4.2 Sensitivity Analysis

Next, we describe a set of sensitivity analyses performed on TECO system, which have been used for contract negotiations and system specification re-evaluations.

#### 2.4.2.1 Transportation Contract Design

Our colleagues at TECO make an effort to customize the (long-term) transportation contract terms in order to achieve affordable electricity rates. Our plan was to test the sensitivity of the overall cost to the current transportation carriers' cost structure parameters, i.e. dead freight/credit thresholds, dead freight penalty, credit, and unit transportation rate. We then draw some insights from the result to recognize the effective parameters.

For example, we noticed that in the base case, i.e. where all parameters are set to their present values, the river transportation carriers were used to a great extend. This observation indicated two possibilities: *(1)* the carriers on the river offer relatively good prices, and *(2)* desirable coal sources are accessible by Mississippi river. Two questions arose during our analysis: *(1)* whether or not negotiating with rail carrier to bring the cost down could shift the load from river-based transportation to railroads. *(2)* if river transportation is still favorable, how much we could gain by negotiating over contract terms. In this regard, we conducted a set of experiments and checked a range of values for rates, credits, and dead freight charges, to analyze dead freight/credit thresholds, and penalty/discount rates of the rail and water-based transportation carriers.

For the current pool of fuel suppliers, our analysis showed that minor changes in the aforementioned contract parameters did not result in changes of carriers nor the main suppliers, which confirmed the importance of river transportation and the robustness of TECO's fuel supply chain configuration. It also indicated that existing transportation cost structures are well designed and balanced for consumers in Florida, given their geographic locations and demand patterns. Those experiments still helped us develop quantitative understanding on the potential of cost savings from modifying the aforementioned contract terms (i.e. parameters in our MIP model). For example, by reducing the base rate of the highly used carriers, i.e. gulf carrier, a river-based carrier, and rail carrier by just one dollar we would save 3.5%, 1.35%, and 1% respectively, on the overall transportation cost, a cost category which represents one third of the total cost of fuel supply chain. The saving on rail would almost be doubled if we reduce the dead freight trigger of rail by 10%. We also explored the possibility of increasing the maximum allowed transportation to reduce cost. For example, consider that river-based carrier which was almost fully utilized in three years of our four-year planning analysis. If it can increase TECO's allowed volume by 10% (with all other rates unchanged), a 0.25% reduction on TECO's total cost could be achieved.

#### 2.4.2.2 Vulnerability to Burn Quality

We incorporated the emission control requirements as hard constraints in the optimization model of Fuelsupport. However, changes in the current regulations may require power plants to meet more stringent standards. Therefore, a set of experiments were conducted to determine the fuel cost sensitivity to such changes. More importantly, we would like to help

TECO to investigate whether it is beneficial to further invest in installing or upgrading facilities to remove sulfur or chlorine. Ideally, with new facilities and upgrades, TECO will be able to explore high-sulfur and/or -chlorine content but less-expensive fuel sources without violating the environmental regulations.

Therefore, we varied the maximum acceptable level of sulfur content in the final blend in the range of [4.2, 5.6] lb/mmbtu and that of chlorine content in the range of [0.075, 0.195]% to observe their impacts on the total cost relative to the existing practice. Results, with respect to the current pool of fuels, are plotted in Figure 5. We noted that TECO's system is very robust against changes in sulfur standards, which verifies the effectiveness of the currently installed scrubbers in handling the sulfur issue. However, it is very sensitive to chlorine restrictions. For the most stringent chlorine restriction, we will see a significant cost increase, ranging from [9.6, 13.1]%, based on different sulfur content restrictions. With such cost information presented in this figure, TECO adminstration can justify a technology upgrade. For example, assuming that one chlorine purification technology costs $p$ million dollars and has $q$% purification rate, we can find the associated cost saving from the chart and provide a quantitative cost-benefit justification on the installation of that technology.

In aforementioned experiments, we made an assumption that TECO designs its fuel supply chain without any existing commitments or inventory, i.e. TECO can implement a completely optimal fuel supply chain given each realization of regulations. This consideration is valid to analyze TECO's strategic decisions and management. However, in practice, after new regulations are imposed, utility companies generally have to deal with existing fuel

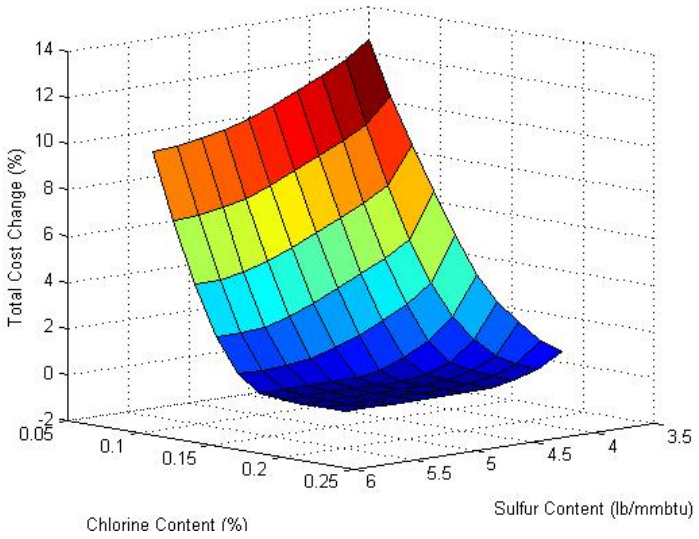


Figure 5: The impact of coal quality standards on total cost

sources in the backyards, fulfill signed contracts or break contracts with penalties. Specifically, TECO's policy is to continue the signed contracts in the first year, and negotiate to excuse the remaining years if necessary, then improve the quality of blends by purchasing better-quality coals, which could be more expensive. Clearly, this approach can also be quantitatively evaluated by slightly modifying our Fuelsupport system in a way similar to the rolling-horizon method. For example, we considered one scenario that concerns TECO: the acceptable thresholds of sulfur contents in final blends are 10% lower than the current values for all units. Our analysis shows that under such situation, TECO's total cost increases by 5.3%. Indeed, provided South American petroleum coke, which are of low sulfur contents and fair prices, is accessible, the total cost will only have 2.7% increase. Hence, it suggests that, if feasible, TECO should seriously consider fuels from South America to construct a portfolio that is of low cost and low risk.

## 2.5 Final Remarks

By benchmarking with TECO's practices over the last couple of years, it was observed that solutions from Fuelsupport lead to 2-3% saving on annual fuel cost, which translates to millions of dollars in savings. Since the fuel cost is directly transferred to the consumers, such saving can benefit the community most by a reduction in their electricity bills. A detailed investigation and comparison between the historical supply chain decisions and Fuelsupport solutions illustrates the main advantages of Fuelsupport system. *(i)* It identifies multiple optimal coal source portfolios; due to the fast computation of the optimization model of Fuelsupport, it evaluates hundreds of combinations of source coals and finds a number of them that result in the minimum cost. *(ii)* We are no longer limited to fixed blending recipes throughout the planning horizon. Fuelsupport instead generates dynamic blending recipes that take the availability and price fluctuation into consideration and makes the best use of the supply portfolio. *(iii)* Effective asset utilization is another advantage of our system. For example, Fuelsupport is programmed to make the most of the storage and handling rate differences between the intermediate depot and Big Bend power station by giving a preference to the depot, with cheaper rates, and optimally scheduling the shipments to Big Bend to assure a reliable operation. *(iv)* It exploits contract terms and conditions to the advantage of TECO. For example, by using the 10% variation limit in monthly transportation when needed, Fuelsupport promotes the purchase and transportation of coals when their purchase or transportation unit costs are less expensive.

# CHAPTER 3: ROBUST SECURITY-CONSTRAINED UNIT COMMITMENT WITH DYNAMIC RATING

## 3.1 Background

Unit Commitment (UC) is one of the most essential problems in the deregulated power market, and the uncertainties appearing in supply and demand sides amplifies its complexity. UC problem attempts at scheduling the generators in a way to meet the forecasted demand with the least commitment and dispatch costs while maintaining various physical, systematical, and reliability requirements. There are two decision making milestones associated with this problem; the status of generators is set in a day-ahead basis, and the generation level of each unit is determined on the real time and is adaptable with the actual load.

Given the importance of reliably generating electricity and the high portion of dispatch cost in total operation cost (%60 of total operating cost), UC attracts a lot of attention. Over the time, many research papers have considered this problem, different mathematical formulations have been proposed for general practices or specific utility company characteristics, and various approaches have been taken to solve this problem. A literature review of UC problem is gathered in [27].

The main challenges faced in UC problem come from the many uncertainties in the system, among them one can mention forecasted demand, renewable energy penetration both by end consumers and the utilities, and systems failures or malfunctions. There have

been many studies conducted to investigate how to avoid system failures and eliminate the consequences of variabilities such as unscheduled generator outages and major load forecasting errors. These approaches can be categorised as follows:

- The traditional approach is to consider a spinning reserve requirement, which is extra generation, in the deterministic model. The level of reserve can be set to be a portion of the forecasted demand or equal the generator loss and based on the satisfactory level of reliability. Although, this method is easy to implement, there is no guarantee it will always work and may not be economically efficient ([28, 29, 30, 31]).
- The next widely applied approach is stochastic optimization which requires probabilistic information of the uncertainties. Examples are ([32, 33, 34]) which considered transmission security issues, and ([35, 36, 37]) which focused on demand and renewable energy sources. For a literature review on stochastic optimization application in unit commitment see [38]. A drawback from the stochastic approach is its reliance on the existence of probability distributions in the data. Also, reaching a solution that's highly reliable requires a large number of scenarios which makes the problem computationally intensive.
- The third approach is robust optimization (RO), in which the decision makers aims at hedging against the worst case of uncertainty realization given a level of conservatism. This approach does not require probabilistic information and merely needs a range of variation. Despite its recent popularity, robust optimization's applications have been restricted to the uncertainties appearing in either right hand

side (demand uncertainty in UC problem [39, 40, 41]) or objective function (cost coefficients). However, there are some practical problems such as gas generator efficiency related to inlet air temperature, in which the uncertainty appears in the body of constraints. [42] presents variants of robust unit commitment and discusses its relationship with stochastic optimization.

The main contributions of our approach are summarized below.

- We formulate two instances of two-stage robust optimization models for the unit commitment problem. In the first instance, we consider the impact of the uncertainty in the inlet air temperature on both gas generators and overhead transmission lines efficiency. Such realization of uncertainty requires dynamic rating for our assets. The proposed model can be solved to optimality. In another instance, we consider both the uncertainty in the inlet air temperature and the forecasted demand. We also capture the relationship between the two uncertainty sets: based on the actual weather data in Tampa, FL, we noticed the demand curve follows temperature curve by up to two time periods. By solving this problem, we can have a good approximation of the optimal solution.
- We develop a practical solution methodology to solve the RO problems in which uncertain factors appear both in the left and right hand sides. Column and constraint generation algorithm is adopted and tailored to the specification of this problem. To the best of our knowledge, this is the first work on modeling and solving a problem with left hand side uncertainty.

- We conduct extensive numerical experiments on a both a single large scale power system operated by the Tampa Electric Company (TECO), as well as a medium scale network.

In this section, we, first, discuss the importance of dynamic rating in section 3.2, then the mathematical formulations are presented in section 3.3, our solution strategy is presented in section 3.4, and some experimental studies are provided in section 3.5 to shed light on the importance of this problem. Table 2 provides the nomenclature used in this chapter.

Table 2: Nomenclature used in chapter 3

| Symbol | Meaning |
|---|---|
| **Index Sets** | |
| $N$ | Set of indices of buses, $n = 1, ..., \|N\|$ |
| $I_n$ | Set of indices of generators connected to bus $n$, $i = 1, ..., \|I_n\|$ |
| $T$ | Set of indices of time periods, $t = 1, ..., \|T\|$ |
| $K$ | Breaking point in fuel cost approximation function, $k = 1, ..., \|K\|$ |
| $L$ | Set of indices of transmission assets, $l = 1, ..., \|L\|$ |
| $o(l)$ | Origin bus of transmission line $l$ |
| $d(l)$ | Destination bus of transmission line $l$ |
| **Parameters** | |
| $c^N_{ni}$ | No-load(fixed) cost of unit $i$, \$/h |
| $c^S_{ni}$ | Startup cost of unit $i$, \$ |
| $c^F_{nik}$ | Fuel cost at output level $G_{nik}$, \$/h |
| $c^M_t$ | Market purchase cost at time $t$, \$/MW |
| $D_{nt}$ | Demand of node $n$ at time $t$, MW |
| $l_i, u_i$ | Minimum/maximum generation limits of unit $i$, MW |
| $m^i_{+/-}$ | Minimum up/down limits, h |
| $\Delta^i_{+/-}$ | Ramping up/down limits of unit $i$, MW |
| $S_{ni}$ | Maximum spinning reserve contribution from unit $i$, MW |
| $R_t$ | Spinning reserve requirement of the whole system at time $t$, MW |
| $G_{nik}$ | Output level of generator $i$ at breaking point $k$, MW |
| $V_{nt}$ | Voltage level at bus $n$ at time $t$, volt |
| $P_{lt}$ | Power flow capacity of transmission line $l$ at time $t$, MW |
| $\bar{\delta}$ | Phase angle capacity of a bus, Radian |

Table 2 (continued)

| Symbol | Meaning |
|---|---|
| $\chi_{l_{pu}}$ | The impedance in the line $l$ |
| $P_l^{NP}$ | Nameplate rating of the line $l$, amperes |
| $A_{nt}$ | Ambient temperature at location $n$ time $t$, $^\circ C$ |
| $A_{max}$ | Maximum equipment temperature, $^\circ C$ |
| $A^{NP}$ | Air temperature specified for nameplate rating, $^\circ C$ |
| $A_{max}^{NP}$ | Maximum equipment temperature specified for nameplate rating, $^\circ C$ |
| $\iota$ | Exponent between 1.6 and 2 |
| **Decision variables** | |
| $\alpha_{nt}$ | Binary variable, (if 1) there is a temperature increase in bus $n$ at time $t$ |
| $\xi_{nt}$ | Binary variable, (if 1) there is a demand increase in bus $n$ at time $t$ |
| $x_{nit}$ | Planed generation level of unit $i$ which belongs to bus $n$ at time $t$, MW |
| $z_{nt}$ | Purchase level of bus $n$ at time $t$, MW |
| $\lambda_{nitk}$ | Positive linear combination of $k$ breaking points of generator $i$ at time $t$ |
| $r_{nit}$ | Spinning reserve from generator $i$ at time $t$, MW |
| $\delta_{nt}$ | Phase angle at node $n$ at time $t$, Radian |
| $p_{lt}$ | Power flow on line between bus $n$ to bus $n'$ at time $t$, MW |

### 3.2 Dynamic Asset Ratings

In this section, we analytically describe the impact of ambient air temperature on gas-fired generating units, as well as transmission network capacity. We also briefly discuss the advantages of dynamic rating vs. static rating which is widely practiced. Next, we describe how exploring the correlation between weather and load uncertainties can improve the operations and reduce the conservatism in decision making.

#### 3.2.1 Generation and Transmission Efficiency

As shown in Figure 6, the power output of a gas-fired generating unit is a linear inverse function of the inlet air temperature. By sampling, [3] built the linear function which basically states that at temperature $A$, there is an output power loss of $\left(\frac{A}{300} - 0.2\right)$ MW due to the ambient air temperature. This function can be used in static rating of generators.

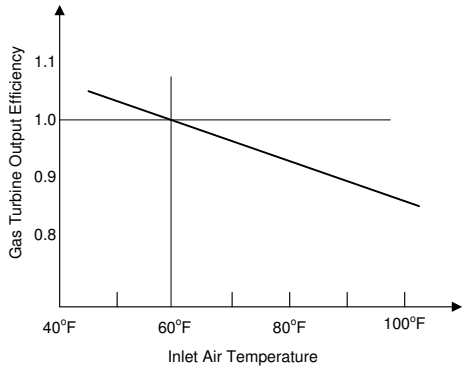


Figure 6: Power output loss due to ambient air temperature ([2])

Moreover, the capacity of an overhead transmission line is directly affected by weather conditions such as wind speed and direction, solar radiation, and ambient temperature. Here, we focus on studying the impact of temperature at each bus and along the transmission lines. The actual power flow $P_{lt}$ as a function of the ambient air temperature can be determined by equation (3.1) ([43]). However, since the exponent, $\iota$, is in the range of $[1.6, 2]$ substituting this expression in the UC formulation makes it nonlinear and more challenging to solve. Instead, in the robust model, we adopted an approximation reported in [44], which states there is a 1.1% reduction in power flow capacity for every $1°C$ increase in the ambient temperature around the transmission line (and vice versa).

$$P_{lt} = \frac{V_0}{S_0} I_l^{NP} \left(\frac{A_{max} - A_{nt}}{A_{max}^{NP} - A_{nt}^{NP}}\right)^{\iota} = P_l^{NP} \left(\frac{A_{max} - A_{nt}}{A_{max}^{NP} - A_{nt}^{NP}}\right)^{\iota} \tag{3.1}$$

In order to approximate the capacity of each line we use the temperature of its ends. The higher temperature will set the actual capacity of the line. Equation (3.2) shows the new range for the transmission lines.

$$|p_{lt}| \leq \min \begin{cases} |P_{lt}(1 - 0.11\frac{\Delta A_{o(l)}}{10}\alpha_{o(l)t})| \\ |P_{lt}(1 - 0.11\frac{\Delta A_{d(l)}}{10}\alpha_{d(l)t})| \end{cases} \tag{3.2}$$

### 3.2.2 Dynamic Rating

A transmission grid's power transfer capacity is primarily controlled by stability, voltage limits, and thermal ratings (dynamic line ratings). The first two factors are functions of transmission line length; stability, which is related to electrical phase shift, may determine power flow capacity on lines with more than 150 miles in length, and voltage drops determine the capacity of lines between 50 and 150 miles in length. However, the thermal limits are not a function of length, but of the weather condition. Indeed, wind speed and direction, solar radiation, and ambient temperature are the main factors that determine the flow capacity of lines, in particular for lines less than 50 miles in length.

There are two approaches to determine the thermal ratings of an overhead transmission line. The first approach is the static one, which assumes constant weather conditions over an extended period of time. The other approach is dynamic or real time approach, which takes the weather variation into account. While it may be easier to operate the network with an static rating, the dynamic ratings can improve system reliability, and optimize grid utilization through determining the actual real-time capacity.

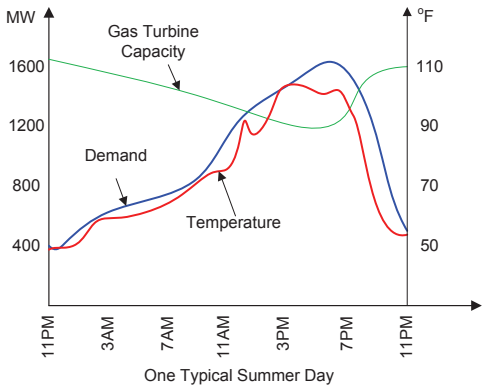


Figure 7: Demand and capacity vs. inlet air temperature ([3])

### 3.2.3 Correlated Uncertainty

As shown in Figure 7, temperature fluctuation not only affects the power generation capacity, but also the demand. In the shown instance, the warmth of a summer day in Florida, has decreased the generation capacity, while the demand, mainly for air conditioning, has followed this temperature increase with a short time lag. Utilizing this observation can result in a less conservative commitment and faster computational time.

## 3.3 Mathematical Models

### 3.3.1 Deterministic SCUC

In this section, a general Security-Constraint Unit Commitment, SCUC, model with thermal limits on the transmission network and generation capability is formulated (constraint sets (3.3)-(3.19)).

$$\min \sum_{n=1}^{|N|} \sum_{t=1}^{|T|} [\sum_{i=1}^{|I_n|} (c_{ni}^N y_{nit} + c_{ni}^S v_{nit}) + \sum_{i=1}^{|I_n|} \sum_{k=1}^{|K|} c_{nik}^F \lambda_{nitk} + c_t^M z_{nt}] \tag{3.3}$$

$$st.\ v_{nit} - w_{nit} = y_{nit} - y_{n,i,t-1}, \forall n \in N, i \in I_n, t \in T \backslash \{1\} \tag{3.4}$$

$$v_{ni1} = y_{ni1},\ \forall n \in N, i \in I_n \tag{3.5}$$

$$\sum_{h=t-m_+^i+1}^{t} v_{nih} \leq y_{nit}, \forall n \in N, i \in I_n, t \in \{m_+^i - 1, T\} \tag{3.6}$$

$$\sum_{h=t-m_-^i+1}^{t} w_{nih} \leq 1 - y_{nit},\ \forall n \in N, i \in I_n, t \in \{m_-^i - 1, T\} \tag{3.7}$$

$$x_{ni,t+1} + r_{ni,t+1} \leq x_{nit} + y_{nit}\Delta_+^i + (1 - y_{nit})u_i,\ \forall n \in N, i \in I_n, t \in T \backslash \{|T|\} \tag{3.8}$$

$$x_{nit} \leq x_{ni,t+1} + y_{n,i,t+1}\Delta_-^i + (1 - y_{n,i,t+1})u_i,\ \forall n \in N, i \in I_n, t \in T \backslash \{|T|\} \tag{3.9}$$

$$x_{nit} = \sum_{k=1}^{|K|} \lambda_{nitk} G_{nik},\ \forall n \in N, i \in I_n, t \in T \tag{3.10}$$

$$\sum_{k=1}^{|K|} \lambda_{nitk} = y_{nit},\ \forall n \in N, i \in I_n, t \in T \tag{3.11}$$

$$\sum_{i=1}^{|I_n|} x_{nit}(1.2 - \frac{A_{nt}}{300}) - \sum_{l|o(l)=n} p_{lt} + \sum_{l|d(l)=n} p_{lt} + z_{nt} = D_{nt},\ \forall n \in N, t \in T \tag{3.12}$$

$$x_{nit} + r_{nit} \leq u_i y_{nit},\ \forall n \in N, i \in I_n, t \in T \tag{3.13}$$

$$r_{nit} \leq S_{ni} y_{nit},\ \forall n \in N, i \in I_n, t \in T \tag{3.14}$$

$$\sum_{n=1}^{|N|} \sum_{i=1}^{|I_n|} r_{nit}(1.2 - \frac{A_{nt}}{300}) \geq R_t,\ \forall t \in T \tag{3.15}$$

$$p_{lt}\chi_{l_{pu}} = \delta_{o(l)t} - \delta_{d(l)t},\ \forall t \in T, l \in L \tag{3.16}$$

$$-P_{lt} \leq p_{lt} \leq P_{lt},\ \forall t \in T, l \in L \tag{3.17}$$

$$-\overline{\delta} \leq \delta_{nt} \leq \overline{\delta}\ \forall n \in N, t \in T \tag{3.18}$$

$$y_{nit} \in \{0, 1\}; v_{nit}, w_{nit} \in [0, 1];\ x_{nit}, r_{nit}, \lambda_{nitk}, z_{nt} \geq 0; \delta_{nt}, p_{lt} \in \mathbb{R} \tag{3.19}$$

The objective function (3.3) consists of start-up costs, no-load costs, fuel costs of gas generators and power purchase cost which is incurred either when generation cannot meet the demand or when it is not profitable to generate. The quadratic fuel cost functions of gas generators are approximated by piecewise linear functions. Figure 8 shows the piecewise linear function for generator $i$ with $K-1$ segments, generating in the range of $(l_i, u_i)$. Start-up operations are shown in constraints (3.4)-(3.5); unit $i$ is started up at the beginning of period $t$ if its status is off at time $t-1$ and is on at time $t$. Minimum up/down requirements, i.e., number of periods a unit has keep its on/off status, are demonstrated in constraints (3.6-3.7). The two aforementioned sets of constraints are proposed as strong (sometimes facet-defining) valid inequalities for UC problems in [45]. Ramping up/down limits, i.e., the maximal increase and decrease in the generation level of a unit at each period, are captured by constraints (3.8)-(3.9) [46]. Constraint set (3.11) illustrate the generation efficiency of unit $i$ as a convex combination of the breakpoints of the piecewise linear cost function. Due to the minimization objective function, unique combination will be achieved. Constraint (3.12) ensures that customer demand is satisfied by network power generation and real-time electricity purchase. Constraints (3.13)-(3.15) represents the spinning reserve requirement [47]. Constraint set (3.16) determines the power flow based on the voltage angle, and finally, constraint sets (3.17)-(3.18) set the feasible ranges for power flow and voltage angle. The planed power generation, $x_{nit}$, can be ommited from the formulation by replacing it with $\sum_{k=1}^{|K|} \lambda_{nitk} G_{nik}$, which is the convex combination of the breakpoints of the piecewise linear cost function.

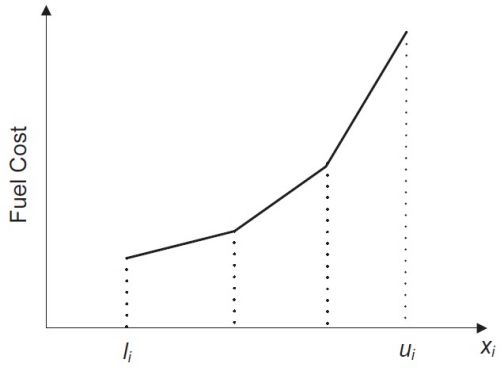


Figure 8: Piecewise linear fuel cost function

### 3.3.2 Two-stage Robust Counterpart

Problem (3.3.2) presents the two stage robust counter part of the UC problem. Set $\mathbb{Y}$ represents the day-ahead decision of when to turn on(off), thus, $y_{nit}, v_{nit}, w_{nit}$ are the first stage decisions. Set $\mathbb{X}$ represented the real time decision of generator load ($x_{nit}$), spinning reserve ($r_{nit}$), and transmission network power flow ($p_{lt},\ and\ \delta nt$) at each time period.

$$inf_{\mathbf{y},\mathbf{v},\mathbf{w}\in\mathbb{Y}} \sum_{n=1}^{|N|}\sum_{i=1}^{|I_n|}\sum_{t=1}^{|T|}(c_{ni}^{N}y_{nit} + c_{ni}^{S}v_{nit}) +$$
$$sup_{\alpha_{\mathbf{nt}}\in\mathbb{A}} inf_{\mathbf{r},\lambda,\mathbf{z},\mathbf{p},\delta\in\mathbb{X}} \sum_{n=1}^{|N|}\sum_{t=1}^{|T|}(\sum_{i=1}^{|I_n|}\sum_{k=1}^{|K|} c_{nik}^{F}\lambda_{nitk} + c_t^{M}Z_{nt}) \tag{3.20}$$

$$\mathbb{Y} = \{\mathbf{y},\mathbf{v},\mathbf{w} : (3.4) - (3.7); y_{nit} \in \{0,1\}, v_{nit}, w_{nit} \in [0,1]\}$$

$$\mathbb{X} = \{\mathbf{r},\lambda,\mathbf{z},\mathbf{p},\delta : (3.8) - (3.18);\ r_{nit}, \lambda_{nitk}, z_{nt} \geq 0; \delta_{nt}, p_{lt} \in \mathbb{R}\}$$

**Proposition 1** *When $\mathbb{A}$ is a hypercubic or discrete set, the two-stage robust optimization problem defined in (3.3.2) can be rewritten as problem (3.21).*

*Proof.* It is clear that when $\mathbb{A}$ is finite, (3.3.2) reduces to (3.21). For the case where $\mathbb{A}$ is a hypercubic set, given first-stage decisions (i.e., $\hat{y}$), we consider $\sup_{\alpha\in\mathbb{A}} f(\alpha)$ where $f(\alpha) = \inf_{\{x,r,z,p,\delta\}\in\mathbb{X}} (obj)$. Because $f(\alpha)$ is a non-increasing function over $\mathbb{A}$ for all $n, t$, (i.e., $f(\cdot,\alpha^1) \leq f(\cdot,\alpha^2)$ if $\alpha^1 \geq \alpha^2$ for all $n, t$), the supremum can be achieved at the lower corner point of the hypercubic set. Then the conclusion follows immediately. □

$$\min_{\mathbf{y},\mathbf{v},\mathbf{w}\in\mathbb{Y}} \sum_{n=1}^{|N|}\sum_{i=1}^{|I_n|}\sum_{t=1}^{|T|}(c^N_{ni}y_{nit} + c^S_{ni}v_{nit}) + \max_{\alpha_{\mathbf{nt}}\in\mathbb{A}} \min_{\mathbf{r},\lambda,\mathbf{z},\mathbf{p},\delta\in\mathbb{X}} \sum_{n=1}^{|N|}\sum_{t=1}^{|T|}(\sum_{i=1}^{|I_n|}\sum_{k=1}^{|K|} c^F_{nik}\lambda_{nitk} + c^M_t Z_{nt}) \tag{3.21}$$

The uncertainty set $\mathbb{A}$ is defined based on the variant of robust model. When a single uncertain factor, i.e., temperature, is considered, $\mathbb{A}$ is defined as $\mathbb{A}^S$ in equation (3.22), and in the case with two correlated uncertainty sets, it is written as $\mathbb{A}^C$ in equation (3.23).

$$\mathbb{A}^S = \{\alpha_{\mathbf{nt}} : A_{nt} = \underline{A}_{nt} + \alpha_{nt}\Delta A_n \ \forall n \in N, t \in T; \sum_{t=1}^{|T|} \alpha_{nt} \leq \Gamma^A \ \forall n \in N; \alpha_{nt} \in [0,1]\} \tag{3.22}$$

$$\begin{aligned}\mathbb{A}^C = \{\alpha_{\mathbf{nt}}, \xi_{\mathbf{nt}} : {} & A_{nt} = \underline{A}_{nt} + \alpha_{nt}\Delta A_{nt} \ \forall n \in N, t \in T; \ \sum_{t=1}^{|T|} \alpha_{nt} \leq \Gamma^A \ \forall n \in N \\ & D_{nt} = \underline{D}_{nt} + \xi_{nt}\Delta D_{nt} \ \forall n \in N, t \in T; \ \sum_{t=1}^{|T|} \xi_{nt} \leq \Gamma^D \ \forall n \in N \\ & \sum_{t=0}^{t+1} \xi_{nt} \geq \alpha_{nt} \ \forall n \in N, t \in T; \ \Gamma^A \leq \Gamma^D; \ \alpha_{nt}, \xi_{nt} \in [0,1]\}\end{aligned} \tag{3.23}$$

### 3.4 Solution Approach

Two-level decomposition algorithms have proven to be effective in solving two-stage robust optimization problems. Thus, we implemented Column and Constraint Generation algorithm (C&CG), also used in [1, 48]. Algorithm 1 describes the implementation procedure, and the description of this implementation is provided as follows.

**Step 0**

Set $LB = -\infty,\ UB = +\infty,\ m = 1,\ \{l\} = \emptyset$;

Solve the master problem (3.24). Let $y^m$ denote the optimal first-stage decision.

**while** $\epsilon = (UB - LB)/UB$ *is greater than the tolerance* **do**

> **Step** $m$**.(a)**
>
> For a given $y^m$, solve the subproblem (3.25) to obtain the worst case uncertainty scenario $\hat{A}^{(m)}$.
>
> Update $\{l\} = \{l\} \bigcup \{m\}$ and $UB = \min\{UB, \text{subproblem objective}\}$.
>
> **Step** $m$**.(b)**
>
> Create extra variables $x^{(m)}, r^{(m)}, z^{(m)}, p^{(m)}, \delta^{(m)}$ and add second stage constraints with respect to $\hat{A}^{(m)}$ to the master problem.
>
> Set $m = m + 1$, Solve the master problem (3.24).
>
> Update $y^m$ and $LB = \{\text{the objective value of the master problem}\}$

**end**

**Algorithm 1:** Column and constraint generation algorithm

The master problem consists of the first stage constraints (3.4)-(3.7), and the cutting planes, generated iteratively in the subproblem. Given the solution of master problem, i.e., on/off status of generators, solving the subproblem identifies the worst realization of uncertainty and the best dispatch decision in that case. Incorporating the solution information from the subproblem, we then develop the mentioned cutting planes to protect the master

problem from such realization of uncertainty. The master problem and subproblem for the case with just temperature uncertainty are problems (3.24) and (3.25), respectively.

$$\min \sum_{n=1}^{|N|}\sum_{i=1}^{|I_n|}\sum_{t=1}^{|T|}(c_{ni}^{N}y_{nit} + c_{ni}^{S}v_{nit}) + \chi \tag{3.24}$$

$$st.\ v_{nit} - w_{nit} = y_{nit} - y_{n,i,t-1},\ \forall n \in N, i \in I_n, t \in T\backslash\{1\}$$

$$v_{ni1} = y_{ni1},\ \forall n \in N, i \in I_n$$

$$\sum_{h=t-m_{+}^{i}+1}^{t} v_{nih} \leq y_{nit} \forall n \in N, i \in I_n, t \in \{m_{+}^{i} - 1, |T|\}$$

$$\sum_{h=t-m_{-}^{i}+1}^{t} w_{nih} \leq 1 - y_{nit} \forall n \in N, i \in I_n, t \in \{m_{-}^{i} - 1, |T|\}$$

$$\chi \geq \sum_{n=1}^{|N|}\sum_{t=1}^{|T|}(\sum_{i=1}^{|I_n|}\sum_{k=1}^{|K|} c_{ik}^{F}\lambda_{itk}^{(m)} + c_{t}^{M}z_{nt}^{(m)})\ \forall 1 \leq m \leq o$$

$$\sum_{k=1}^{|K|}\lambda_{n,i,t+1,k}^{(m)}G_{nik} + r_{n,i,t+1}^{(m)} \leq \sum_{k=1}^{|K|}\lambda_{nitk}^{(m)}G_{nik} + y_{nit}\Delta_{+}^{i} + (1 - y_{nit})u_i$$

$$\forall n \in N, i \in I_n, t \in T\backslash\{|T|\}, 1 \leq m \leq o$$

$$\sum_{k=1}^{|K|}\lambda_{nitk}^{(m)}G_{nik} \leq \sum_{k=1}^{|K|}\lambda_{i,t+1,k}^{(m)}G_{nik} + y_{i,t+1}\Delta_{-}^{i} + (1 - y_{i,t+1})u_i$$

$$\forall n \in N, i \in I_n, t \in T\backslash\{|T|\}, 1 \leq m \leq o$$

$$\sum_{k=1}^{|K|}\lambda_{nitk}^{(m)} = y_{nit}\ \forall n \in N, i \in I_n, t, 1 \leq m \leq o$$

$$\sum_{i=1}^{|I_n|}\sum_{k=1}^{|K|}\lambda_{nitk}^{(m)}G_{nik}(1.2 - \frac{A_{nt}^{T^*}}{300}) - \sum_{l|o(l)=n} p_{lt}^{(m)} + \sum_{l|d(l)=n} p_{lt}^{(m)} + z_{nt}^{(m)} = D_{nt},$$

$$\forall n \in N, t \in T, 1 \leq m \leq o$$

$$\sum_{k=1}^{|K|}\lambda_{nitk}^{(m)}G_{nik} + r_{nit}^{(m)} \leq u_i y_{nit}, \forall n \in N, i \in I_n, t \in T, 1 \leq m \leq o$$

$$r_{nit}^{(m)} \leq S_{ni} y_{nit} \forall n \in N, i \in I_n, t \in T, 1 \leq m \leq o$$

$$\sum_{N=1}^{|N|} \sum_{i=1}^{|I_n|} r_{nit}^{(m)} (1.2 - \frac{A_{nt}^{T^*}}{300}) \geq R_t \ \forall t \in T, 1 \leq m \leq o$$

$$p_{lt}^{(m)} \chi_{l_{pu}} = \delta_{o(l)t}^{(m)} - \delta_{d(l)t}^{(m)}, \ \forall t \in T, l \in L, 1 \leq m \leq o$$

$$-P_{lt}^{*} \leq p_{lt}^{(m)} \leq P_{lt}^{*}, \ \forall t \in T, l \in L, 1 \leq m \leq o$$

$$-\overline{\delta} \leq \delta_{nt}^{(m)} \leq \overline{\delta}, \ \forall n \in N, t \in T, 1 \leq m \leq o$$

$$y_{nit} \in \{0,1\}, v_{nit}, w_{nit} \in [0,1], \forall n \in N, i \in I_n, t \in T;$$

$$r_{it}^{(m)}, \lambda_{nitk}^{(m)}, z_{nt}^{(m)}, \chi \in \mathbb{R}^{+}; p_{lt}^{(m)}, \delta_{nt}^{(m)} \in \mathbb{R} \ \forall n \in N, i \in I_n, t \in T, k \in K$$

**Remark 1** *Given a feasible* $\{y_{nit}\} \in \mathbb{Y}$*,* $\alpha_{nt}$ *takes values at either* 0 *or* 1 *except for (at most) one* $(n,t)$ *where it takes a value in between.*

The intuition behind this remark is that given a commitment plan, the most vulnerable bus/time combinations can be found and sorted. The worst case will occur when the $\Gamma$ most risk-prone combinations take value. Given an integer $\Gamma$, there will not be a non-binary $\alpha_{nt}$. The nonlinear *max-min* subproblem can be converted to a single bilinear maximization problem through utilizing Remark 1, which sets the uncertainty set domain to $\alpha_{nt} \in \mathbb{B}$, and dualizing the resulted innermost bilinear minimization problem.

$$\max \ -\sum_{n}\sum_{i}\sum_{t=0}^{T-2}[(\hat{y}_{nit}\Delta_{+}^{i} + (1-\hat{y}_{nit})u_i)\beta_{nit} + (\hat{y}_{it+1}\Delta_{-}^{i} + (1-\hat{y}_{n,i,t+1})u_i)\theta_{nit}] + \sum_{t} R_t \pi_t +$$

$$\sum_{n}\sum_{i}\sum_{t}(\hat{y}_{nit}\zeta_{nit} - u_i\hat{y}_{nit}\vartheta_{nit} - S_{ni}\hat{y}_{nit}\mu_{nit}) + \sum_{n}\sum_{t}[D_{nt}\eta_{nt} - \overline{\delta}(\epsilon_{nt} + \phi_{nt})] -$$

$$\sum_{l}\sum_{t}[P_{lt}(1-0.11P_{lt}\frac{\Delta A_{o(l)}}{10}\alpha_{o(l)t})(\iota_{lt}+\xi_{lt})+P_{lt}(1-0.11\frac{\Delta A_{d(l)t}}{10}\alpha_{d(l)t})(\kappa_{lt}+\nu_{lt})] \quad (3.25)$$

$$G_{nik}(\beta_{ni0}-\theta_{ni0})+\zeta_{ni0}+G_{nik}(1.2-\frac{A_{n0}}{300})\eta_{n0}-G_{nik}\vartheta_{ni0}\leq c^{F}_{nik},\ \forall n\in N, i\in I_n, t=0, k\in K$$

$$G_{nik}(-\beta_{ni,t-1}+\theta_{ni,t-1}+\beta_{nit}-\theta_{nit})+\zeta_{nit}+G_{nik}(1.2-\frac{A_{nt}}{300})\eta_{nt}-G_{nik}\vartheta_{nit}\leq c^{F}_{nik},$$

$$\forall n\in N, i\in I_n, t\in T\backslash 1,|T|, k\in K$$

$$G_{nik}(-\beta_{ni,T-2}+\theta_{ni,T-2})+\zeta_{ni,T-1}+G_{nik}(1.2-\frac{A_{nT-1}}{300})\eta_{nT-1}-G_{nik}\vartheta_{ni,T-1}\leq c^{F}_{nik},$$

$$\forall n\in N, i\in I_n, t=T-1, k\in K$$

$$\eta_{nt}\leq c^{M}_{t},\ \forall n\in N, t\in T$$

$$-\beta_{ni,t-1}-\vartheta_{nit}-\mu_{nit}+(1.2-\frac{A_{nt}}{300})\pi_t\leq 0,\ \forall n, i\in I_n, t$$

$$-\eta_{n|o(l)=n,t}+\eta_{n|d(l)=n,t}+\chi_{l_{pu}}\rho_{lt}+\iota_{lt}-\xi_{lt}+\kappa_{lt}-\nu_{lt}=0,\ \forall l\in L, t\in T$$

$$-\sum_{l}\rho_{l|o(l)=n,t}+\sum_{l}\rho_{l|d(l)=n,t}+\epsilon_{nt}-\phi_{nt}=0,\ \forall n\in N, t\in T$$

$$\beta_{nit},\theta_{nit},\vartheta_{nit},\mu_{nit},\pi_t,\xi_{lt},\nu_{lt},\epsilon_{nt},\phi_{nt}\in\mathbb{R}^{+};\ \zeta_{nit},\eta_{nt},\rho_{lt}\in\mathbb{R}$$

Note that the terms $\alpha_{nt}\xi_{lt}$, $\alpha_{nt}\iota_{lt}$, $\alpha_{nt}\kappa_{lt}$, $\alpha_{nt}\nu_{lt}$, $\frac{A_{nt}}{300}\eta_{nt}$ and $\frac{A_{nt}}{300}\pi_t$ are nonlinear. Again, using the result from Remark 1, we can reformulate the nonlinear terms with McCormick linearization technique. The linearized model is omitted to avoid repetition.

### 3.5 Computational Study

In this section, a computational study is presented, and the impact of asset dynamic rating is investigated. The models are implemented in C++ with CPLEX 12.5 on a PC desktop with an Intel Core(TM)2QUAD 3.00 GHz CPU and 8 GB of memory. The relative gap is set to be $1e-3$ for terminating the algorithm. The experiments are conducted in two

categories: first we study the impact of dynamic rating on a power system with transmission network, and then we study the joint impact of demand and temperature uncertainties on a single bus.

### 3.5.1 Dynamic Rating

The experiments are conducted on a case study based on RTS 96 data set. There are 24 buses, including 8 generators with different capacity. Figure 9 presents a graph-view of the network where the green nodes represent the generator buses and the orange ones represent the demand points. The generator characteristics are described in Table 3. The total capacity is approximately 1975 MW, and the average demand per hour is around 57% of the capacity. All generators have a $min(150, Max\ output - Min\ output)(MW)$ ramping up rate and $min(50, Max\ output - Min\ output)(MW)$ ramping down rate. Both minimum up and down times are 2 hours. The fuel cost is a quadratic function in form of $f(x) = \alpha x^2 + \beta x$, however, we use a three-segmented piecewise linear approximation with breaking points $\{l, (u + 2l)/3, (2u + l)/3, u$ where $l \leq x \leq u$. The parameters $\alpha, \beta$ are randomly generated in a range of $[0.019, 0.024]$ and $[14, 18]$. Each generator can contribute up to 10% of its capacity to spinning reserve which is 10% of the demand at each hour.

Table 3: Parameters of gas generators in a power network

| Generator | G1 | G2 | G3 | G4 | G5,6,8 | G7 |
|---|---|---|---|---|---|---|
| Max output (MW) | 150 | 300 | 150 | 50 | 375 | 200 |
| Min output (MW) | 94 | 38 | 38 | 94 | 20 | 30 |
| Startup cost ($) | 4000 | 4000 | 2000 | 1000 | 4000 | 8000 |
| No load cost ($/hour) | 500 | 1000 | 300 | 1000 | 500 | 600 |

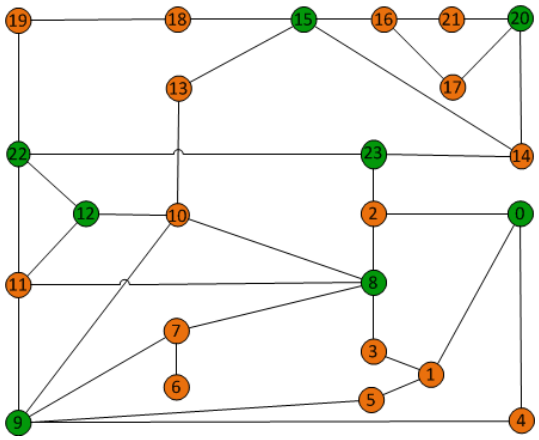


Figure 9: 24 bus system

We first demonstrate the impact of temperature on the generation and transmission network capacity. Figure 10(a) and (b)-(f) respectively display the planned vs actual generation and transmission of a randomly selected asset in an optimal deterministic UC solution with respect to temperature. As seen, the temperature impact can be significant specially during the peak hours.

Next, we investigate the impact of ignoring the temperature effect on the generation and transmission by feeding its commitment solution to two extreme cases: the optimistic case where the temperature always remain in its lower bound, and the pessimistic case in which all buses will suffer from temperature increase. Note that the optimistic case is actually only considering generator rating as the transmission line capacity in our model is vulnerable to temperature change. The result indicated a cost increase of at least 13% and rise in load shedding for more than 20%. However if static and dynamic temperature impact would have been considered, the commitment status would change which could result in lowering down the cost. Figure 11(a)-(c) presents the commitment results. The commitment percentages

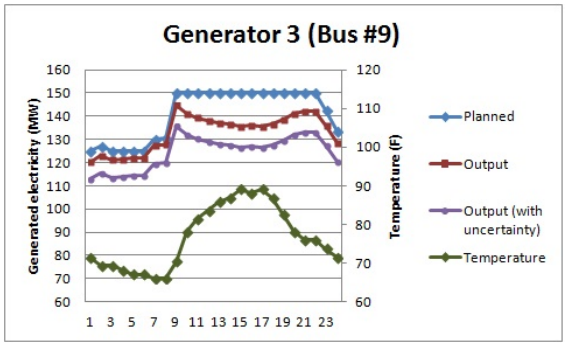


(a)

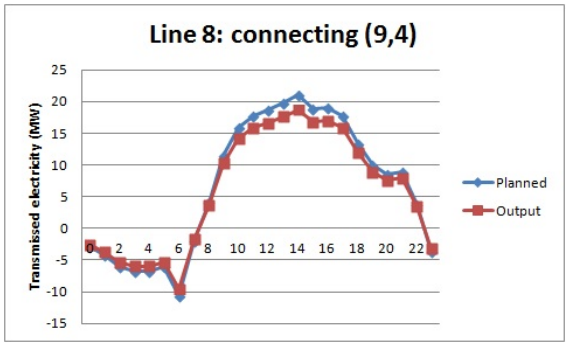


(b)

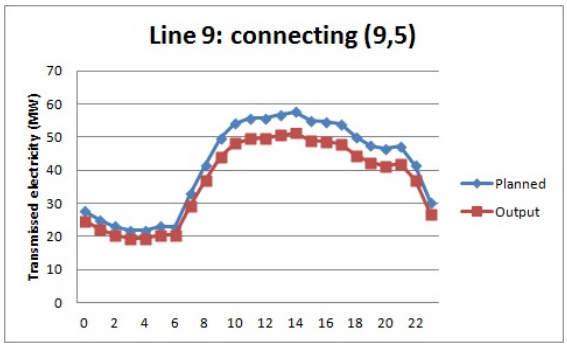


(c)

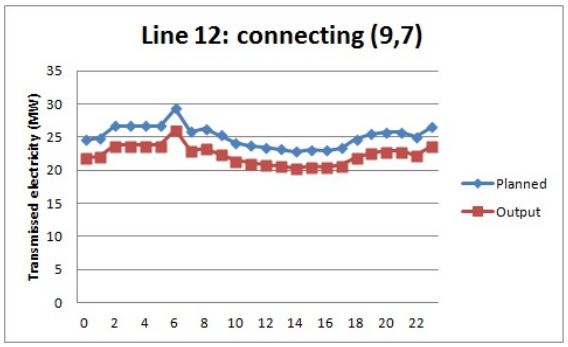


(d)

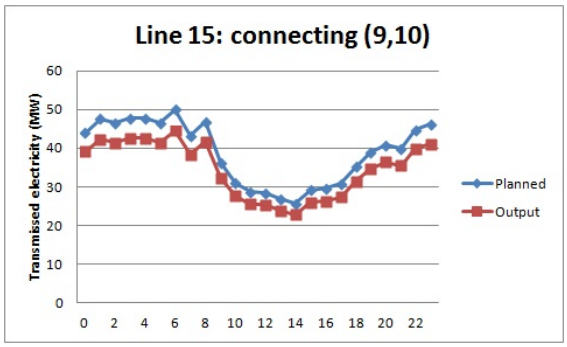


(e)

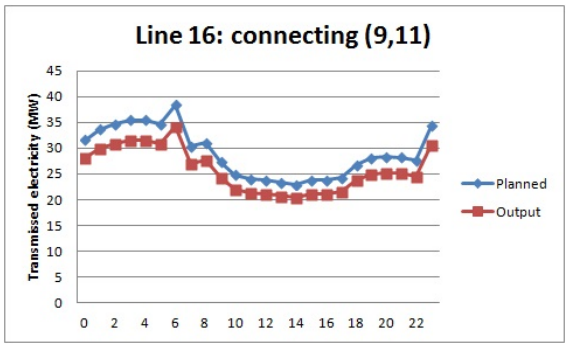


(f)

Figure 10: Temperature uncertainty impact on a generator and its transmission connections

(defined by the ratio of on statuses of all generators throughout the planning horizon) have changed very slightly, 0.6% and 1.1% in the optimistic and pessimistic cases, respectively. However, with the pessimistic approach, more load have been put on generator 2 (bus 8) instead of generator 7 (bus 22).

Since the likelihood of optimistic and pessimistic cases are low, adoption of our robust UC would be closer to reality. We ran the model for a range of possibilities in $\Gamma^A$, and compared the commitment schedule and total cost. Clearly, with a more conservative approach the total cost would be higher. However, in the unit commitment problem, the total cost is not the main comparing measure. The reason is that a considerable amount of cost is from the fuel cost and load shedding penalty. These cost items are associated with the dispatch decisions which can be corrected in the real time. As the result, in order to demonstrate the necessity of considering temperature uncertainty, we compare the commitment status in different cases. Figure 12 includes the commitment plan of two instances with different realization of temperature uncertainty. Note that $\Gamma^A$ should not necessarily remain constant over the time periods. Thus in these set of experiments we adopted $\Gamma^A_t$ which the level of conservatism at time $t$. Figure 12(a) is the commitment status of the case with $\Gamma^A_{6\leq t\leq 18} = 2$, and Figure 12(b) is the commitment status of the case with $\Gamma^A_{t\leq 8} = 2$. In both cases we have assumed a deterministic demand to study the temperature uncertainty impact. The commitment percentage in these cases are respectively 93% and 92% respectively, but they have different combination of generators and lines being active. It is also important to note that the $\Gamma^A_{t\leq 8} = 2$ case has the lower commitment percentage than the optimistic case, however in

| Bus # \ Hour | 12-1AM | 1-2 AM | 2-3 AM | 3-4 AM | 4-5 AM | 5-6 AM | 6-7 AM | 7-8 AM | 8-9 AM | 9-10 AM | 10-11 AM | 11-12 PM | 12-1 PM | 1-2 PM | 2-3 PM | 3-4 PM | 4-5 PM | 5-6 PM | 6-7 PM | 7-8 PM | 8-9 PM | 9-10 PM | 10-11 PM | 11-12 AM |
|---|---|---|---|---|---|---|---|---|---|---|---|---|---|---|---|---|---|---|---|---|---|---|---|---|
| 0 | 1 | 1 | 1 | 1 | 1 | 1 | 1 | 1 | 1 | 1 | 1 | 1 | 1 | 1 | 1 | 1 | 1 | 1 | 1 | 1 | 1 | 1 | 1 | 1 |
| 1 | 0 | 0 | 0 | 0 | 0 | 0 | 0 | 0 | 0 | 0 | 0 | 0 | 0 | 0 | 0 | 0 | 0 | 0 | 0 | 0 | 0 | 0 | 0 | 0 |
| 2 | 0 | 0 | 0 | 0 | 0 | 0 | 0 | 0 | 0 | 0 | 0 | 0 | 0 | 0 | 0 | 0 | 0 | 0 | 0 | 0 | 0 | 0 | 0 | 0 |
| 3 | 0 | 0 | 0 | 0 | 0 | 0 | 0 | 0 | 0 | 0 | 0 | 0 | 0 | 0 | 0 | 0 | 0 | 0 | 0 | 0 | 0 | 0 | 0 | 0 |
| 4 | 0 | 0 | 0 | 0 | 0 | 0 | 0 | 0 | 0 | 0 | 0 | 0 | 0 | 0 | 0 | 0 | 0 | 0 | 0 | 0 | 0 | 0 | 0 | 0 |
| 5 | 0 | 0 | 0 | 0 | 0 | 0 | 0 | 0 | 0 | 0 | 0 | 0 | 0 | 0 | 0 | 0 | 0 | 0 | 0 | 0 | 0 | 0 | 0 | 0 |
| 6 | 0 | 0 | 0 | 0 | 0 | 0 | 0 | 0 | 0 | 0 | 0 | 0 | 0 | 0 | 0 | 0 | 0 | 0 | 0 | 0 | 0 | 0 | 0 | 0 |
| 7 | 0 | 0 | 0 | 0 | 0 | 0 | 0 | 0 | 0 | 0 | 0 | 0 | 0 | 0 | 0 | 0 | 0 | 0 | 0 | 0 | 0 | 0 | 0 | 0 |
| 8 | 0 | 0 | 0 | 0 | 0 | 0 | 0 | 1 | 1 | 1 | 1 | 1 | 1 | 1 | 1 | 1 | 1 | 1 | 1 | 1 | 1 | 1 | 1 | 1 |
| 9 | 1 | 1 | 1 | 1 | 1 | 1 | 1 | 1 | 1 | 1 | 1 | 1 | 1 | 1 | 1 | 1 | 1 | 1 | 1 | 1 | 1 | 1 | 1 | 1 |
| 10 | 0 | 0 | 0 | 0 | 0 | 0 | 0 | 0 | 0 | 0 | 0 | 0 | 0 | 0 | 0 | 0 | 0 | 0 | 0 | 0 | 0 | 0 | 0 | 0 |
| 11 | 0 | 0 | 0 | 0 | 0 | 0 | 0 | 0 | 0 | 0 | 0 | 0 | 0 | 0 | 0 | 0 | 0 | 0 | 0 | 0 | 0 | 0 | 0 | 0 |
| 12 | 1 | 1 | 0 | 0 | 0 | 0 | 0 | 0 | 1 | 1 | 1 | 1 | 1 | 1 | 1 | 1 | 1 | 1 | 1 | 1 | 1 | 1 | 1 | 0 |
| 13 | 0 | 0 | 0 | 0 | 0 | 0 | 0 | 0 | 0 | 0 | 0 | 0 | 0 | 0 | 0 | 0 | 0 | 0 | 0 | 0 | 0 | 0 | 0 | 0 |
| 14 | 0 | 0 | 0 | 0 | 0 | 0 | 0 | 0 | 0 | 0 | 0 | 0 | 0 | 0 | 0 | 0 | 0 | 0 | 0 | 0 | 0 | 0 | 0 | 0 |
| 15 | 1 | 1 | 1 | 1 | 1 | 1 | 1 | 1 | 1 | 1 | 1 | 1 | 1 | 1 | 1 | 1 | 1 | 1 | 1 | 1 | 1 | 1 | 1 | 1 |
| 16 | 0 | 0 | 0 | 0 | 0 | 0 | 0 | 0 | 0 | 0 | 0 | 0 | 0 | 0 | 0 | 0 | 0 | 0 | 0 | 0 | 0 | 0 | 0 | 0 |
| 17 | 0 | 0 | 0 | 0 | 0 | 0 | 0 | 0 | 0 | 0 | 0 | 0 | 0 | 0 | 0 | 0 | 0 | 0 | 0 | 0 | 0 | 0 | 0 | 0 |
| 18 | 0 | 0 | 0 | 0 | 0 | 0 | 0 | 0 | 0 | 0 | 0 | 0 | 0 | 0 | 0 | 0 | 0 | 0 | 0 | 0 | 0 | 0 | 0 | 0 |
| 19 | 0 | 0 | 0 | 0 | 0 | 0 | 0 | 0 | 0 | 0 | 0 | 0 | 0 | 0 | 0 | 0 | 0 | 0 | 0 | 0 | 0 | 0 | 0 | 0 |
| 20 | 1 | 1 | 1 | 1 | 1 | 1 | 1 | 1 | 1 | 1 | 1 | 1 | 1 | 1 | 1 | 1 | 1 | 1 | 1 | 1 | 1 | 1 | 1 | 1 |
| 21 | 0 | 0 | 0 | 0 | 0 | 0 | 0 | 0 | 0 | 0 | 0 | 0 | 0 | 0 | 0 | 0 | 0 | 0 | 0 | 0 | 0 | 0 | 0 | 0 |
| 22 | 1 | 1 | 1 | 1 | 1 | 1 | 1 | 1 | 1 | 1 | 1 | 1 | 1 | 1 | 1 | 1 | 1 | 1 | 1 | 1 | 1 | 1 | 1 | 0 |
| 23 | 1 | 1 | 1 | 1 | 1 | 1 | 1 | 1 | 1 | 1 | 1 | 1 | 1 | 1 | 1 | 1 | 1 | 1 | 1 | 1 | 1 | 1 | 1 | 1 |

(a) Ignoring temperature effect

| Bus # \ Hour | 12-1AM | 1-2 AM | 2-3 AM | 3-4 AM | 4-5 AM | 5-6 AM | 6-7 AM | 7-8 AM | 8-9 AM | 9-10 AM | 10-11 AM | 11-12 PM | 12-1 PM | 1-2 PM | 2-3 PM | 3-4 PM | 4-5 PM | 5-6 PM | 6-7 PM | 7-8 PM | 8-9 PM | 9-10 PM | 10-11 PM | 11-12 AM |
|---|---|---|---|---|---|---|---|---|---|---|---|---|---|---|---|---|---|---|---|---|---|---|---|---|
| 0 | 1 | 1 | 1 | 1 | 1 | 1 | 1 | 1 | 1 | 1 | 1 | 1 | 1 | 1 | 1 | 1 | 1 | 1 | 1 | 1 | 1 | 1 | 1 | 1 |
| 1 | 0 | 0 | 0 | 0 | 0 | 0 | 0 | 0 | 0 | 0 | 0 | 0 | 0 | 0 | 0 | 0 | 0 | 0 | 0 | 0 | 0 | 0 | 0 | 0 |
| 2 | 0 | 0 | 0 | 0 | 0 | 0 | 0 | 0 | 0 | 0 | 0 | 0 | 0 | 0 | 0 | 0 | 0 | 0 | 0 | 0 | 0 | 0 | 0 | 0 |
| 3 | 0 | 0 | 0 | 0 | 0 | 0 | 0 | 0 | 0 | 0 | 0 | 0 | 0 | 0 | 0 | 0 | 0 | 0 | 0 | 0 | 0 | 0 | 0 | 0 |
| 4 | 0 | 0 | 0 | 0 | 0 | 0 | 0 | 0 | 0 | 0 | 0 | 0 | 0 | 0 | 0 | 0 | 0 | 0 | 0 | 0 | 0 | 0 | 0 | 0 |
| 5 | 0 | 0 | 0 | 0 | 0 | 0 | 0 | 0 | 0 | 0 | 0 | 0 | 0 | 0 | 0 | 0 | 0 | 0 | 0 | 0 | 0 | 0 | 0 | 0 |
| 6 | 0 | 0 | 0 | 0 | 0 | 0 | 0 | 0 | 0 | 0 | 0 | 0 | 0 | 0 | 0 | 0 | 0 | 0 | 0 | 0 | 0 | 0 | 0 | 0 |
| 7 | 0 | 0 | 0 | 0 | 0 | 0 | 0 | 0 | 0 | 0 | 0 | 0 | 0 | 0 | 0 | 0 | 0 | 0 | 0 | 0 | 0 | 0 | 0 | 0 |
| 8 | 0 | 0 | 0 | 0 | 0 | 0 | 0 | 1 | 1 | 1 | 1 | 1 | 1 | 1 | 1 | 1 | 1 | 1 | 1 | 1 | 1 | 1 | 1 | 1 |
| 9 | 1 | 1 | 1 | 1 | 1 | 1 | 1 | 1 | 1 | 1 | 1 | 1 | 1 | 1 | 1 | 1 | 1 | 1 | 1 | 1 | 1 | 1 | 1 | 1 |
| 10 | 0 | 0 | 0 | 0 | 0 | 0 | 0 | 0 | 0 | 0 | 0 | 0 | 0 | 0 | 0 | 0 | 0 | 0 | 0 | 0 | 0 | 0 | 0 | 0 |
| 11 | 0 | 0 | 0 | 0 | 0 | 0 | 0 | 0 | 0 | 0 | 0 | 0 | 0 | 0 | 0 | 0 | 0 | 0 | 0 | 0 | 0 | 0 | 0 | 0 |
| 12 | 1 | 1 | 0 | 0 | 0 | 0 | 0 | 0 | 1 | 1 | 1 | 1 | 1 | 1 | 1 | 1 | 1 | 1 | 1 | 1 | 1 | 1 | 1 | 0 |
| 13 | 0 | 0 | 0 | 0 | 0 | 0 | 0 | 0 | 0 | 0 | 0 | 0 | 0 | 0 | 0 | 0 | 0 | 0 | 0 | 0 | 0 | 0 | 0 | 0 |
| 14 | 0 | 0 | 0 | 0 | 0 | 0 | 0 | 0 | 0 | 0 | 0 | 0 | 0 | 0 | 0 | 0 | 0 | 0 | 0 | 0 | 0 | 0 | 0 | 0 |
| 15 | 1 | 1 | 1 | 1 | 1 | 1 | 1 | 1 | 1 | 1 | 1 | 1 | 1 | 1 | 1 | 1 | 1 | 1 | 1 | 1 | 1 | 1 | 1 | 1 |
| 16 | 0 | 0 | 0 | 0 | 0 | 0 | 0 | 0 | 0 | 0 | 0 | 0 | 0 | 0 | 0 | 0 | 0 | 0 | 0 | 0 | 0 | 0 | 0 | 0 |
| 17 | 0 | 0 | 0 | 0 | 0 | 0 | 0 | 0 | 0 | 0 | 0 | 0 | 0 | 0 | 0 | 0 | 0 | 0 | 0 | 0 | 0 | 0 | 0 | 0 |
| 18 | 0 | 0 | 0 | 0 | 0 | 0 | 0 | 0 | 0 | 0 | 0 | 0 | 0 | 0 | 0 | 0 | 0 | 0 | 0 | 0 | 0 | 0 | 0 | 0 |
| 19 | 0 | 0 | 0 | 0 | 0 | 0 | 0 | 0 | 0 | 0 | 0 | 0 | 0 | 0 | 0 | 0 | 0 | 0 | 0 | 0 | 0 | 0 | 0 | 0 |
| 20 | 1 | 1 | 1 | 1 | 1 | 1 | 1 | 1 | 1 | 1 | 1 | 1 | 1 | 1 | 1 | 1 | 1 | 1 | 1 | 1 | 1 | 1 | 1 | 1 |
| 21 | 0 | 0 | 0 | 0 | 0 | 0 | 0 | 0 | 0 | 0 | 0 | 0 | 0 | 0 | 0 | 0 | 0 | 0 | 0 | 0 | 0 | 0 | 0 | 0 |
| 22 | 1 | 1 | 1 | 1 | 1 | 1 | 1 | 1 | 1 | 1 | 1 | 1 | 1 | 1 | 1 | 1 | 1 | 1 | 1 | 1 | 1 | 1 | 1 | 1 |
| 23 | 1 | 1 | 1 | 1 | 1 | 1 | 1 | 1 | 1 | 1 | 1 | 1 | 1 | 1 | 1 | 1 | 1 | 1 | 1 | 1 | 1 | 1 | 1 | 1 |

(b) Optimistic approach

| Bus # \ Hour | 12-1AM | 1-2 AM | 2-3 AM | 3-4 AM | 4-5 AM | 5-6 AM | 6-7 AM | 7-8 AM | 8-9 AM | 9-10 AM | 10-11 AM | 11-12 PM | 12-1 PM | 1-2 PM | 2-3 PM | 3-4 PM | 4-5 PM | 5-6 PM | 6-7 PM | 7-8 PM | 8-9 PM | 9-10 PM | 10-11 PM | 11-12 AM |
|---|---|---|---|---|---|---|---|---|---|---|---|---|---|---|---|---|---|---|---|---|---|---|---|---|
| 0 | 1 | 1 | 1 | 1 | 1 | 1 | 1 | 1 | 1 | 1 | 1 | 1 | 1 | 1 | 1 | 1 | 1 | 1 | 1 | 1 | 1 | 1 | 1 | 1 |
| 1 | 0 | 0 | 0 | 0 | 0 | 0 | 0 | 0 | 0 | 0 | 0 | 0 | 0 | 0 | 0 | 0 | 0 | 0 | 0 | 0 | 0 | 0 | 0 | 0 |
| 2 | 0 | 0 | 0 | 0 | 0 | 0 | 0 | 0 | 0 | 0 | 0 | 0 | 0 | 0 | 0 | 0 | 0 | 0 | 0 | 0 | 0 | 0 | 0 | 0 |
| 3 | 0 | 0 | 0 | 0 | 0 | 0 | 0 | 0 | 0 | 0 | 0 | 0 | 0 | 0 | 0 | 0 | 0 | 0 | 0 | 0 | 0 | 0 | 0 | 0 |
| 4 | 0 | 0 | 0 | 0 | 0 | 0 | 0 | 0 | 0 | 0 | 0 | 0 | 0 | 0 | 0 | 0 | 0 | 0 | 0 | 0 | 0 | 0 | 0 | 0 |
| 5 | 0 | 0 | 0 | 0 | 0 | 0 | 0 | 0 | 0 | 0 | 0 | 0 | 0 | 0 | 0 | 0 | 0 | 0 | 0 | 0 | 0 | 0 | 0 | 0 |
| 6 | 0 | 0 | 0 | 0 | 0 | 0 | 0 | 0 | 0 | 0 | 0 | 0 | 0 | 0 | 0 | 0 | 0 | 0 | 0 | 0 | 0 | 0 | 0 | 0 |
| 7 | 0 | 0 | 0 | 0 | 0 | 0 | 0 | 0 | 0 | 0 | 0 | 0 | 0 | 0 | 0 | 0 | 0 | 0 | 0 | 0 | 0 | 0 | 0 | 0 |
| 8 | 1 | 1 | 1 | 1 | 1 | 1 | 1 | 1 | 1 | 1 | 1 | 1 | 1 | 1 | 1 | 1 | 1 | 1 | 1 | 1 | 1 | 1 | 1 | 1 |
| 9 | 1 | 1 | 1 | 1 | 1 | 1 | 1 | 1 | 1 | 1 | 1 | 1 | 1 | 1 | 1 | 1 | 1 | 1 | 1 | 1 | 1 | 1 | 1 | 1 |
| 10 | 0 | 0 | 0 | 0 | 0 | 0 | 0 | 0 | 0 | 0 | 0 | 0 | 0 | 0 | 0 | 0 | 0 | 0 | 0 | 0 | 0 | 0 | 0 | 0 |
| 11 | 0 | 0 | 0 | 0 | 0 | 0 | 0 | 0 | 0 | 0 | 0 | 0 | 0 | 0 | 0 | 0 | 0 | 0 | 0 | 0 | 0 | 0 | 0 | 0 |
| 12 | 0 | 0 | 0 | 0 | 0 | 0 | 0 | 1 | 1 | 1 | 1 | 1 | 1 | 1 | 1 | 1 | 1 | 1 | 1 | 1 | 1 | 1 | 1 | 1 |
| 13 | 0 | 0 | 0 | 0 | 0 | 0 | 0 | 0 | 0 | 0 | 0 | 0 | 0 | 0 | 0 | 0 | 0 | 0 | 0 | 0 | 0 | 0 | 0 | 0 |
| 14 | 0 | 0 | 0 | 0 | 0 | 0 | 0 | 0 | 0 | 0 | 0 | 0 | 0 | 0 | 0 | 0 | 0 | 0 | 0 | 0 | 0 | 0 | 0 | 0 |
| 15 | 1 | 1 | 1 | 1 | 1 | 1 | 1 | 1 | 1 | 1 | 1 | 1 | 1 | 1 | 1 | 1 | 1 | 1 | 1 | 1 | 1 | 1 | 1 | 1 |
| 16 | 0 | 0 | 0 | 0 | 0 | 0 | 0 | 0 | 0 | 0 | 0 | 0 | 0 | 0 | 0 | 0 | 0 | 0 | 0 | 0 | 0 | 0 | 0 | 0 |
| 17 | 0 | 0 | 0 | 0 | 0 | 0 | 0 | 0 | 0 | 0 | 0 | 0 | 0 | 0 | 0 | 0 | 0 | 0 | 0 | 0 | 0 | 0 | 0 | 0 |
| 18 | 0 | 0 | 0 | 0 | 0 | 0 | 0 | 0 | 0 | 0 | 0 | 0 | 0 | 0 | 0 | 0 | 0 | 0 | 0 | 0 | 0 | 0 | 0 | 0 |
| 19 | 0 | 0 | 0 | 0 | 0 | 0 | 0 | 0 | 0 | 0 | 0 | 0 | 0 | 0 | 0 | 0 | 0 | 0 | 0 | 0 | 0 | 0 | 0 | 0 |
| 20 | 1 | 1 | 1 | 1 | 1 | 1 | 1 | 1 | 1 | 1 | 1 | 1 | 1 | 1 | 1 | 1 | 1 | 1 | 1 | 1 | 1 | 1 | 1 | 1 |
| 21 | 0 | 0 | 0 | 0 | 0 | 0 | 0 | 0 | 0 | 0 | 0 | 0 | 0 | 0 | 0 | 0 | 0 | 0 | 0 | 0 | 0 | 0 | 0 | 0 |
| 22 | 0 | 0 | 0 | 0 | 0 | 0 | 1 | 1 | 1 | 1 | 1 | 1 | 1 | 1 | 1 | 1 | 1 | 1 | 1 | 1 | 1 | 1 | 1 | 1 |
| 23 | 1 | 1 | 1 | 1 | 1 | 1 | 1 | 1 | 1 | 1 | 1 | 1 | 1 | 1 | 1 | 1 | 1 | 1 | 1 | 1 | 1 | 1 | 1 | 1 |

(c) Pessimistic approach

Figure 11: The commitment status given different temperature effect consideration strategies

Hour

| Bus # | 12-1AM | 1-2 AM | 2-3 AM | 3-4 AM | 4-5 AM | 5-6 AM | 6-7 AM | 7-8 AM | 8-9 AM | 9-10 AM | 10-11 AM | 11-12 PM | 12-1 PM | 1-2 PM | 2-3 PM | 3-4 PM | 4-5 PM | 5-6 PM | 6-7 PM | 7-8 PM | 8-9 PM | 9-10 PM | 10-11 PM | 11-12 AM |
|---|---|---|---|---|---|---|---|---|---|---|---|---|---|---|---|---|---|---|---|---|---|---|---|---|
| 0 | 1 | 1 | 1 | 1 | 1 | 1 | 1 | 1 | 1 | 1 | 1 | 1 | 1 | 1 | 1 | 1 | 1 | 1 | 1 | 1 | 1 | 1 | 1 | 1 |
| 1 | 0 | 0 | 0 | 0 | 0 | 0 | 0 | 0 | 0 | 0 | 0 | 0 | 0 | 0 | 0 | 0 | 0 | 0 | 0 | 0 | 0 | 0 | 0 | 0 |
| 2 | 0 | 0 | 0 | 0 | 0 | 0 | 0 | 0 | 0 | 0 | 0 | 0 | 0 | 0 | 0 | 0 | 0 | 0 | 0 | 0 | 0 | 0 | 0 | 0 |
| 3 | 0 | 0 | 0 | 0 | 0 | 0 | 0 | 0 | 0 | 0 | 0 | 0 | 0 | 0 | 0 | 0 | 0 | 0 | 0 | 0 | 0 | 0 | 0 | 0 |
| 4 | 0 | 0 | 0 | 0 | 0 | 0 | 0 | 0 | 0 | 0 | 0 | 0 | 0 | 0 | 0 | 0 | 0 | 0 | 0 | 0 | 0 | 0 | 0 | 0 |
| 5 | 0 | 0 | 0 | 0 | 0 | 0 | 0 | 0 | 0 | 0 | 0 | 0 | 0 | 0 | 0 | 0 | 0 | 0 | 0 | 0 | 0 | 0 | 0 | 0 |
| 6 | 0 | 0 | 0 | 0 | 0 | 0 | 0 | 0 | 0 | 0 | 0 | 0 | 0 | 0 | 0 | 0 | 0 | 0 | 0 | 0 | 0 | 0 | 0 | 0 |
| 7 | 0 | 0 | 0 | 0 | 0 | 0 | 0 | 0 | 0 | 0 | 0 | 0 | 0 | 0 | 0 | 0 | 0 | 0 | 0 | 0 | 0 | 0 | 0 | 0 |
| 8 | 0 | 0 | 0 | 0 | 0 | 0 | 0 | 1 | 1 | 1 | 1 | 1 | 1 | 1 | 1 | 1 | 1 | 1 | 1 | 1 | 1 | 1 | 1 | 1 |
| 9 | 1 | 1 | 1 | 1 | 1 | 1 | 1 | 1 | 1 | 1 | 1 | 1 | 1 | 1 | 1 | 1 | 1 | 1 | 1 | 1 | 1 | 1 | 1 | 1 |
| 10 | 0 | 0 | 0 | 0 | 0 | 0 | 0 | 0 | 0 | 0 | 0 | 0 | 0 | 0 | 0 | 0 | 0 | 0 | 0 | 0 | 0 | 0 | 0 | 0 |
| 11 | 0 | 0 | 0 | 0 | 0 | 0 | 0 | 0 | 0 | 0 | 0 | 0 | 0 | 0 | 0 | 0 | 0 | 0 | 0 | 0 | 0 | 0 | 0 | 0 |
| 12 | 1 | 1 | 0 | 0 | 0 | 0 | 0 | 0 | 1 | 1 | 1 | 1 | 1 | 1 | 1 | 1 | 1 | 1 | 1 | 1 | 1 | 1 | 1 | 0 |
| 13 | 0 | 0 | 0 | 0 | 0 | 0 | 0 | 0 | 0 | 0 | 0 | 0 | 0 | 0 | 0 | 0 | 0 | 0 | 0 | 0 | 0 | 0 | 0 | 0 |
| 14 | 0 | 0 | 0 | 0 | 0 | 0 | 0 | 0 | 0 | 0 | 0 | 0 | 0 | 0 | 0 | 0 | 0 | 0 | 0 | 0 | 0 | 0 | 0 | 0 |
| 15 | 1 | 1 | 1 | 1 | 1 | 1 | 1 | 1 | 1 | 1 | 1 | 1 | 1 | 1 | 1 | 1 | 1 | 1 | 1 | 1 | 1 | 1 | 1 | 1 |
| 16 | 0 | 0 | 0 | 0 | 0 | 0 | 0 | 0 | 0 | 0 | 0 | 0 | 0 | 0 | 0 | 0 | 0 | 0 | 0 | 0 | 0 | 0 | 0 | 0 |
| 17 | 0 | 0 | 0 | 0 | 0 | 0 | 0 | 0 | 0 | 0 | 0 | 0 | 0 | 0 | 0 | 0 | 0 | 0 | 0 | 0 | 0 | 0 | 0 | 0 |
| 18 | 0 | 0 | 0 | 0 | 0 | 0 | 0 | 0 | 0 | 0 | 0 | 0 | 0 | 0 | 0 | 0 | 0 | 0 | 0 | 0 | 0 | 0 | 0 | 0 |
| 19 | 0 | 0 | 0 | 0 | 0 | 0 | 0 | 0 | 0 | 0 | 0 | 0 | 0 | 0 | 0 | 0 | 0 | 0 | 0 | 0 | 0 | 0 | 0 | 0 |
| 20 | 1 | 1 | 1 | 1 | 1 | 1 | 1 | 1 | 1 | 1 | 1 | 1 | 1 | 1 | 1 | 1 | 1 | 1 | 1 | 1 | 1 | 1 | 1 | 1 |
| 21 | 0 | 0 | 0 | 0 | 0 | 0 | 0 | 0 | 0 | 0 | 0 | 0 | 0 | 0 | 0 | 0 | 0 | 0 | 0 | 0 | 0 | 0 | 0 | 0 |
| 22 | 1 | 1 | 1 | 1 | 1 | 1 | 1 | 1 | 1 | 1 | 1 | 1 | 1 | 1 | 1 | 1 | 1 | 1 | 1 | 1 | 1 | 1 | 1 | 1 |
| 23 | 1 | 1 | 1 | 1 | 1 | 1 | 1 | 1 | 1 | 1 | 1 | 1 | 1 | 1 | 1 | 1 | 1 | 1 | 1 | 1 | 1 | 1 | 1 | 1 |

(a) $\Gamma^A_{6\leq t\leq 18} = 2$

Hour

| Bus # | 12-1AM | 1-2 AM | 2-3 AM | 3-4 AM | 4-5 AM | 5-6 AM | 6-7 AM | 7-8 AM | 8-9 AM | 9-10 AM | 10-11 AM | 11-12 PM | 12-1 PM | 1-2 PM | 2-3 PM | 3-4 PM | 4-5 PM | 5-6 PM | 6-7 PM | 7-8 PM | 8-9 PM | 9-10 PM | 10-11 PM | 11-12 AM |
|---|---|---|---|---|---|---|---|---|---|---|---|---|---|---|---|---|---|---|---|---|---|---|---|---|
| 0 | 1 | 1 | 1 | 1 | 1 | 1 | 1 | 1 | 1 | 1 | 1 | 1 | 1 | 1 | 1 | 1 | 1 | 1 | 1 | 1 | 1 | 1 | 1 | 1 |
| 1 | 0 | 0 | 0 | 0 | 0 | 0 | 0 | 0 | 0 | 0 | 0 | 0 | 0 | 0 | 0 | 0 | 0 | 0 | 0 | 0 | 0 | 0 | 0 | 0 |
| 2 | 0 | 0 | 0 | 0 | 0 | 0 | 0 | 0 | 0 | 0 | 0 | 0 | 0 | 0 | 0 | 0 | 0 | 0 | 0 | 0 | 0 | 0 | 0 | 0 |
| 3 | 0 | 0 | 0 | 0 | 0 | 0 | 0 | 0 | 0 | 0 | 0 | 0 | 0 | 0 | 0 | 0 | 0 | 0 | 0 | 0 | 0 | 0 | 0 | 0 |
| 4 | 0 | 0 | 0 | 0 | 0 | 0 | 0 | 0 | 0 | 0 | 0 | 0 | 0 | 0 | 0 | 0 | 0 | 0 | 0 | 0 | 0 | 0 | 0 | 0 |
| 5 | 0 | 0 | 0 | 0 | 0 | 0 | 0 | 0 | 0 | 0 | 0 | 0 | 0 | 0 | 0 | 0 | 0 | 0 | 0 | 0 | 0 | 0 | 0 | 0 |
| 6 | 0 | 0 | 0 | 0 | 0 | 0 | 0 | 0 | 0 | 0 | 0 | 0 | 0 | 0 | 0 | 0 | 0 | 0 | 0 | 0 | 0 | 0 | 0 | 0 |
| 7 | 0 | 0 | 0 | 0 | 0 | 0 | 0 | 0 | 0 | 0 | 0 | 0 | 0 | 0 | 0 | 0 | 0 | 0 | 0 | 0 | 0 | 0 | 0 | 0 |
| 8 | 1 | 1 | 1 | 1 | 1 | 1 | 1 | 1 | 1 | 1 | 1 | 1 | 1 | 1 | 1 | 1 | 1 | 1 | 1 | 1 | 1 | 1 | 1 | 1 |
| 9 | 1 | 1 | 1 | 1 | 1 | 1 | 1 | 1 | 1 | 1 | 1 | 1 | 1 | 1 | 1 | 1 | 1 | 1 | 1 | 1 | 1 | 1 | 1 | 1 |
| 10 | 0 | 0 | 0 | 0 | 0 | 0 | 0 | 0 | 0 | 0 | 0 | 0 | 0 | 0 | 0 | 0 | 0 | 0 | 0 | 0 | 0 | 0 | 0 | 0 |
| 11 | 0 | 0 | 0 | 0 | 0 | 0 | 0 | 0 | 0 | 0 | 0 | 0 | 0 | 0 | 0 | 0 | 0 | 0 | 0 | 0 | 0 | 0 | 0 | 0 |
| 12 | 0 | 0 | 0 | 0 | 0 | 0 | 0 | 0 | 1 | 1 | 1 | 1 | 1 | 1 | 1 | 1 | 1 | 1 | 1 | 1 | 1 | 1 | 1 | 0 |
| 13 | 0 | 0 | 0 | 0 | 0 | 0 | 0 | 0 | 0 | 0 | 0 | 0 | 0 | 0 | 0 | 0 | 0 | 0 | 0 | 0 | 0 | 0 | 0 | 0 |
| 14 | 0 | 0 | 0 | 0 | 0 | 0 | 0 | 0 | 0 | 0 | 0 | 0 | 0 | 0 | 0 | 0 | 0 | 0 | 0 | 0 | 0 | 0 | 0 | 0 |
| 15 | 1 | 1 | 1 | 1 | 1 | 1 | 1 | 1 | 1 | 1 | 1 | 1 | 1 | 1 | 1 | 1 | 1 | 1 | 1 | 1 | 1 | 1 | 1 | 1 |
| 16 | 0 | 0 | 0 | 0 | 0 | 0 | 0 | 0 | 0 | 0 | 0 | 0 | 0 | 0 | 0 | 0 | 0 | 0 | 0 | 0 | 0 | 0 | 0 | 0 |
| 17 | 0 | 0 | 0 | 0 | 0 | 0 | 0 | 0 | 0 | 0 | 0 | 0 | 0 | 0 | 0 | 0 | 0 | 0 | 0 | 0 | 0 | 0 | 0 | 0 |
| 18 | 0 | 0 | 0 | 0 | 0 | 0 | 0 | 0 | 0 | 0 | 0 | 0 | 0 | 0 | 0 | 0 | 0 | 0 | 0 | 0 | 0 | 0 | 0 | 0 |
| 19 | 0 | 0 | 0 | 0 | 0 | 0 | 0 | 0 | 0 | 0 | 0 | 0 | 0 | 0 | 0 | 0 | 0 | 0 | 0 | 0 | 0 | 0 | 0 | 0 |
| 20 | 1 | 1 | 1 | 1 | 1 | 1 | 1 | 1 | 1 | 1 | 1 | 1 | 1 | 1 | 1 | 1 | 1 | 1 | 1 | 1 | 1 | 1 | 1 | 1 |
| 21 | 0 | 0 | 0 | 0 | 0 | 0 | 0 | 0 | 0 | 0 | 0 | 0 | 0 | 0 | 0 | 0 | 0 | 0 | 0 | 0 | 0 | 0 | 0 | 0 |
| 22 | 0 | 0 | 0 | 0 | 0 | 0 | 1 | 1 | 1 | 1 | 1 | 1 | 1 | 1 | 1 | 1 | 1 | 1 | 1 | 1 | 1 | 1 | 1 | 1 |
| 23 | 1 | 1 | 1 | 1 | 1 | 1 | 1 | 1 | 1 | 1 | 1 | 1 | 1 | 1 | 1 | 1 | 1 | 1 | 1 | 1 | 1 | 1 | 1 | 1 |

(b) $\Gamma^A_{t\leq 8} = 2$

Figure 12: The commitment status in two instance with single uncertainty set

this case different generator have been active due to the realization of worst case. The commitment schedule in case $\Gamma^A_{6\leq t\leq 18} = 2$ is more similar to the optimistic case, simply because most of the uncertainty instances are forced to occur during the time that the generators were on based on the optimistic approach. Of course, this case will incur higher cost due to the longer period of time affected by weather volatility; the total cost and load shed in this case are 7% and 14% higher than the case with $\Gamma^A_{t\leq 8} = 2$. This observation indicate the high portion of fuel cost in the total power generation cost.

### 3.5.2 Demand and Temperature Correlation

The join uncertainty realizations is tested on single power system in Florida. The information presented in this document has been slightly changed for confidentiality purposes. Table 4 provides the information about the 11 gas generators at TECO which have been

used in our experiments, and Figure 13 depicts the forecasted demand vs weather prediction for a summer day. We have considered a time lag of 2 hours in the study, and stopped the model after 10 minutes. Figure 14 presents the result of running the robust model when both the uncertainties vary in the range of [0,4]. When either uncertainty factor is at 0, the problem can be solved to optimality, while the other cases provide an approximation for the total cost. As you can see, the demand uncertainty can increase the cost up to 3.3%, while this rate is 2.4% for temperature uncertainty. This observation illustrates that temperature uncertainty, while widely neglected, can be a source of congestion and blackouts. Moreover, the combination of two uncertainties leave the system vulnerable by up to 6.4%.

Unit commitment problem is NP-hard and computationally challenging. As you can see in Table 5, while the $C\&CG$ algorithm is very efficient and can solve the two-stage robust problems in a few iterations, in the correlated cases after 10 minutes the gap has not be completely closed.

Table 4: Parameters of gas generators in a single power system

| Gen. | G1 | G2 | G3 | G4- G6 | G7 | G8 | G9-G11 |
|---|---|---|---|---|---|---|---|
| $u$ | 32 | 130 | 135 | 32 | 32 | 275 | 105 |
| $l$ | 57 | 710 | 940 | 57 | 57 | 290 | 155 |
| $m_+$ | 6 | 4 | 4 | 6 | 6 | 2 | 2 |
| $m_-$ | 2 | 1 | 1 | 2 | 2 | 1 | 1 |
| $\Delta_{+/-}$ | 57 | 267 | 267 | 57 | 57 | 120 | 160 |
| $\hat{\text{CS}}$ | 18000 | 13000 | 16000 | 15000 | 10000 | 13000 | 19000 |
| $\hat{\text{CN}}$ | 134 | 178 | 100 | 113 | 113 | 112 | 112 |
| $\hat{\text{CF}}$ | 537 | 2633 | 2751 | 601 | 601 | 6139 | 1934 |
| | 684 | 8110 | 10924 | 765 | 765 | 6283 | 2287 |
| | 836 | 15457 | 22697 | 933 | 933 | 6428 | 2653 |
| | 990 | 24673 | 38070 | 1104 | 1104 | 6574 | 3033 |

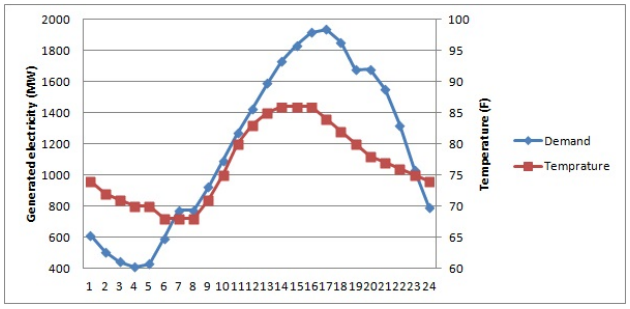


Figure 13: Demand and temperature forecast

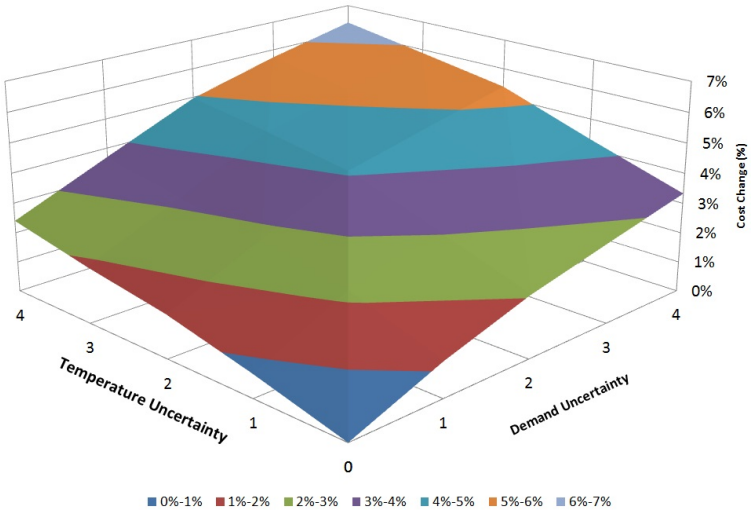


Figure 14: Impact of correlated temperature and demand uncertainty on cost

Table 5: C&CG algorithm performance on unit commitment

| | | $\Gamma^D$ | | | | |
|---|---|---|---|---|---|---|
| | | 0 | 1 | 2 | 3 | 4 |
| $\Gamma^A$ | 0 | | | | | |
| | 1 | | 0.06% | 0.04% | 0.07% | |
| | 2 | | | 0.04% | 0.07% | 0.08% |
| | 3 | | | 0.08% | 0.03% | 0.05% |
| | 4 | 0.11% | 0.08% | 0.06% | 0.08% | 0.03% |

## 3.6 Final Remarks

The generation and transmission systems are constrained by the capacities of the generators and transmission lines. Normally, these capacities are calculated statically which puts the system at risk of shortage and or congestion. In this chapter, we proposed a two-stage robust optimization unit commitment model and incorporated the dynamic rating concept into it. The uncertain elements in our model are the ambient air temperature and forecasted demand. The experiment results indicate the importance of investigating these factors as they lead to different commitment schedule.

# CHAPTER 4: ROBUST JOB SCHEDULING WITH UNCERTAIN LOCAL GENERATION IN SMART BUILDINGS[1]

## 4.1 Background

Distributed energy generation has gained a significant popularity over the last few years. Typical examples include solar panels on the roofs and small wind turbines for buildings in remote areas. Such locally generated energies can be consumed and stored on-site, or possibly sold back to the grid. Moreover, restructuring of the power system and emergence of smart grids have enabled end-consumers to receive timely price information. With this information, consumers can manage their load by transferring flexible jobs or tasks (i.e., electricity-consuming applications) to *off-peak* hours to avoid expensive peak-time charges [49]. Clearly, it would be more beneficial for consumers to arrange their jobs by jointly considering both local generation and price information.

Although providing more accurate and frequent price information allows for more *informed* decision makings about the energy consumption, it does not seem realistic to expect consumers to be willing and able to go through the information and make an optimal decision. As mentioned in [50], "while over 80% of consumers are very interested in being able to cut their energy costs, less than one-half want to learn more about smart grids". So in order to benefit the most, consumers must be provided with state-of-the-art hardware and software

[1]This chapter was partially published in [1]. Permission is included in Appendix A.

such as communication devices and technologies, modern platforms, and an automatic and reliable scheduler/planner that takes electricity price and local generation information.

Due to the complicated nature and various requirements in job scheduling problem, e.g., complex jobs' specifications as well as the logical relationships between them, it is very challenging to develop and implement a reliable model in the scheduler. Over the past few years, many models and scheduling methods have been proposed to generate cost-effective schedules for both residential and industrial applications. Generally, there are three types of scheduling models. The first type consists of basic deterministic scheduling models solved by exact or heuristic algorithms ([51, 52, 53, 54, 55, 56, 57, 58, 59, 60]). For example, deterministic mixed integer programming formulations are developed in [53, 55] for a set of home appliances and solved by existing solver packages. Due to the complexity of scheduling problem, sequential approximation [51] and ranking based heuristics [56] are developed for fast computing. A more complicated industrial job scheduling formulation is presented in [58] where a genetic algorithm is developed and tested. The second type extends from deterministic models and develops more sophisticated scheduling formulations to consider random demand and distributed generation from solar panels or wind turbines ([61, 62, 63, 64]). For example, [61] considers random load within an industrial environment and investigates load control through Monte Carlo simulation. More analytical models using stochastic programming approaches are developed for home appliances in [62, 63] where random scenarios are used to capture the randomness in loads. The last type is price-based load control methods ([65, 66, 67, 68]) that dynamically adjust job schedules given real-time

price information. An analytical dynamic-programming-based control method is presented in [67] and solved by a Q-learning algorithm. Similar stochastic control model is also developed for multiple households in [68], and an online Lyapunov-based cost minimization algorithm is designed.

Traditionally, stochastic scheduling models capture the randomness in local generation or demand by probabilistic scenarios ([63, 64, 67]). However, because of the inconsistent patterns of many data sets, it is often difficult to obtain the probability distribution, or additionally, the obtained information might not be reliable, like inaccurate local generation forecasts. Given an unreliable forecast, the optimal schedule from a stochastic programming model may still leave the consumer vulnerable to an unexpectedly-high electricity bill. To eliminate this possibility, robust optimization models, which simply use uncertainty sets to capture randomness, are adopted to solve operational problems in power systems [69, 70, 40]. In particular, we observe that two-stage robust optimization provides a flexible modeling framework to deal with multi-period scheduling problem. For example, in the study of two-stage robust unit commitment problems [69, 70, 40], which are essentially machine scheduling problems, generators' (i.e., machines') on/off status must be determined ahead of time as the first-stage decisions and their generation levels can be adjusted in the second stage after the random load or renewable generation is revealed. It is noted that two-stage robust models are more aligned with reliability considerations to hedge against randomness [71].

As demonstrated in [72, 73, 74], there are many situations where scheduling of jobs in residential and industrial building environments can be made in two different stages or scales.

For residential houses, on one hand, we observe that some activities or tasks/jobs, such as the lengthy jobs, e.g., electrical vehicle charging; those undertaken by external workers or professionals, e.g., pest control, carpet cleaning, pump or AC reparation; and the multi-family activities, e.g., neighborhood parties, must be determined ahead of time as "here-and-now" decision. On the other hand, many small-scale jobs, e.g., laundry, ironing, or entertainment activities are more flexible and deferrable. Then, as in [53], and [56], we can schedule them according to price information and the revelation of local generation, as "wait-and-see" decisions. Similarly, in service industry, such as hotels, convention centers, and warehouses, some jobs, e.g., maintenance or large-scale events, should be scheduled ahead of time. Other jobs, e.g., cleaning, small-scale events, and ventilation, are more flexible and deferrable to a near real-time scheduling.

One may think it is possible to decompose job scheduling issue into two disjoint decision problems for the aforementioned stages respectively. Nevertheless, overlooking the logical relationships among those tasks/jobs significantly reduces their scheduling flexibility and can lead to expensive job schedules. For example, the pest control task needs to be performed after an entertainment activity for a safety consideration. If we ignore precedence relationship in scheduling the pest control task, either we may not be able to arrange the entertainment activity or it will be done during a period with a high price and low local generation.

Noting the advantage of robust optimization in dealing with randomness, a robust scheduling model is developed in [72] and implemented in a rolling-horizon fashion for real-time scheduling. Note that the model is a single-stage robust model, which is overly con-

servative and generally produces costly solutions. With current progress in modeling and solution aspects of two-stage robust optimization, we develop a two-stage robust scheduling model for tasks/jobs scheduling in a building environment with time-of-use price information and uncertain local generation, to minimize energy cost. Specifically, our two-stage scheduling model has the following features:

- It considers two sets of jobs: the first set includes the jobs that must be scheduled ahead of time and the second set includes jobs that are flexible and deferrable for real-time scheduling;
- Each job can have multiple modes with different durations and energy consumptions;
- Some jobs are interruptible, while some other ones are not. Considering these job characteristics makes the model applicable for both residential and industrial settings;
- If distributed generation is more than enough, it can be sold back to the grid.

To the best of our knowledge, the presented two-stage robust scheduling model is the first two-stage robust optimization formulation for the job scheduling problem. In particular, due to the nature of scheduling problem, it carries discrete (binary) variables in the second-stage decision problem, which places our model as one of the first robust formulations with a mixed integer program (MIP) in the second stage. To solve this complicated formulation, we prove some properties and then employ a novel algorithm, the *nested column-and-constraint generation* (NC&CG) method [75], to find an optimal solution. As a result, this chapter presents a decision support tool, including both the scheduling formulation and the solution

algorithm, for consumers to manage their activities, risks and financial benefits in an uncertain environment. We recognize that when randomness can be well captured by stochastic scenarios or decision makers are less sensitive towards risks, stochastic scheduling models are appropriate.

This chapter is organized as follows: Section 4.2 describes the formulation, including both the deterministic model and its robust counterpart; section 4.3 describes the exact solution approach; the computational results, along with some discussion are shown in Section4.4; and finally section 6 concludes the chapter.

## 4.2 Mathematical Model

Table 6: Nomenclature used in chapter 4

| Symbol | Meaning |
|---|---|
| **Index Sets** | |
| $n$ | Time period, $n = 0, ..., N-1$ |
| $i$ | Job, $i = 0, ..., I-1$ |
| $k$ | Working mode, $k = 0, ...., K-1$ |
| $t$ | Segment of job $i$ in mode $k$, $t = 0, ..., L_{ik}-1$ |
| **Parameters** | |
| $C_n^b$ | Base electricity price at time $n$ |
| $C_n^e$ | Non-base electricity price at time $n$ |
| $A_i$ | Earliest start time for job $i$ |
| $B_i$ | Due time for job $i$ |
| $\mathbb{P}^G$ | Uncertainty set of local generation |
| $L_{ik}$ | Length of job $i$ in mode $k$ |
| $D_{ikt}$ | Workload of job $i$ in mode $k$ at segment $t$ |
| $P_n^{max}$ | Consumption limit at base price at time $n$ |
| $R_i$ | Whether job $i$ is interruptible or not |
| $nrho_n$ | The ratio of selling price to base purchase price at time period $n$, $(0 < \rho_n < 1)$ |
| $Pr_i$ | The set of precedents of job $i$ |
| **Decision variables** | |
| $\theta_{iktn}$ | Binary variable, 1 if the segment $t$ in mode $k$ of job $i$ is assigned to period $n$ |
| $y_{ik}$ | Binary variable, 1 if job $i$ runs in mode $k$ |

Table 6 (continued)

| Symbol | Meaning |
|---|---|
| $s_n$ | Continuous variable, extra generation at period $n$ |
| $w_n^b$ | Billed consumption at a base price at time $n$ |
| $w_n^e$ | Billed consumption at an extra price at time $n$ |
| $p_n^G$ | Local generation at time period $n$ |

### 4.2.1 Deterministic Model

We consider an electricity market in which the local generation, owned by a prosumer, is from a renewable energy source, of no cost and can be sold back to the grid at a price lower than purchase price. In each time period, a prosumer will make a purchase if the local generation is not sufficient, and will sell electricity back to the grid in case of extra generation. We consider a step-wise price structure ([52, 76]), also known as inclining block rate (IBR) [77], where the unit/base price, $C_n^b$, is applied if the amount of power purchased is less than a predefined level, $P_n^{max}$. A higher price, $C_n^e$, will be applicable for the amount of purchase above $P_n^{max}$.

The following job characteristics are factored into our model formulation:

- There is a time window (i.e., earliest start time $A_i$ and due time $B_i$) for a job $i$.
- There are multiple modes for each job $i$ with corresponding length $L_{ik}$ and workload distribution $D_{ikt}$; e.g., a cooking appliance will have two modes, slow cooking or regular cooking.
- Precedent relationships existing between jobs are observed.
- Some jobs need to be scheduled ahead of time, while the decisions for other jobs could be made during the day.

- Some jobs are interruptible like HVAC, charging or ironing, while others have to be completed without interruption, such as running a dish washer.
- The segments of a job $i$ should be scheduled in order (i.e., a job segment can only be executed if all the previous segments are finished).

Given a fixed hourly local generation, $p_n^G$, the deterministic scheduling problem is formulated as follows:

$$\min \sum_{n=0}^{N-1}(w_n^b C_n^b + w_n^e C_n^e - \rho_n C_n^b s_n) \tag{4.1}$$

$$st. \sum_{t=0}^{L_{ik}-1} \theta_{iktn} \leq y_{ik}, \ \forall i,k,n \tag{4.2}$$

$$\sum_{n=0}^{N-1} \theta_{iktn} = y_{ik}, \ \forall i,k,t \tag{4.3}$$

$$\sum_{n=0}^{u} \theta_{iktn} \geq \sum_{n=0}^{u} \theta_{ikt'n}, \forall i,k,t,t' \geq t, u = 0,...,N-1 \tag{4.4}$$

$$\theta_{iktn} \leq \sum_{n'=n+1}^{N-1} \theta_{ikt'n'}, \ \forall i,k,t,t' \geq t+1,n \tag{4.5}$$

$$\sum_{k=0}^{K-1} y_{ik} = 1, \ \forall i \tag{4.6}$$

$$\sum_{n=0}^{N-1} n \sum_{k=0}^{K-1} \theta_{ik0n} \geq A_i, \ \forall i \tag{4.7}$$

$$\sum_{n=0}^{N-1} n \sum_{k=0}^{K-1} \theta_{ik,L_{ik}-1,n} \leq B_i, \ \forall i \tag{4.8}$$

$$\sum_{n=0}^{N-1} n \sum_{k=0}^{K-1} \theta_{ik,L_{ik}-1,n} - \sum_{n=0}^{N-1} n \sum_{k=0}^{K-1} \theta_{ik0n} \leq R_i N + \sum_{k=0}^{K-1}(L_{ik}-1)y_{ik}, \ \forall i \tag{4.9}$$

$$\sum_{n=0}^{N-1} n \sum_{k=0}^{K-1} \theta_{ik,L_{ik}-1,n} + 1 \leq \sum_{n=0}^{N-1} n \sum_{k=0}^{K-1} \theta_{jk0n}, \forall i,j \in Pr_i \tag{4.10}$$

$$\sum_{i=0}^{I-1}\sum_{k=0}^{K-1}\sum_{t=0}^{L_{ik}-1} d_{ikt}\theta_{iktn} \leq P_n^{max} + w_n^e + p_n^G,\ \forall n \tag{4.11}$$

$$w_n^b - s_n \geq \sum_{i=0}^{I-1}\sum_{k=0}^{K-1}\sum_{t=0}^{L_{ik}-1} d_{ikt}\theta_{iktn} - p_n^G - w_n^e,\ \forall n \tag{4.12}$$

$$w_n^b, w_n^e, s_n \geq 0, \theta_{iktn}, y_{ik} \in \{0,1\} \tag{4.13}$$

The objective (4.1) is to minimize total cost from purchase at base or extra rate. The profit from selling local generation back to the grid is considered as a negative cost. Constraint set (4.2) indicates that each time period $n$ can only accommodate one segment of each job $i$ in its active mode (i.e., two segments of one job cannot be scheduled in one time period $n$). Constraint set (4.3) ensures that all segments of a job are scheduled exactly once. Constraint set (4.4) assures each job is scheduled in the right order. Constraint set (4.5) makes sure that a job segment can only be executed if the previous segments are finished. E.g., if the LHS of (4.5) is 1 (the segment $t$ is assigned to period $n$), the RHS will be forced to be 1 (the proceeding segments must be scheduled after $n$). Constraint set (4.6) guarantees that only one mode is selected for a job. Constraint sets (4.7)-(4.8) introduce each job's time window. Constraint set (4.9) states if the job $i$ is not interruptible (i.e., $R_i = 0$), the time between its start and finish time, is exactly equal to its length, forcing it to run without interruption. Constraint set (4.10) represents the precedent relationships existing between jobs. Constraint sets (4.11) and (4.12) capture energy balance as well as the impact of step-wise price on energy consumption. Let $f_n$ represent total consumption at time $n$, i.e., $f_n = \sum_i \sum_k \sum_t d_{ikt}\theta_{iktn}$. The following three cases are the possibilities for total cost:

- If the local generation is enough for the demand in time $n$ ($f_n \leq p_n^G$), the $w_n^e$ will be forced to be zero by the objective function and $w_n^b$ will be zero by (4.12), resulting in no charge. In this case $s_n$ will take a value equal to the excess generation so the owners earn some money by selling their extra generation at a lower price than the market's;
- If $0 \leq f_n - p_n^G \leq P_n^{max}$, the $w_n^e$ will, again, be forced to be zero, $w_n^b = f_n - P_n^G$ and $s_n = 0$ by constraint sets (4.12). In this case we pay at base rate;
- If $f_n - p_n^G \geq P_n^{max}$, constraint (4.11) will become active with $w_n^e \geq 0$ and $w_n^b$ will be forced to be $P_n^{max}$. Thus, we pay at both base and extra rates.

### 4.2.2 Two-stage Robust Counterpart

Although the deterministic model can help the consumers schedule their jobs, the randomness and intermittency in the distributed local generation (e.g., the power from solar panels) decreases its accuracy drastically. Moreover, the probability information corresponding to local generation is often unreliable, which diminishes the utility of stochastic programming. In order to improve the accuracy, we develop a robust optimization model in which the randomness in local generation is represented by a general polyhedron denoted by $\mathbb{P}^G$.

As mentioned previously, all jobs are partitioned into two sets, $J$ and $H$, based on when their schedules are determined, denoted as *job determination time*. Specifically, the mode selection and schedule of each job in set $J$ needs to be determined ahead of time (i.e., in the first stage). The decision regarding the rest of the jobs in set $H$ (i.e., recourse problem) is made in real time, after the first-stage decision is made and the information of

the uncertain distributed local generation is revealed. The two-stage robust counterpart, also called *adjustable* or *adaptable* robust optimization formulation ([78, 69]), is as follows:

$$\inf_{\{\theta_{jktn},y_{jk}\}\in\Psi^J} \sup_{p^G\in\mathbb{P}^G} \inf_{\{\theta_{hktn},y_{hk},w^b,w^e,s_n\}\in\Phi} (4.1) \tag{4.14}$$

$$\Psi^J = \{(4.2)-(4.10), \theta_{jktn}, y_{jk} \in \{0,1\}, \forall j,k,t,n\}$$

$$\Psi^H = \{(4.2)-(4.10), \theta_{hktn}, y_{hk} \in \{0,1\}, \forall h,k,t,n\}$$

$$\Phi = \Psi^H \bigcap \{(4.11)-(4.12)\}$$

Similar to Proposition 1 in Chapter 3, one can show that the two-stage robust optimization problem defined in (4.14) can be rewritten as follows:

$$\min_{\{\theta_{jktn},y_{jk}\}\in\Psi^J} \max_{p^G\in\mathbb{P}^G} \min_{\{\theta_{hktn},y_{hk},w^b,w^e,s_n\}\in\Phi} (4.1) \tag{4.15}$$

When $\mathbb{P}^G$ is a general polyhedron set, such reduction may not be valid and the optimality may not be achievable. Nevertheless, we can always achieve an $\varepsilon$-optimal solution for any $\varepsilon > 0$, which is generally sufficient for engineering applications.

### 4.3 Exact Solution Approach

The majority of the existing algorithms applied on two-stage RO essentially depend on the strong duality of the recourse problem. Thus, these algorithms cannot be applied to problems with discrete recourse problem such as our proposed two-stage robust model (with binary variables $\theta_{hktn}, y_{hk}$ in the second stage). Because of its two-stage nature, a few two-

level algorithms are used to solve this type of problems (see [40, 69]). A recent algorithm, called the "Nested Column-and-Constraint Generation" ($NC\&CG$) method [79], extends the column-and-constraint generation ($C\&CG$) algorithm ([40, 80]) for two-stage RO and is proven to be effective in dealing with MIP recourse problems. Therefore, it is adopted in this chapter to solve the two-stage robust scheduling problem. The detailed mathematical derivations, proofs and analysis of this algorithm are referred to [79]. A general overview of this algorithm is presented in Figure 15. For completeness, we first present the kernel formulations in subsection 4.3.1 and 4.3.2, then we provide a detailed description of the algorithm (for the outer level) and its performance analysis in subsection 4.3.3. The detailed formulations of inner level problems are omitted for simplicity, but the inner level algorithm description is provided in section 4.3.4.

### 4.3.1 Outer-Level Problem

The algorithm starts with a feasible schedule for the jobs in set $J$ (i.e., ahead of time jobs), which is fed to the inner-level problem. At each iteration, for a given first-stage decision, solving the inner-level problems gives the corresponding worst case local generation $\hat{p}^{G(m)}$. Then, extra variables $w_n^{b(m)}, w_n^{e(m)}, \theta_{hktn}^{(m)}, y_{hk}^{(m)}, s_n^{(m)}$ and the related constraints (4.17)-(4.28) are generated and added to the following formulation to find a better first-stage decision. Note that $\hat{p}^{G(m)}$ is a parameter in the outer-level problem.

$$\min \ \eta \tag{4.16}$$

$$st. \ \eta \geq \sum_{n=0}^{N-1} (w_n^{b(m)} C_n^b + w_n^{e(m)} C_n^e - \rho C_n^b s_n^{(m)}), \ \forall m \tag{4.17}$$

$$\sum_{t=0}^{L_{hk}-1} \theta_{hktn}^{(m)} \leq y_{hk}^{(m)},\ \forall h,k,n,m \tag{4.18}$$

$$\sum_{n=0}^{N-1} \theta_{hktn}^{(m)} = y_{hk}^{(m)},\ \forall h,k,t,m \tag{4.19}$$

$$\sum_{n=0}^{u} \theta_{iktn}^{(m)} \geq \sum_{n=0}^{u} \theta_{ikt'n}^{(m)}, \forall i,k,t,t' \geq t, u < N, m \tag{4.20}$$

$$\theta_{hktn}^{(m)} \leq \sum_{n'=n+1}^{N-1} \theta_{hkt'n'}^{(m)},\ \forall h,k,m,t,t' > t,n \tag{4.21}$$

$$\sum_{k=0}^{K-1} y_{hk}^{(m)} = 1,\ \forall m,h \tag{4.22}$$

$$\sum_{n=0}^{N-1} n \sum_{k=0}^{K-1} \theta_{hk0n}^{(m)} \geq A_h,\ \forall m,h \tag{4.23}$$

$$\sum_{n=0}^{N-1} n \sum_{k=0}^{K-1} \theta_{hk,L_{ik}-1,n}^{(m)} \leq B_h,\ \forall m,h \tag{4.24}$$

$$\sum_{n=0}^{N-1} n \sum_{k=0}^{K-1} \theta_{hk,L_{ik}-1,n}^{(m)} - \sum_{n=0}^{N-1} n \sum_{k=0}^{K-1} \theta_{hk0n}^{(m)} \leq R_h N + \sum_{k=0}^{K-1} (L_{hk}-1) y_{hk}^{(m)},\ \forall m,h \tag{4.25}$$

$$\sum_{n=0}^{N-1} n \sum_{k=0}^{K-1} \theta_{hk,L_{hk}-1,n}^{(m)} + 1 \leq \sum_{n=0}^{N-1} n \sum_{k=0}^{K-1} \theta_{h'k0n}(m), \forall h,h' \in Pr_h \tag{4.26}$$

$$\sum_{j} \sum_{k=0}^{K-1} \sum_{t=0}^{L_{jk}-1} d_{jkt}\theta_{jktn} + \sum_{h} \sum_{k=0}^{K-1} \sum_{t=0}^{L_{hk}-1} d_{hkt}\theta_{hktn}^{(m)} \leq P_n^{max} + w_n^{e(m)} + \hat{p}_n^{G(m)}, \forall m,n \tag{4.27}$$

$$\sum_{j} \sum_{k=0}^{K-1} \sum_{t=0}^{L_{jk}-1} d_{jkt}\theta_{jktn} - \hat{p}_n^{G(m)} - w_n^{e(m)} + \sum_{h} \sum_{k=0}^{K-1} \sum_{t=0}^{L_{hk}-1} d_{hkt}\theta_{hktn}^{(m)} \leq w_n^{b(m)} - s_n^{(m)},\ \forall m,n \tag{4.28}$$

$$\theta_{jktn}, y_{jk} \in \Psi^J,\ \forall j,k,t,n \tag{4.29}$$

$$w_n^{b(m)}, w_n^{e(m)}, s_n^{(m)} \geq 0,\ \theta_{hktn}^{(m)}, y_{hk}^{(m)} \in \{0,1\}, \tag{4.30}$$

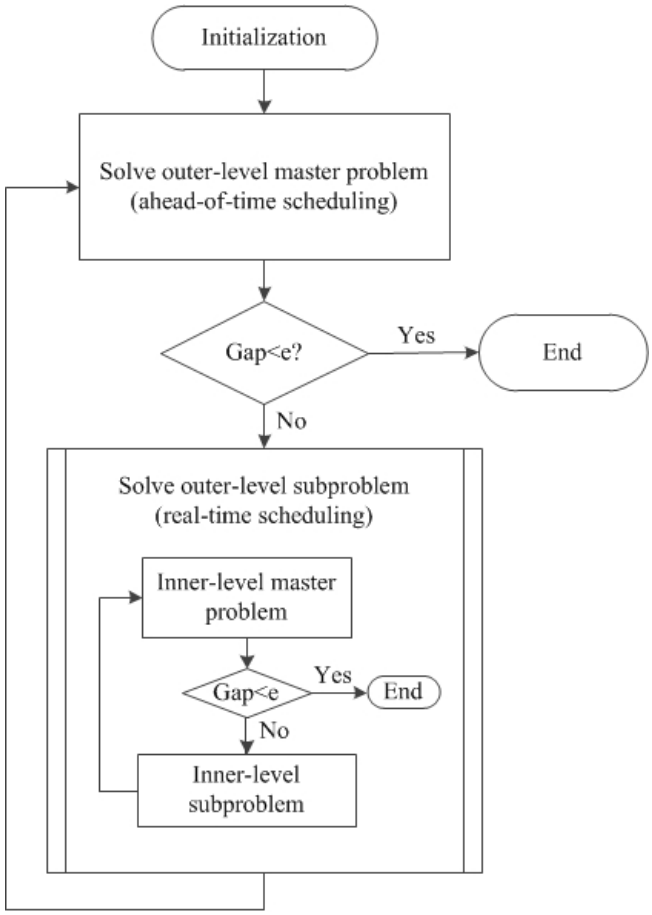


Figure 15: $NC\&CG$ algorithm steps

### 4.3.2 Inner-Level Problem

We solve the inner-level problem in order to obtain a worst case scenario of local generation given the first-stage decision. To be specific, given $\hat{\theta}_{jktn}, \hat{y}_{jk}$ for jobs in set $J$, the inner level problem is as follows:

$$\max_{p^G \in \mathbb{P}^G} \min_{\{\theta, y, w^b, w^e, s\}} (4.1) \tag{4.31}$$

$$st. \sum_{j} \sum_{k=0}^{K-1} \sum_{t=0}^{L_{jk}-1} d_{jkt} \hat{\theta}_{jktn} + \sum_{h} \sum_{k=0}^{K-1} \sum_{t=0}^{L_{hk}-1} d_{hkt} \theta_{hktn} \leq P_n^{max} + w_n^e + p_n^G, \ \forall n \tag{4.32}$$

$$w_n^b - s_n \geq \sum_j \sum_{k=0}^{K-1} \sum_{t=0}^{L_{jk}-1} d_{jkt}\hat{\theta}_{jktn} - p_n^G - w_n^e + \sum_h \sum_{k=0}^{K-1} \sum_{t=0}^{L_{hk}-1} d_{hkt}\theta_{hktn},\ \forall n \tag{4.33}$$

$$\theta_{hktn}, y_{hk} \in \Psi^H, w_n^b, w_n^e, s_n, p_n^G \geq 0,\ \forall h, t, k, n \tag{4.34}$$

By separating binary and continuous variables in the second stage, the above bi-level formulation can be converted into a tri-level equivalent formulation in the form of (4.35), along with constraints (4.32-4.34). Such a tri-level problem can be effectively solved using the classical Karush-Kuhn-Tucker (KKT) condition for the innermost linear programming problem with a $C\&CG$ implementation.

$$\max_{p^G \in \mathbb{P}^G} \min_{\{\theta, y\}} \min_{\{w^b, w^e, s\}} (4.1) \tag{4.35}$$

### 4.3.3 Outer-Level Algorithm

We provide a detailed description for the outer level procedure in algorithm 2 and prove its convergence. In the following algorithm description, $LB$ and $UB$ represent the lower bound and upper bound of the outer-level problem, respectively. $m$ tracks the number of iterations, and $l$ represents the set of explored extreme points.

**Proposition 2** *This algorithm converges to an optimal solution in finite steps.*

*Proof.* First, by observing that $\Psi^H$ is a finite set, the inner-level algorithm will converge in finite steps by Proposition 4 in [75]. Secondly, given that the inner level will find a worst case scenario in finite steps, the outer level algorithm will terminate with an optimal solution in finite steps based on Proposition 2 in [75]; the conclusion follows immediately. □

Note that although we use enumeration to prove finite convergence, the average number of iterations of both outer and inner algorithms is very small in practice. We show this in the numerical study in the next section.

**Step 0**

Set $LB = -\infty,\ UB = +\infty,\ m = 1,\ \{l\} = \emptyset$;

Solve the outer-level problem (4.16)-(4.30). Let $\theta^m$ denote the optimal first-stage decision.

**while** $\epsilon = (UB - LB)/UB$ *is greater than the tolerance* **do**

**Step** $m$**.(a)**

For a given $\theta^m$, use the $NC\&CG$ inner-level algorithm in section 4.3.4 to obtain the worst case uncertainty scenario $\hat{p}^{G(m)}$.

Update $\{l\} = \{l\} \bigcup \{m\}$ and $UB = \min\{UB, \text{inner-level problem objective}\}$.

**Step** $m$**.(b)**

Create extra variables $w_n^{b(m)}, w_n^{e(m)}, \theta_{hktn}^{(m)}, y_{hk}^{(m)}, s_n^{(m)}$ and add related constraints (4.17)-(4.28) with respect to $\hat{p}^{G(m)}$ to the outer-level problem.

Set $m = m + 1$, Solve the outer-level problem.

Update $\theta^m$ and $LB = \{\text{the objective value of the outer-level master problem}\}$

**end**

**Algorithm 2:** Outer-Level of $NC\&CG$ Algorithm

### 4.3.4 Inner-level Algorithm

We describe the inner-level algorithm 3 which is used to find a worst case scenario of the uncertainty set. Here, $LB'$ and $UB'$ represent the lower bound and upper bound of the inner-level problem, respectively. $r$ tracks the number of iterations, and set $q$ consists of the explored extreme points of the uncertainty set (i.e., local generation realization).

**Step 0**

Set $LB' = -\infty$, $UB' = +\infty$, and $\{q\} = \emptyset$.

Let $r = 1$. Pick an arbitrary point $p^{G(1)}$ in the uncertainty set.

**while** $\epsilon' = (UB' - LB')/UB'$ *is greater than the tolerance* **do**

**Step $r$.(a)**

For a revealed uncertainty set $p^{G(r)}$, solve the inner-level subproblem (i.e., $\{\theta_{hktn}, y_{hk} \in \Psi^H\}$), and obtain the optimal solution $\hat{\theta}^{(r)}_{hktn}, \hat{y}^{(r)}_{hk}$ in response to $p^{G(r)}$.

Update $\{q\} = \{q\} \bigcup \{r\}$ and

$LB' = \max\{LB', \text{the objective value of the subproblem}\}$.

**Step $r$.(b)**

Set $r = r + 1$. Create extra variables $w^{b(r)}_n, w^{e(r)}_n, s^{(r)}_n, \delta^{(r)}_n, \gamma^{(r)}_n$ and add related constraints with respect to $\hat{\theta}^{(r)}_{hktn}, \hat{y}^{(r)}_{hk}$ to the inner-level master problem and solve it. Let $p^{G(r)}$ denote its optimal solution.

Update $UB'$= the optimal objective value of the inner-level master problem.

**end**

pass $\hat{p}^{G(r)} = p^{G(r)}$ to the outer-level algorithm.

**Algorithm 3:** Inner-Level of $NC\&CG$ Algorithm

### 4.4 Numerical Results

We perform a set of experiments to investigate our two-stage robust scheduling model and the solution algorithm. The computation algorithm is implemented in C++ with CPLEX MIP solver. All experiments are performed on a PC desktop with Intel Core(TM) i7 2.93 GHz CPU and 8GB memory. Time limit is set to 3,600 seconds, and the tolerance gaps for both outer and inner level algorithms of $NC\&CG$ are set to $10^{-3}$.

The jobs in each group are divided into two categories: The ones that are scheduled ahead of time ($I_d$), and the ones that are scheduled after realization of uncertainty ($I_r$).

The experiments are, therefore, aptly named as $(I : I_d/I_r)$, where $I$ is the total number of jobs. The scheduling horizon is over $N = 12$ time periods (hours), from 8AM to 8PM. The consumption limit with the base price, $P_n^{max}$, is assumed to be 200 KW for all time periods. The base electricity prices in the planning horizon are adopted from [81] in winter season:

- 11.7 (cents/KWh) for the *on-peak* periods (8AM-11AM, 5PM-7PM),
- 10.0 (cents/KWh) for the *mid-peak* periods (11AM-5PM),
- 6.5 (cents/KWh) for the *off-peak* periods (7PM-8PM).

The non-base or extra electricity price is assumed to be three times the base price, i.e., $c_n^e = 3c_n^b \ \forall n$. When extra electricity is available from the local generation, it can be sold back to the grid with $\rho = 80\%$.

To capture the randomness in local generation, similar to [69] and [70], we adopt a hypercube with a budget constraint to represent the uncertainty set of the local generation, i.e., $p_n^G = \underline{p}_n^G + \zeta_n \tilde{p}_n^G, \zeta_n \in [0,1] \ \forall n$ and $\sum_n \zeta_n \geq \Gamma$ where $\Gamma$ is an *uncertainty budget* to reflect decision maker's level of conservativeness. In the numerical study, the forecasted local generation, $\underline{p}_n^G$, is randomly generated following a bell shape (in the range of [15,90]) over time so that peak values are achieved around mid-day. We consider different forecasting variation levels in the form of $\tilde{p}_n^G = \alpha\% \underline{p}_n^G$.

### 4.4.1 Management Insights

In order to investigate the impact of job determination times, i.e., the impact of ahead-of-time and real-time scheduling, we consider two variants of a total of 10 jobs (the first ten jobs in Table 7) with different number of jobs for real-time scheduling. In the first variant,

seven jobs must be determined ahead of time (and the remaining three are scheduled after uncertainty of distributed local generation is revealed, aptly named $(10 : 7/3)$. In the second variant the decision about the first five must be determined ahead of time, and the position of later five is determined in real time, i.e., $(10 : 5/5)$. Table 7 provides all the jobs that are used in the experiments with their characteristics. Jobs (1-10), (1-15), and (1-20) are respectively used in experiments $(10 : I_d/I_r)$, $(15 : I_d/I_r)$, and $(20 : I_d/I_r)$.

Earliest start time and due time values are randomly generated in the ranges of [0, 4] and [7,12], respectively. Nine out of 20 jobs are randomly selected to be interruptible, and six out of 20 jobs are picked to have a precedent. Load distribution values are randomly generated in [0, 100]. We continue until we reach to a negative value. The number of segments of each job in each of its modes, $L_{ik}$, its total load and hourly load distribution are also provided in Table 7. In total, the 20 instances and their numerical result, including the computation time and objective value in the worst cases are listed in Table 8. Based on these results, we observe that:

- Due to the possible selling opportunity, the objective function is decreasing with respect to $\Gamma$; i.e., the worst case cost decreases when $\Gamma$ increases (more local generation is forecasted optimistically). If the consumer could not sell the extra generation to the market, then the cost would be non-increasing;
- Job determination time could affect total costs. The reason is that the mode selection and scheduling of real-time jobs can be adjusted according to actual uncertainty realizations, so the consumers can benefit from the more information they get.

- As mentioned in section 4.3.3, the average number of iterations is small. Figure 16 depicts the longest computation time among the 20 instances.

Table 7: Parameters of all 20 jobs

| **Job** | $A_i$ | $B_i$ | $R_i$ | **precedent** | **K** | $L_{ik}$ **(h)** | **Total Load (MWh)** | $D_{ikt}$ **(MWh)** | | | | | | |
|---|---|---|---|---|---|---|---|---|---|---|---|---|---|---|
| **1** | 8 | 20 | 1 | - | 0 | 5 | 510 | 150 | 120 | 120 | 60 | 60 | | |
| | | | | | 1 | 3 | 510 | 150 | 180 | 180 | | | | |
| **2** | 9 | 20 | 1 | 1 | 0 | 5 | 532.5 | 112.5 | 105 | 105 | 105 | 105 | | |
| | | | | | 1 | 4 | 525 | 150 | 135 | 135 | 105 | | | |
| **3** | 8 | 19 | 0 | - | 0 | 6 | 295 | 100 | 45 | 45 | 45 | 45 | 15 | |
| | | | | | 1 | 4 | 305 | 125 | 75 | 60 | 45 | | | |
| **4** | 8 | 20 | 0 | - | 0 | 6 | 267.5 | 87.5 | 45 | 45 | 30 | 30 | 30 | |
| | | | | | 1 | 4 | 300 | 75 | 75 | 75 | 75 | | | |
| **5** | 9 | 19 | 1 | - | 0 | 6 | 245 | 50 | 45 | 45 | 45 | 45 | 15 | 15 |
| | | | | | 1 | 3 | 267.5 | 87.5 | 75 | 105 | | | | |
| **6** | 10 | 20 | 0 | - | 0 | 6 | 282.5 | 87.5 | 75 | 45 | 45 | 15 | 15 | |
| | | | | | 1 | 3 | 275 | 125 | 105 | 45 | | | | |
| **7** | 10 | 18 | 0 | 6 | 0 | 3 | 177.5 | 87.5 | 45 | 45 | | | | |
| | | | | | 1 | 2 | 165 | 75 | 90 | | | | | |
| **8** | 8 | 20 | 0 | - | 0 | 5 | 362.5 | 62.5 | 75 | 75 | 75 | 75 | | |
| | | | | | 1 | 4 | 295 | 100 | 75 | 75 | 45 | | | |
| **9** | 8 | 19 | 1 | - | 0 | 6 | 202.5 | 37.5 | 45 | 30 | 30 | 30 | 30 | |
| | | | | | 1 | 2 | 217.5 | 112.5 | 105 | | | | | |
| **10** | 9 | 20 | 1 | 9 | 0 | 4 | 357.5 | 87.5 | 90 | 90 | 90 | | | |
| | | | | | 1 | 4 | 372.5 | 87.5 | 120 | 120 | 45 | | | |
| **11** | 9 | 19 | 0 | - | 0 | 5 | 190 | 68 | 44 | 44 | 27 | 7 | | |
| | | | | | 1 | 3 | 211 | 82 | 70 | 59 | | | | |
| **12** | 8 | 20 | 0 | - | 0 | 5 | 272 | 99 | 70 | 58 | 28 | 17 | | |
| | | | | | 1 | 4 | 268 | 100 | 72 | 59 | 37 | | | |
| **13** | 8 | 19 | 0 | 12 | 0 | 4 | 214 | 92 | 67 | 40 | 15 | | | |
| | | | | | 1 | 3 | 199 | 83 | 68 | 48 | | | | |
| **14** | 8 | 20 | 1 | - | 0 | 6 | 163 | 50 | 30 | 28 | 24 | 19 | 12 | |
| | | | | | 1 | 4 | 186 | 86 | 46 | 37 | 17 | | | |
| **15** | 11 | 20 | 1 | - | 0 | 5 | 184 | 66 | 54 | 36 | 14 | 14 | | |
| | | | | | 1 | 4 | 208 | 84 | 65 | 37 | 22 | | | |
| **16** | 9 | 15 | 0 | - | 0 | 2 | 76 | 38 | 38 | | | | | |
| | | | | | 1 | 1 | 86 | 86 | | | | | | |
| **17** | 10 | 20 | 1 | 16 | 0 | 4 | 138 | 63 | 41 | 20 | 14 | | | |
| | | | | | 1 | 3 | 160 | 64 | 59 | 37 | | | | |
| **18** | 8 | 20 | 1 | - | 0 | 5 | 263 | 93 | 68 | 58 | 28 | 16 | | |
| | | | | | 1 | 4 | 297 | 100 | 85 | 69 | 43 | | | |
| **19** | 9 | 19 | 0 | - | 0 | 3 | 112 | 55 | 39 | 18 | | | | |
| | | | | | 1 | 2 | 161 | 90 | 71 | | | | | |
| **20** | 8 | 20 | 0 | 19 | 0 | 5 | 134 | 55 | 31 | 26 | 12 | 10 | | |
| | | | | | 1 | 4 | 141 | 71 | 42 | 18 | 10 | | | |

Table 8: The experiment result

| Case | Forecasting Var. | Γ | Time (s) | Obj Value ($) | Itrs. |
|---|---|---|---|---|---|
| **10: 7/3** | $\tilde{p}_n^G = 20\%\overline{p}_n^G$ | 1 | 47.203 | 284.185 | 2 |
| | | 2 | 51.946 | 283.483 | 2 |
| | | 3 | 60.016 | 282.781 | 2 |
| | | 4 | 553.361 | 281.494 | 3 |
| | | 5 | 1079.24 | 280.194 | 4 |
| | $\tilde{p}_n^G = 40\%\overline{p}_n^G$ | 1 | 47.303 | 283.6 | 2 |
| | | 2 | 61.548 | 282.196 | 2 |
| | | 3 | 369.613 | 280.592 | 3 |
| | | 4 | 763.221 | 277.792 | 4 |
| | | 5 | 1561.53 | 274.195 | 5 |
| **10: 5/5** | $\tilde{p}_n^G = 20\%\overline{p}_n^G$ | 1 | 42.741 | 284.185 | 3 |
| | | 2 | 214.521 | 283.483 | 3 |
| | | 3 | 309.678 | 282.781 | 3 |
| | | 4 | 654.481 | 281.494 | 4 |
| | | 5 | 320.506 | 280.194 | 3 |
| | $\tilde{p}_n^G = 40\%\overline{p}_n^G$ | 1 | 174.731 | 283.6 | 3 |
| | | 2 | 223.678 | 282.123 | 3 |
| | | 3 | 1347.85 | 280.612 | 4 |
| | | 4 | 1941.72 | 277.558 | 4 |
| | | 5 | 2264.32 | 273.326 | 4 |

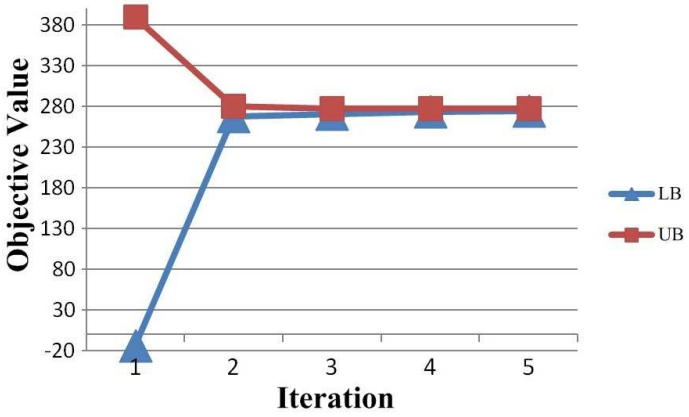


Figure 16: Upper bound and lower bound vs. iteration in the worst case (the case of $(10:7/3)$, $\Gamma = 5$, and 40% uncertainty variation)

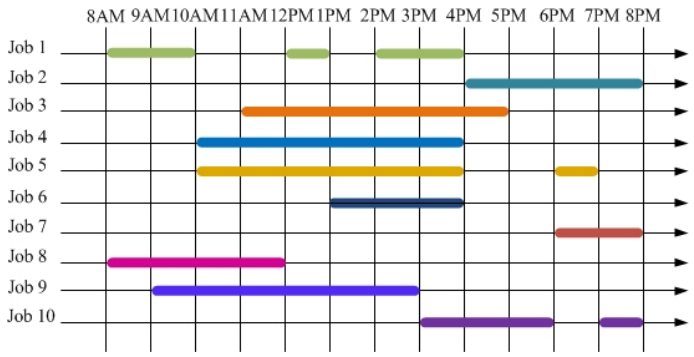


Figure 17: Detailed schedule for the case of $(10 : 7/3)$, $\Gamma = 2$, and 20% uncertainty variation

The detailed schedule of a $(10 : 7/3)$ instance with $\Gamma = 2$ and 20% variation can be seen in Figure 17. Figure 18 represents the corresponding total load in each period based on the optimal schedule, and shows the contribution of local generation and purchased energy at base and extra prices. In this example, jobs $\{1, 3, 4, 5, 6, 10\}$ are scheduled to be running in modes 0 and the remaining jobs are to be performed in their mode 1. As seen in the Gantt chart (Figure 17), we still have some jobs $\{1, 2, 5, 6, 7, 10\}$ being partially or fully scheduled during *on-peak* periods. However, due to the availability of local generation the amount charged at extra-rate is minor. Also it is good to notice that although the load density during mid-day is high, high local generation during that time period, i.e., from 1PM to 5PM, flattens the purchase (mainly base rate purchase) and the lower rate of *mid-peak* period alleviates the total cost. In general, load peaks (12PM-4PM) happen when either local generation has its peak or during *off-peak* period (7PM-8PM).

### 4.4.2 Algorithm Performance

In order to evaluate the efficiency of the algorithm, two larger sets of jobs are tested, i.e., 15 jobs and 20 $(= 15 + 5)$ jobs. Characteristics of 20 jobs, including the earliest start time,

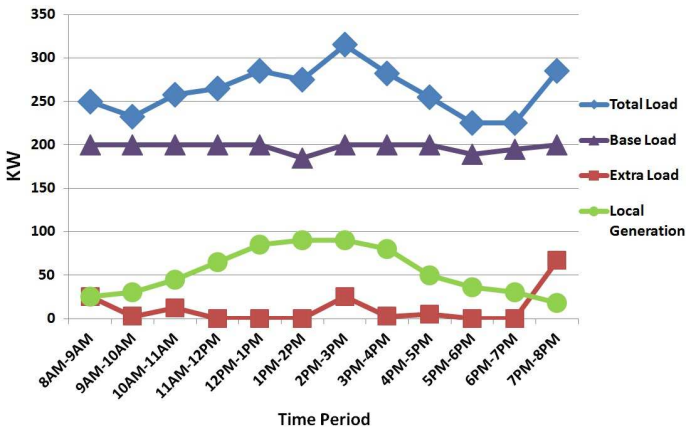


Figure 18: Load distribution: case $(10 : 7/3)$, $\Gamma = 2$, variation=20%

due time, precedent relationships, and their energy consumption at each of their modes, are randomly generated. Please see Table 7 and the way of generating parameters. The corresponding sizes of formulations, including number of constraints and variables are listed in Table 9. Since many constraints are shared by the first and second stages, we do not partition constraints into these two stages.

The computational time, final gaps for non-optimal cases, and number of iterations are reported in Table 10. We can see that although the problem size is small, the computation time is not negligible. Also, the computation time increases significantly with respect to the problem size, which highlights the challenge level of two-stage RO with discrete recourse problem. Clearly, advanced solution strategies are definitely needed for better computational performance.

### 4.4.3 Performances in the Worst Case Situations

In this part, we study the advantages of two-stage robust model over the deterministic one in handling the worst case situations due to the uncertain nature of local generation. Two

Table 9: Number of variables and constraint in experiments

| Case | Stage | Bin. Vars | Cont. Vars | Total Vars | Consts |
|---|---|---|---|---|---|
| **15:8/7** | 1 | 868 | - | 1638 | 837 |
| | 2 | 722 | 48 | | |
| **15:10/5** | 1 | 1064 | - | | |
| | 2 | 526 | 48 | | |
| **20:10/10** | 1 | 1064 | - | 2044 | 1056 |
| | 2 | 932 | 48 | | |
| **20:15/5** | 1 | 1590 | - | | |
| | 2 | 406 | 48 | | |

sets of experiments are conducted to evaluate the performance of each model with respect to local generation level ($\underline{p}_n^G$) and level of conservatism ($\Gamma$). In each set of experiments, we consider the pessimistic deterministic scheduling model, i.e., $p_n^G = \underline{p}_n^G \ \forall n$; and the optimistic one, i.e., $p_n^G = \underline{p}_n^G + \tilde{p}_n^G \ \forall n$ where $\tilde{p}_n^G = 30\%\underline{p}_n^G$. To have a fair comparison, we compare the pessimistic deterministic model with the two-stage robust model with a small $\Gamma$ (=2). Such a situation indicates that local generation is typically close to its lower bound and only in two time periods we have extra generation, which corresponds to the pessimistic intention. In the same spirit, we compare the optimistic deterministic case with the robust model with $\Gamma = 10$, which indicates local generation typically goes to its upper bounds and corresponds to the optimistic intention.

To match the nature of robust optimization in dealing with worst case situations, we identify the worst case situation for any solution produced by the deterministic model. Specifically, given a schedule obtained from the deterministic model, we solve a simple optimization problem to maximize its cost with respect to the uncertainty set, which leads to the worst case situation for that schedule. Then, we can benchmark the performances of the

Table 10: Algorithm performance

| **Case** | $\alpha$ | $\Gamma$ | **Time (s)** | **Gap** | **# of Iterations** |
|---|---|---|---|---|---|
| **15:8/7** | 10% | 1 | 18.642 | | 2 [2,2] |
| | | 2 | 9.485 | | 2 [2,2] |
| | | 3 | 25.896 | | 3 [2,2,2] |
| | 20% | 1 | 9.75 | | 2[3,2] |
| | | 2 | 28.018 | | 3 [3,2,2] |
| | | 3 | 26.38 | | 3 [3,3,2] |
| | 30% | 1 | 8.736 | | 2 [3,3] |
| | | 2 | 68.187 | | 4 [4,3,2,3] |
| | | 3 | 30.857 | | 3 [3,3,2] |
| **15:10/5** | 10% | 1 | 20.202 | | 3 [2,3,2] |
| | | 2 | 9.079 | | 2 [2,2] |
| | | 3 | 9.282 | | 2 [2,2] |
| | 20% | 1 | 9.188 | | 2 [2,3] |
| | | 2 | 20.92 | | 3 [2,3,3] |
| | | 3 | 46.706 | | 4 [2,2,3,2] |
| | 30% | 1 | 7.722 | | 2 [2,3] |
| | | 2 | 24.632 | | 3 [2,3,3] |
| | | 3 | 56.816 | | 4 [2,3,3,2] |
| **20:15/5** | 10% | 1 | 169.291 | | 2 [2,2] |
| | | 2 | 176.92 | | 2 [2,2] |
| | | 3 | 225.03 | | 4 [2,2,2,2] |
| | 20% | 1 | 96.283 | | 2 [2,3] |
| | | 2 | 118.045 | | 3 [2,3,2] |
| | | 3 | 161.476 | | 4 [3,3,2,2] |
| | 30% | 1 | 9.188 | | 2 [3,3] |
| | | 2 | 39.546 | | 3 [3,3,3] |
| | | 3 | 83.101 | | 4 [3,3,3,2] |
| **20:10/10** | 10% | 1 | $\geq$ 3600 | 0.16% | 9 [2,2,2,2,2,2,2,2,2] |
| | | 2 | $\geq$ 3600 | 0.16% | 11 [2,2,2,...,2] |
| | | 3 | $\geq$ 3600 | 0.16% | 7 [2,2,2,2,2,2,2] |
| | 20% | 1 | 13.01 | | 2 [2,3] |
| | | 2 | $\geq$ 3600 | 0.11% | 9 [2,5,4,4,4,4,4,4,4] |
| | | 3 | 183.114 | | 3 [2,4,2] |
| | 30% | 1 | 13.878 | | 2 [2,3] |
| | | 2 | $\geq$ 3600 | 0.18% | 9 [2,6,6,6,6,6,6,6,6] |
| | | 3 | 114.282 | | 4 [2,5,3,2] |

two models in their respective worst case situations. In the first set of experiments, we vary the intensity of local generation from $1 \times \underline{p}_n^G$ to $5 \times \underline{p}_n^G$ for all $n$ to evaluate the deterministic and robust solutions with respect to this parameter. Results, as shown in Figure 19(a), are represented as relative cost increase/decreases with respect to those from deterministic solutions. Generally, we note that regardless of being pessimistic or optimistic, solutions from robust model always have equal or less costs. Indeed, cost reduction with respect to optimistic deterministic model is much more significant (up to 30%) even though there are only two periods in which local generation fails to produce more than its lower bound. Such an observation can be explained by two reasons. First, the robust model produces solutions that wisely hedge against worst case situations. Second, the deterministic model produces solutions that often involve costly purchases at extra rate.

In another experiment, fixing local generation to $5 \times \underline{p}_n^G$, we vary $\Gamma$ which actually controls the size of uncertainty set from 0 to 12, and compare the performances of those two models. As we see in Figure 19(b), compared to the pessimistic case, robust approach can save up to 7%. Moreover, the bigger the uncertainty size is, the lower the cost is. The advantage of robust approach is even more clear when compared to the optimistic deterministic model where we have up to 30% reduction in cost. Note that when $\Gamma = 0$ and 12, our robust model reduces to the pessimistic deterministic model and the optimistic deterministic one respectively, which explains zero cost reduction in these two situations.

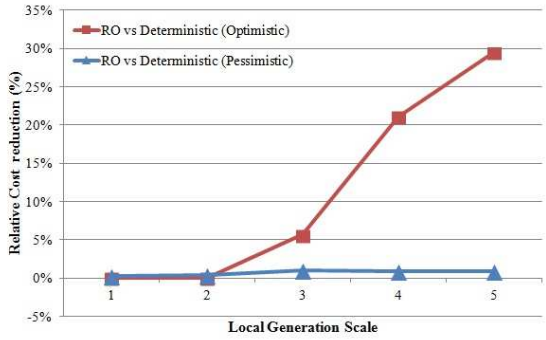


(a) Relative Cost Reduction with Respect to Local Generation Level

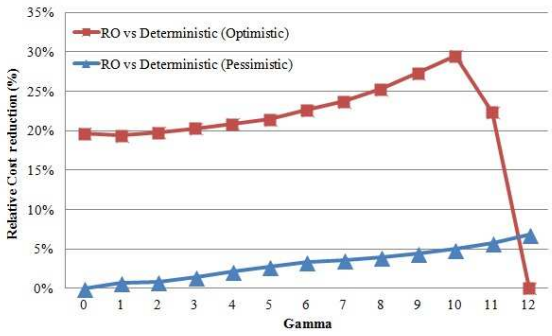


(b) Relative Cost Reduction with Respect to Size of Uncertainty Set

Figure 19: Cost comparisons in worst case situations

## 4.5 Final Remarks

In this chapter, we present a two-stage robust optimization model to schedule jobs with a time-of-use price information and a random local generation. Such model is suitable for the situations where the probabilistic information for the random local generation is not available or not reliable. To the best of our knowledge, it is the first two-stage robust optimization scheduling model with random local generation. A computation study is performed to demonstrate the effectiveness of the resulting schedules, study the impacts of job determination time and randomness of local generation, as well as compare the robust optimization approach with respect to the deterministic approach in handling the worst case situations. Given the complexity of scheduling problems and their computational challenge, one future research direction is to solve large-scale instances with algorithm improvement.

# CHAPTER 5: A CUTTING PLANE METHOD FOR ROBUST MIXED INTEGER PROGRAMMING

## 5.1 Background

As discussed in the previous chapters, unpredictability of the future and imperfect information are some of the main challenges in decision making which can be addressed by robust optimization. In order to solve a (multi-stage) robust optimization problem, we need to solve one or more Mixed Integer Programming (MIP) problems, which are, unfortunately, hard to solve. An extensive amount of research has been conducted on developing efficient solution approaches to solve MIPs. For a comprehensive list of exact and heuristic algorithms see [82] and [83], respectively. The focus of this chapter is on the exact algorithms which are mainly Branch and Bound (B&B) and cutting plane methods.

B&B is a general-purpose algorithm which uses the bounds obtained from the LP relaxation of the MIP to eliminate the parts of the feasible region that do not contain the optimal solution. Interested readers are suggested to read [84, 85, 86, 87] on this algorithm. The key to find an optimal solution via B&B algorithm is to find tight lower and upper bounds. While lower bounds are usually achieved by heuristic methods, cutting plane algorithms have been proven to be effective in finding strong upper bounds.

Cutting planes are linear inequalities that are valid to the feasible region except for a portion of its LP relaxation. The motivation behind this approach is as follows: For a set of

points $S \subseteq \mathbb{R}^n$, convex hull of $S$ ($conv(S)$) is the smallest convex set that contains $S$. It can be shown that if $conv(S)$ is identical to to its $L(P)$, then the MIP can be solved as a linear program because it shares the same set of extreme points, and thus, has the same optimal solution as its $L(P)$. Therefore, in the cutting plane method, starting from a LP relaxation, we add valid inequalities in such a way that the solution of $conv(S)$ can be found by solving the linear program. The difficulty is that there is generally not an efficient way to obtain a complete description of $conv(S)$ or it might be very time-consuming. However, adding such cuts in a sequential way, and as needed, can reduce the computational challenges. This process will be discussed in the following sections.

In the late 1950's, Gomory [88] and Dantzig [89] proposed to use cutting planes to solve MIPs. However, this approach did not gain much popularity until Johnson and Padberg [90] proposed to use cutting planes in conjunction with B&B algorithm in the early 1980's. Over the past decades, the polyhedral structure of many MIPs has been studied and efficient cutting plane generating methods have been developed and implemented in the MIP solvers. Most of such methods generate cuts from a single constraint. We believe, however, that generating strong cuts from multiple constraints can reduce the computational time, particulary for optimization problems under uncertainty. In this research, we attempt to derive strong valid inequalities for a widely-encountered class of optimization problems, the binary knapsack problem, with uncertain constraint coefficients affecting the feasible solutions. Each combination of uncertainty allocation can be considered as a knapsack constraint itself, and thus we face a large-scale structured MIP to solve.

### 5.1.1 Robust Binary Knapsack Problem

The knapsack problem (5.1) determines the amount of items to include in a collection. Each item has utility and weight coefficients, and the goal is that the total utility is maximized while total weight is below the capacity. Resource allocation problems are usually in the form of knapsack problem. A special variant of this combinatorial optimization problem is the binary knapsack problem, i.e. $x \in \mathbb{B}^n$. This problem is commonly used to model a selection between discrete choices such as the on/off status of generators in the unit commitment problem.

$$\begin{aligned} &\max\ cx \\ &Ax \leq b \\ &x \in \mathbb{R}^n_+ \end{aligned} \tag{5.1}$$

Since early 1970's, developing strong cutting planes for this problem has been investigated extensively [91, 92, 93, 94]. Examples of studies of sequential and simultaneous lifting can be found in [95, 96, 97], and the generalization of sequence-independent lifting for general MIP are described in [98, 99]. While these studies were concerned with one-dimensional lifting, applications of multidimensional lifting are limited to the work of [100, 101, 102].

In this research we are interested in studying the robust knapsack problem (RKP) with uncertain $A$ matrix. Let $\mathbb{X} = conv\{\mathbf{x} \in \mathbb{B}^n : A\mathbf{x} \leq b\ \forall A \in \tilde{A}\}$ be the convex hull of the robust solution parameterized by $\tilde{A} = \{a_{ij} | a_{ij} = \underline{a}_{ij} + \Delta_{ij}\lambda_{ij}, \sum_j \lambda_{ij} \leq \Gamma\ \forall i,\ \lambda_{ij} \in [0,1]\}$ as defined in [103]. In this definition, the uncertainty budget, $\Gamma$, controls the number of

coefficients which take their upper bounds. While not necessary in general, here we assume that the parameter $\Gamma$ is a nonnegative integer. If the randomness is independent, $\tilde{A}$ will be reduced to points with $\lambda_{ij} \in \mathbb{B}$, and the worst case is obtained by $\sum_j \lambda_{ij} = \Gamma \ \forall i$. Thus, we can redefine $\mathbb{X}$ in equation (5.2).

$$\mathbb{X}(\Gamma) = conv\Big\{\mathbf{x} \in \mathbb{B}^n | \forall S \subseteq J \ s.t. \ |S| = \Gamma : \sum_{j \in J \setminus S} \underline{a}_{ij} x_j + \sum_{j \in S} (\underline{a}_{ij} + \Delta_{ij}) x_j \leq b_i \ \forall i\Big\} \quad (5.2)$$

Next, we review valid inequalities for robust optimization in Section 5.2, then present our proposed dynamic programming procedure to generate multi-scenario lifted robust covers in Section 5.3. A framework to incorporate these cuts in a general algorithm along with a computation study to illustrate the potential of this method is in Section 5.4. Finally, we point out the future research directions in Section 5.5.

## 5.2 Polyhedral Study of RKP

**Lemma 3** *Let $\mathbb{X}(\Gamma)$ represent the intersection of polyhedra defined by any $\mathbf{A} \in \tilde{A}$. $\mathbb{X}(\Gamma)$ is a polyhedron.*

**Lemma 4** *$\mathbb{X}(\Gamma)$ is full dimensional if and only if $\underline{a}_j + \Delta_j \leq b \ \forall j \in J$.*

In this study, we assume full dimensionality for $\mathbb{X}(\Gamma)$, because, if it is not, it can be modified (by setting the violating variable to zero) so that it is. For simplicity, we also omit index $i$ which represents constraints.

### 5.2.1 Generating Valid Inequalities for RKP

**Lemma 5** *Let $\mathbb{X}^k$ represent $\mathbb{X}_{|A=A^k}$. If an inequality $\alpha^T \boldsymbol{x} \leq \alpha_0$ is valid for $\mathbb{X}^k$, it is also valid for $\mathbb{X}(\Gamma)$.*

This result can be simply seen as $\mathbb{X}(\Gamma) \subseteq \mathbb{X}^k$. We can now extend Lemma 3 and Lemma 5 to obtain Definition 1.

**Definition 1** *An inequality $\alpha^T \boldsymbol{x} \leq \alpha_0$ is valid for $\mathbb{X}(\Gamma)$ if it holds for the intersection of polyhedra defined by any $\mathbf{A} \in \tilde{A}$.*

The terms robust cover and minimal robust cover can be generalized from the deterministic case [104]:

**Definition 2** *The set $C \subseteq J$ is a robust cover if $\exists\ S \subseteq C$ s.t. $|S| = min\{\Gamma, |C|\}$ and $\sum_{j \in C \setminus S} \underline{a}_j + \sum_{j \in S}(\underline{a}_j + \Delta_j) > b$.*

**Definition 3** *A robust cover $C$ is minimal if for any $j \in C$, $C \setminus \{j\}$ is not a robust cover.*

For any robust cover $C$, the inequality (5.3) is valid for $\mathbb{X}(\Gamma)$, simply because of its definition.

$$\sum_{j \in C} x_j \leq |C| - 1 \tag{5.3}$$

**Remark 2** *A robust cover inequality is at least as strong as a nominal cover inequality.*

Robust cover $C$ can be further strengthened to either a robust extended cover $E(C)$ or a robust lifted cover. [104] proposes equation (5.4) to obtain an extended cover whose corresponding inequality is the equation (5.5). The intuition behind (robust) extend cover is that if a variable's coefficient is larger than the coefficients already in the cover, then that variable belongs to the extended set.

$$E(C) = \begin{cases} C \bigcup \{j \notin C | \underline{a}_j + \Delta_j \geq \max_{k \in C}(\underline{a}_k + \Delta_k)\}, & |C| \leq \Gamma; \\ C \bigcup \{j \notin C | \underline{a}_j \geq \max_{k \in C} \underline{a}_k \& \ \underline{a}_j + \Delta_j \geq \max_{k \in C}(\underline{a}_k + \Delta_k)\}, & |C| > \Gamma. \end{cases} \tag{5.4}$$

$$\sum_{j \in E(C)} x_j \leq |C| - 1 \tag{5.5}$$

Similarly, a robust lifted cover as in equation (5.6) is derived by including all the variables that are not in the $C$.

$$\sum_{j \in C} x_j + \sum_{j' \in J \setminus C} \beta_{j'} x_{j'} \leq |C| - 1 \tag{5.6}$$

**Remark 3** *A robust lifted cover inequality is at least as strong as a robust cover inequality.*

Furthermore, it can be shown that the cuts from lifted covers can be stronger than extended covers as lifting allows for coefficients greater than one ($\beta_{j'} \geq 1$).

### 5.3 Robust Lifting

Let $\hat{x}$ represent the solution from solving the LP relaxation of the robust MIP. A corresponding robust cover inequality can be generated by solving the separation problem (5.7). The optimal objective value of the separation problem is strictly less than one if and only if a violated robust cover inequality exists. Such robust cover is characterized by the optimal vector $r$. There are also heuristic methods that can result in robust covers in a faster time. Next, we describe how to obtain a robust lifted cover from the robust cover.

$$\min_{j} \sum_{j} (1 - \hat{x_j}) r_j \tag{5.7}$$

$$st.\ \underline{a}_j r_j + \Delta_j s_j \geq b + 1$$

$$\sum_{j} s_j \leq \Gamma$$

$$s_j \leq r_j\ \forall j$$

$$r_j, s_j \in \mathbb{B}$$

### 5.3.1 Robust Lifting Procedure

In [105], Zemel has proposed a dynamic programming approach for lifting nominal covers. Extending this framework to incorporate all realizations of uncertainty, we propose Algorithm 4 to derive robust lifted (minimal) covers. This algorithm is a sequential lifting procedure. For each item in the sequence $\pi$ of the variables outside of the cover, we create a two-dimensional table (of size $|C| \times \min\{|C|, \Gamma\}$). The original table is filled by partial sum, $l_{z,\lambda}$, which is the summation of the smallest $z$ items in the cover where $\lambda$ number of them take their upper bounds. $z_{\pi_j}$, calculated for each column $\lambda$, is the maximum number of items in the cover that can remain in the set with the addition of $x_{\pi_j}$. The minimum capacity, will then set the lifting coefficient. Note that, there are two cases for $x_{\pi_j}$:

- It takes its lower bound if $|S| = \Gamma$
- It takes its upper bound if $|S| < \Gamma$

For the next items, the table will be updated via a recursive relationship for forward induction. The algorithm is a polynomially solvable procedure as sorting is of complexity $O(nlog(n))$ and the remaining parts have complexity $O(n^2)$.

**Data**: a sequence $\pi \subset J \backslash C$, and the partial sums $l_{z,\lambda}$
**Result**: the lifted facet $\sum_{j \in C} x_j + \sum_{j' \in J \backslash C} \beta_{j'} x_{j'} \leq |C| - 1$ corresponding to $\pi$
Let $A_{\pi_1,\lambda}(0) = 0,\ A_{\pi_1,\lambda}(z_{>0}) = l_{z,\lambda}$;
**foreach** $j \in \pi$ **do**

$$z_{\pi_j} = \min \left\{ z_\lambda | z_\lambda = \max\{z | \begin{array}{ll} A_{\pi_j,\lambda}(z) \leq b - (a_j + \Delta_j), & \lambda < \Gamma; \\ A_{\pi_j,\lambda}(z) \leq b - a_j, & \lambda = \Gamma. \end{array} \} \right\}$$

$\beta_{\pi_j} = |C| - 1 - z_{\pi_j}$;
**for** *z=1* **to** $|C| - 1$ **do**
**if** $OR(\beta_{\pi_j} = 0,\ z < \beta_{\pi_j})$ **then**
$A_{\pi_{j+1},\lambda}(z) = A_{\pi_j,\lambda}(z)$;
**else**

$$A_{\pi_{j+1},\lambda}(z) = \begin{cases} min\{A_{\pi_j,\lambda}(z), A_{\pi_j,\lambda}(z - \beta_{\pi_j}) + a_{\pi_j}, A_{\pi_j,\lambda-1}(z - \beta_{\pi_j}) + (a_{\pi_j} + \Delta_{\pi_j})\}, & \lambda < z; \\ min\{A_{\pi_j,\lambda}(z), A_{\pi_j,\lambda-1}(z - \beta_{\pi_j}) + (a_{\pi_j} + \Delta_{\pi_j})\}, & \lambda = z; \\ A_{\pi_{j+1},\lambda-1}(z), & \lambda > z. \end{cases}$$

**end**
**end**
**end**

**Algorithm 4:** Multi-scenario Lifting Procedure

### 5.3.2 Lifting Algorithm Demonstration

We present a small case in order to demonstrate the lifting procedure. There are six variables in the set, the right hand side, or capacity, is 25, and we allow for up to three variables to take their upper bounds. Table 11 presents the lower bound and upper bound for the coefficients in and out of cover $C$.

Just by considering the lower bounds, one could obtain the cover inequality $x_1 + x_2 + x_3 + x_4 + x_6 \leq 4$, however, taking uncertainty into consideration, we can have a stronger

Table 11: Sample problem ($N = 6, |C| = 4, \Gamma = 3,\ b = 25$)

| | $C$ | | | | $J \setminus C$ | |
|---|---|---|---|---|---|---|
| $\underline{a}_j$ | 3 | 7 | 9 | 5 | 1 | 8 |
| $\overline{a}_j$ | 6 | 9 | 11 | 8 | 6 | 14 |

robust cover inequality $x_1 + x_2 + x_3 + x_4 \leq 3$. We then apply algorithm 4 on the remaining variables in the order of $\pi = (x_5, x_6)$ to obtain a robust lifted cover, and compare it with nominal lifted cover. Table 12 presents the implementation of Algorithm 4. While, both variables could be lifted into the inequality, robust lifting resulted in a larger coefficient for $x_6$ and thus a stronger cut was obtained. The nominal and robust cuts are respectively $x_1 + x_2 + x_3 + x_4 + x_5 + x_6 \leq 4$ and $x_1 + x_2 + x_3 + x_4 + x_5 + 2x_6 \leq 3$.

Table 12: Recursive lifting algorithm demonstration

| | j= 5 | | | | j= 6 | | | |
|---|---|---|---|---|---|---|---|---|
| | 0 | 1 | 2 | 3 | 0 | 1 | 2 | 3 |
| 0 | 0 | 0 | 0 | 0 | 0 | 0 | 0 | 0 |
| 1 | 3 | 6 | 6 | 6 | 1 | 6 | **6** | 6 |
| 2 | 8 | 11 | **14** | 14 | 4 | **7** | 12 | **12** |
| 3 | **15** | **17** | 20 | **23** | **9** | 12 | 15 | 20 |
| cap | 19 | 19 | 19 | 24 | 11 | 11 | 11 | 17 |
| $Z_\lambda$ | 3 | 3 | 2 | 3 | 3 | 2 | 1 | 2 |
| $\beta_j$ | 1 | | | | 2 | | | |

### 5.4 Computational Study

Detailed computational performance is needed in order to determine the level of effectiveness of this approach. Here we propose a framework to implement the obtained valid inequalities and compare them with the case with no robust cover inequality.

### 5.4.1 Proposed Implementation Framework

Consider the robust optimization problem $\max\{c\mathbf{x}|\mathbf{x} \in \mathbb{X}(\Gamma)\}$. In Figure 20 we present an implementation framework to solve this problem using the proposed multi-scenario lifting algorithm. The framework consists of a master problem, which is a scenario-relaxation of the robust problem, and a subproblem, which finds the optimal solution to the found scenarios. To solve the subproblem, an MIP solver would solve its LP relaxation and then using branch and bound technique and adding cuts would find the integer feasible solution before passing the upper bound. We would next, check the robust feasibility, i.e. whether or not the solution is optimal given other realizations of uncertainty, and generate the violating scenario to the master problem, if there is such a scenario. Otherwise, the optimal solution is obtained.

Note that the computational burden in such procedure is mainly associated with solving master problem whose size is increasing over iterations. We, thus, propose to adopt the multi-scenario lifting procedure in the traditional cutting plane generation in the subproblem so that we can find a solution that not only is optimal with respect to the given scenario, but may also be optimal given other realizations of uncertainty. We expect that by finding tighter upper bounds to the optimal solution, we can solve such problems faster. In general, this adoption can improve the convergence rate of any algorithm such as the restart solution strategy introduced by Fischetti and Monaci in [106].

### 5.4.2 Implementation Results

For the purpose of computational experiments, we have randomly generated matrix $A$ in the range of $[10, 100]$, and the corresponding objective function vector $c = 10 + \overline{A}$,

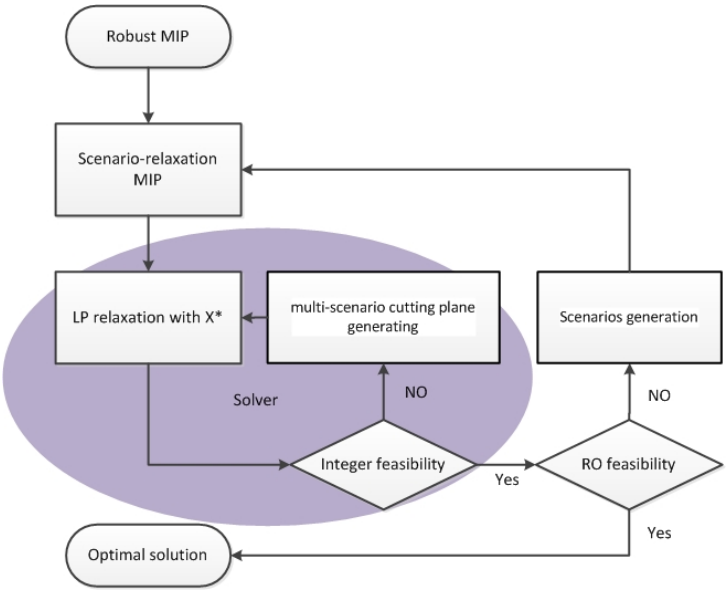


Figure 20: Cutting plane procedure to solve robust MIP

where $\overline{A}$ is the average of body coefficients. $\Gamma$ has been assumed to be half of the number of variables, and other parameters, i.e., number of constraints, variables, and uncertainty rate have been changed in different instances of the experiment. The instances consist of five different number of constraints: 1, 2, 5, and 10 knapsack constraints. Number of variables in each case have been either 20 or 30, and $\Delta$ takes three values of 5%, 10%, and 20% of the matrix coefficient. Table 13 presents the results.

For each case, we have reported the number of master problem solves with each strategy. The fourth column is the result when only robust feasibility cuts are generated, and the fifth column is the result when we had multi-scenario cuts, added in the subproblem solve, in addition to the robust feasibility cuts. Each case has been repeated for four randomly generated cases, and the single and average improvement rates are reported. While we have 13% improvement on average, the number of iterations in different cases varies. Note that,

for instances with higher number of iterations, the size of master problem is increasing which slows down the computation time. Therefore, even slight reduction in the total number of iterations can speed the total solve time. Moreover, in these experiments the number of cuts generated was limited to one per iteration. The performance would drastically improve by incorporating multiple cuts in each round.

In another set of experiments we compared the time spend on each approach. Table 14 presents the results. As we can see, while the save on the number of outer-loop iterations is a positive outcome, the difference in total computation time is considerable, especially in larger problem sizes. We believe that by solving the separation problem in a heuristic way, and adopting a backward induction method, which itself shrinks the size of matrix $A$ by a factor of $2/min(|C|, \Gamma)$, we can overcome this challenge.

Table 13: The experiment result ($\Gamma = n/2$)

| # Cons | # Vars | $\Delta$ | RC | RLC | Change | Ave. Change |
|---|---|---|---|---|---|---|
| 1 | 20 | 5% | 67 | 64 | -4% | -16% |
| | | | 33 | 26 | -21% | |
| | | | 40 | 33 | -18% | |
| | | | 19 | 15 | -21% | |
| 2 | 20 | 5% | 40 | 32 | -20% | -13% |
| | | | 19 | 17 | -11% | |
| | | | 18 | 16 | -11% | |
| | | | 101 | 89 | -12% | |
| 5 | 20 | 5% | 17 | 13 | -24% | -26% |
| | | | 9 | 7 | -22% | |
| | | | 32 | 28 | -13% | |
| | | | 18 | 10 | -44% | |
| 10 | 20 | 5% | 17 | 14 | -18% | -15% |
| | | | 11 | 9 | -18% | |
| | | | 24 | 20 | -17% | |
| | | | 91 | 84 | -8% | |

Table 13 (continued)

| # Cons | # Vars | Δ | RC | RLC | Change | Ave. Change |
|---|---|---|---|---|---|---|
| 1 | 30 | 5% | 28 | 24 | -14% | -10% |
| | | | 68 | 56 | -18% | |
| | | | 223 | 220 | -1% | |
| | | | 84 | 79 | -6% | |
| 2 | 30 | 5% | 104 | 94 | -10% | -12% |
| | | | 15 | 13 | -13% | |
| | | | 106 | 92 | -13% | |
| | | | 15 | 13 | -13% | |
| 5 | 30 | 5% | 32 | 28 | -13% | -9% |
| | | | 80 | 72 | -10% | |
| | | | 18 | 17 | -6% | |
| | | | 190 | 176 | -7% | |
| 10 | 30 | 5% | 31 | 16 | -48% | -15% |
| | | | 144 | 137 | -5% | |
| | | | 23 | 22 | -4% | |
| | | | 268 | 263 | -2% | |
| 1 | 20 | 10% | 481 | 469 | -2% | -7% |
| | | | 156 | 151 | -3% | |
| | | | 74 | 69 | -7% | |
| | | | 133 | 114 | -14% | |
| 2 | 20 | 10% | 206 | 186 | -10% | -8% |
| | | | 71 | 67 | -6% | |
| | | | 66 | 58 | -12% | |
| | | | 80 | 77 | -4% | |
| 5 | 20 | 10% | 16 | 13 | -19% | -13% |
| | | | 57 | 47 | -18% | |
| | | | 56 | 52 | -7% | |
| | | | 72 | 65 | -10% | |
| 10 | 20 | 10% | 139 | 134 | -4% | -12% |
| | | | 49 | 43 | -12% | |
| | | | 16 | 12 | -25% | |
| | | | 122 | 112 | -8% | |
| 1 | 20 | 20% | 100 | 88 | -12% | -9% |
| | | | 22 | 20 | -9% | |
| | | | 214 | 198 | -7% | |
| | | | 449 | 411 | -8% | |
| 2 | 20 | 20% | 110 | 105 | -5% | -14% |
| | | | 218 | 202 | -7% | |
| | | | 125 | 118 | -6% | |
| | | | 71 | 44 | -38% | |

Table 13 (continued)

| # Cons | # Vars | Δ | RC | RLC | Change | Ave. Change |
|---|---|---|---|---|---|---|
| 5 | 20 | 20% | 106 | 89 | -16% | -11% |
| | | | 288 | 257 | -11% | |
| | | | 293 | 267 | -9% | |
| | | | 128 | 119 | -7% | |
| 10 | 20 | 20% | 77 | 63 | -18% | -13% |
| | | | 186 | 168 | -10% | |
| | | | 46 | 40 | -13% | |
| | | | 129 | 117 | -9% | |

Table 14: The time vs number of iteration experiment result ($\Gamma = n/2$)

| # Cons | # Vars | Δ | Time (s) | | | Iteration (#) | | |
|---|---|---|---|---|---|---|---|---|
| | | | RC | RLC | Change | RC | RLC | Change |
| 1 | 10 | 5% | 0.17 | 0.63 | 271% | 6 | 3 | -50% |
| | | | 0.23 | 0.93 | 304% | 8 | 6 | -25% |
| | | | 0.21 | 0.90 | 329% | 8 | 6 | -25% |
| | | | 0.16 | 0.83 | 419% | 5 | 3 | -40% |
| 2 | 10 | 5% | 0.12 | 0.78 | 550% | 4 | 2 | -50% |
| | | | 0.11 | 1.04 | 845% | 3 | 2 | -33% |
| | | | 0.17 | 1.02 | 500% | 5 | 4 | -20% |
| | | | 0.12 | 0.79 | 558% | 3 | 2 | -33% |
| 1 | 20 | 10% | 32.10 | 98.66 | 207% | 191 | 185 | -3% |
| | | | 0.21 | 2.70 | 1186% | 7 | 5 | -29% |
| | | | 0.83 | 12.01 | 1347% | 29 | 28 | -3% |
| | | | 0.90 | 8.63 | 859% | 30 | 26 | -13% |
| 2 | 20 | 10% | 5.56 | 49.52 | 791% | 88 | 79 | -10% |
| | | | 2.61 | 27.00 | 934% | 62 | 60 | -3% |
| | | | 17.22 | 98.38 | 471% | 167 | 156 | -7% |
| | | | 1.27 | 11.56 | 810% | 41 | 39 | -5% |

### 5.5 Final Remarks

In this chapter we presented a framework to derive strong valid inequalities for robust 0-1 knapsack constraints. This multi-scenario cut generation procedure was implemented

in a generic algorithm in order to demonstrate its effectiveness. We see a clear potential for further improvements, and possible improvements include, but are not limited to the followings:

- Adoption of backward induction in the dynamic programming procedure which reduced the size of $A_j$ by a factor $2/min(|c|, \Gamma)$
- Investigating the superadditivity conditions for sequence-independent lifting
- Increasing the number of cuts generated in the subproblem

## REFERENCES


[1] A. Danandeh, L. Zhao, and B. Zeng, "Job scheduling with uncertain local generation in smart buildings: Two-stage robust approach," *Smart Grid, IEEE Transactions on*, vol. 5, pp. 2273–2282, Sept 2014.

[2] E. William, "Turbine inlet air cooling," *ASHRAE Journal article*, 1998.

[3] L. Zhao, B. Zeng, and B. Buckley, "A stochastic unit commitment model with cooling systems," *Power Systems, IEEE Transactions on*, vol. 28, no. 1, pp. 211–218, 2013.

[4] Coal Industry Advisory Board of International Energy Agency, "The impact of global coal supply on worldwide electricity prices." http://www.iea.org/publications, 2014.

[5] Benetech, "Coal blending system method presentation." http://www.prbcoals.com, 2007.

[6] U.S. Energy Information Administration, "Electric power annual 2010." http://www.eia.gov/electricity/annual/.

[7] U.S. DOE Information Administration, "Annual energy outlook." www.eia.gov/forecasts/aeo, 2013.

[8] NPR, "Why we still mine coal." http://www.npr.org, 2010.

[9] U.S. Environmental Protection Agency, "Inventory of U.S. greenhouse gas emissions and sinks: 1990-1998." http://www.epa.gov/climatechange/emissions/downloads06/00ES.pdf.

[10] U.S. Energy Information Administration, "What is the role of coal in the united states?." http://www.eia.gov.

[11] U.S. Congress, "Clean air act amendments of 1990." http://www.epa.gov/air/caa, 1990.

[12] S. Nomura, T. Arima, and K. Kato, "Coal blending theory for dry coal charging process," *Fuel*, vol. 83, no. 13, pp. 1771–1776, 2004.

[13] A. Ravindran and D. Hanline, "Optimal location of coal blending plants by mixed-integer programming," *AIIE Transactions*, vol. 12, no. 2, pp. 179–185, 1980.

[14] J. Morgan and D. Mahr, "Evaluation of coal blending systems," *Combustion*, p. 28, 1981.

[15] E. Y. Baafi, "Application of mathematical programming models to coal quality control," 1983.

[16] J. Kondragunta and L. Walker, "Optimal long term acquisition of coal for fuel blending," *Power Apparatus and Systems, IEEE Transactions on*, no. 5, pp. 1000–1007, 1984.

[17] G. Lineberry and E. Gillenwater, "Linear programming to improve raw coal blending: A new twist to an old tool," *Coal Preparation*, vol. 4, no. 3-4, pp. 227–239, 1987.

[18] W. Candler, "Coal blendingwith acceptance sampling," *Computers & operations research*, vol. 18, no. 7, pp. 591–596, 1991.

[19] J. Lyu, A. Gunasekaran, C. Chen, and C. Kao, "A goal programming model for the coal blending problem," *Computers & industrial engineering*, vol. 28, no. 4, pp. 861–868, 1995.

[20] H. Sherali and R. Puri, "Models for a coal blending and distribution problem," *Omega*, vol. 21, no. 2, pp. 235–243, 1993.

[21] R. Sarker and E. Gunn, "A simple SLP algorithm for solving a class of nonlinear programs," *European journal of operational research*, vol. 101, no. 1, pp. 140–154, 1997.

[22] J. Shih and H. Frey, "Coal blending optimization under uncertainty," *European Journal of Operational Research*, vol. 83, no. 3, pp. 452–465, 1995.

[23] C. Liu and H. Sherali, "A coal shipping and blending problem for an electric utility company," *Omega*, vol. 28, no. 4, pp. 433–444, 2000.

[24] C.-M. Liu, "A blending and inter-modal transportation model for the coal distribution problem," *International Journal of Operations Research*, vol. 5, no. 2, pp. 107–116, 2008.

[25] U.S. DOE Energy Information Administration, "Annual coal report." http://www.eia.gov/, 2011.

[26] CSX Transportation, "Private price list and contract general terms and conditions." http://www.csx.com, 2012.

[27] N. P. Padhy, "Unit commitment-a bibliographical survey," *Power Systems, IEEE Transactions on*, vol. 19, no. 2, pp. 1196–1205, 2004.

[28] L. Anstine, R. Burke, J. Casey, R. Holgate, R. John, and H. Stewart, "Application of probability methods to the determination of spinning reserve requirements for the pennsylvania-new jersey-maryland interconnection," *Power Apparatus and Systems, IEEE Transactions on*, vol. 82, no. 68, pp. 726–735, 1963.

[29] R. Billinton and R. Karki, "Capacity reserve assessment using system well-being analysis," *Power Systems, IEEE Transactions on*, vol. 14, no. 2, pp. 433–438, 1999.

[30] R. Billinton and M. Fotuhi-Firuzabad, "A reliability framework for generating unit commitment," *Electric Power Systems Research*, vol. 56, no. 1, pp. 81–88, 2000.

[31] H. Gooi, D. Mendes, K. Bell, and D. Kirschen, "Optimal scheduling of spinning reserve," *Power Systems, IEEE Transactions on*, vol. 14, no. 4, pp. 1485–1492, 1999.

[32] H. Ma and S. M. Shahidehpour, "Unit commitment with transmission security and voltage constraints," *Power Systems, IEEE Transactions on*, vol. 14, no. 2, pp. 757–764, 1999.

[33] K. Hedman, M. Ferris, R. O'Neill, E. Fisher, and S. Oren, "Co-optimization of generation unit commitment and transmission switching with n-1 reliability," *Power Systems, IEEE Transactions on*, vol. 25, no. 2, pp. 1052–1063, 2010.

[34] A. Lotfjou, M. Shahidehpour, Y. Fu, and Z. Li, "Security-constrained unit commitment with ac/dc transmission systems," *Power Systems, IEEE Transactions on*, vol. 25, no. 1, pp. 531–542, 2010.

[35] A. Tuohy, P. Meibom, E. Denny, and M. O'Malley, "Unit commitment for systems with significant wind penetration," *Power Systems, IEEE Transactions on*, vol. 24, no. 2, pp. 592–601, 2009.

[36] J. Wang, M. Shahidehpour, and Z. Li, "Security-constrained unit commitment with volatile wind power generation," *Power Systems, IEEE Transactions on*, vol. 23, no. 3, pp. 1319–1327, 2008.

[37] E. Constantinescu, V. Zavala, M. Rocklin, S. Lee, and M. Anitescu, "A computational framework for uncertainty quantification and stochastic optimization in unit commitment with wind power generation," *Power Systems, IEEE Transactions on*, vol. 26, no. 1, pp. 431–441, 2011.

[38] H. Dai, N. Zhang, and W. Su, "A literature review of stochastic programming and unit commitment," *Journal of Power and Energy Engineering*, vol. 3, no. 04, p. 206, 2015.

[39] D. Bertsimas, E. Litvinov, X. Sun, J. Zhao, and T. Zheng, "Adaptive robust optimization for the security constrained unit commitment problem," tech. rep., Technical report, 2011.

[40] L. Zhao and B. Zeng, "Robust unit commitment problem with demand response and wind energy," in *Power and Energy Society General Meeting, 2012 IEEE*, pp. 1–8, IEEE, 2012.

[41] G. Liu and K. Tomsovic, "Robust unit commitment considering uncertain demand response," *Electric Power Systems Research*, vol. 119, pp. 126–137, 2015.

[42] Y. An and B. Zeng, "Exploring the modeling capacity of two-stage robust optimization: Variants of robust unit commitment model," *Power Systems, IEEE Transactions on*, vol. 30, no. 1, pp. 109–122, 2015.

[43] D. A. Douglass and A.-A. Edris, "Real-time monitoring and dynamic thermal rating of power transmission circuits," *Power Delivery, IEEE Transactions on*, vol. 11, no. 3, pp. 1407–1418, 1996.

[44] T. V. Group, "Dynamic linne ratings for optimal and reliable power flow," 2010.

[45] D. Rajan and S. Takriti, "Minimum up/down polytopes of the unit commitment problem with start-up costs," *IBM Research Report*, 2005.

[46] A. Frangioni and C. Gentile, "Solving nonlinear single-unit commitment problems with ramping constraints," *Operations Research*, vol. 54, no. 4, pp. 767–775, 2006.

[47] Q. Zhai, X. Guan, J. Cheng, and H. Wu, "Fast identification of inactive security constraints in SCUC problems," *Power Systems, IEEE Transactions on*, vol. 25, pp. 1946 –1954, nov. 2010.

[48] B. Zeng and L. Zhao, "Solving two-stage robust optimization problems using a column-and-constraint generation method," *Operations Research Letters*, vol. 41, no. 5, pp. 457 – 461, 2013.

[49] B. Davito, H. Tai, and R. Uhlaner, "Mckinsey on smart grid: The smart grid and the promise of demand-side management," *Americas The*, no. 1, pp. 38–44, 2010.

[50] T. Hubert and S. Grijalva, "Realizing smart grid benefits requires energy optimization algorithms at residential level," in *Innovative Smart Grid Technologies (ISGT), 2011 IEEE PES*, pp. 1–8, IEEE.

[51] P. Du and N. Lu, "Appliance commitment for household load scheduling," *Smart Grid, IEEE Transactions on*, vol. 2, no. 2, pp. 411–419, 2011.

[52] A.-H. Mohsenian-Rad and A. Leon-Garcia, "Optimal residential load control with price prediction in real-time electricity pricing environments," *Smart Grid, IEEE Transactions on*, vol. 1, no. 2, pp. 120–133, 2010.

[53] K. C. Sou, J. Weimer, H. Sandberg, and K. H. Johansson, "Scheduling smart home appliances using mixed integer linear programming," in *Decision and Control and European Control Conference (CDC-ECC), 2011 50th IEEE Conference on*, pp. 5144–5149, IEEE, 2011.

[54] J.-W. Lee and D.-H. Lee, "Residential electricity load scheduling for multi-class appliances with time-of-use pricing," in *GLOBECOM Workshops (GC Wkshps), 2011 IEEE*, pp. 1194–1198, IEEE, 2011.

[55] Z. Zhu, J. Tang, S. Lambotharan, W. Chin, and Z. Fan, "An integer linear programming and game theory based optimization for demand-side management in smart grid," in *GLOBECOM Workshops (GC Wkshps), 2011 IEEE*, pp. 1205–1210, IEEE, 2011.

[56] Y. Simmhan, S. Aman, B. Cao, M. Giakkoupis, A. Kumbhare, Q. Zhou, D. Paul, C. Fern, A. Sharma, and V. Prasanna, "An informatics approach to demand response optimization in smart grids," *NATURAL GAS*, vol. 31, p. 60, 2011.

[57] H. Goudarzi, S. Hatami, and M. Pedram, "Demand-side load scheduling incentivized by dynamic energy prices," in *Smart Grid Communications (SmartGridComm), 2011 IEEE International Conference on*, pp. 351–356, IEEE, 2011.

[58] J.-Y. Moon, K. Shin, and J. Park, "Optimization of production scheduling with time-dependent and machine-dependent electricity cost for industrial energy efficiency," *The International Journal of Advanced Manufacturing Technology*, pp. 1–13, 2013.

[59] D. Zhang, L. G. Papageorgiou, N. J. Samsatli, and N. Shah, "Optimal scheduling of smart homes energy consumption with microgrid," in *ENERGY 2011, The First International Conference on Smart Grids, Green Communications and IT Energy-aware Technologies*, pp. 70–75, 2011.

[60] D. Zhang, N. Shah, and L. G. Papageorgiou, "Efficient energy consumption and operation management in a smart building with microgrid," *Energy Conversion and Management*, vol. 74, pp. 209–222, 2013.

[61] C. Spezia, "Monte carlo analysis of real-time electricity pricing for industrial loads," *Journal of Industrial Technology*, vol. 25, no. 3, 2009.

[62] X. Chen, T. Wei, and S. Hu, "Uncertainty-aware household appliance scheduling considering dynamic electricity pricing in smart home," *Smart Grid, IEEE Transactions on*, vol. 99, pp. 1–10.

[63] M. Pedrasa, E. Spooner, and I. MacGill, "Robust scheduling of residential distributed energy resources using a novel energy service decision-support tool," in *Innovative Smart Grid Technologies (ISGT), 2011 IEEE PES*, pp. 1–8, IEEE.

[64] L. Jia, Z. Yu, M. C. Murphy-Hoye, A. Pratt, E. G. Piccioli, and L. Tong, "Multi-scale stochastic optimization for home energy management," in *Computational Advances in Multi-Sensor Adaptive Processing (CAMSAP), 2011 4th IEEE International Workshop on*, pp. 113–116, IEEE, 2011.

[65] S. Kishore and L. Snyder, "Control mechanisms for residential electricity demand in smartgrids," in *Smart Grid Communications (SmartGridComm), 2010 First IEEE International Conference on*, pp. 443–448, IEEE, 2010.

[66] G. Xiong, C. Chen, S. Kishore, and A. Yener, "Smart (in-home) power scheduling for demand response on the smart grid," in *Innovative Smart Grid Technologies (ISGT), 2011 IEEE PES*, pp. 1–7, IEEE, 2011.

[67] Y. Liang and Z. Shen, "Stochastic control for smart grid users with flexible demand," tech. rep., working paper, University of California, Berkely, September, 2011.

[68] Y. Guo, M. Pan, Y. Fang, and P. P. Khargonekar, "Coordinated energy scheduling for residential households in the smart grid," in *Smart Grid Communications (SmartGridComm), 2012 IEEE Third International Conference on*, pp. 121–126, IEEE, 2012.

[69] D. Bertsimas, E. Litvinov, X. Sun, J. Zhao, and T. Zheng, "Adaptive robust optimization for the security constrained unit commitment problem," technical report, submitted to *IEEE Transactions on Power Systems*, 2011.

[70] R. Jiang, J. Wang, and Y. Guan, "Robust unit commitment with wind power and pumped storage hydro," *Power Systems, IEEE Transactions on*, vol. 27, no. 2, pp. 800–810, 2012.

[71] J. Zhao, T. Zheng, E. Litvinov, and I. N. England, "Enhancing reliability unit commitment with robust optimization," in *FERC technical conference: Enhanced ISO and RTO unit commitment models, Washington DC*, 2010.

[72] Z. Chen, L. Wu, and Y. Fu, "Real-time price-based demand response management for residential appliances via stochastic optimization and robust optimization," *Smart Grid, IEEE Transactions on*, vol. 3, no. 4, pp. 1822–1831, 2012.

[73] Z. Yu, L. McLaughlin, L. Jia, M. C. Murphy-Hoye, A. Pratt, and L. Tong, "Modeling and stochastic control for home energy management," in *Power and Energy Society General Meeting, 2012 IEEE*, pp. 1–9, IEEE, 2012.

[74] Z. Chen and L. Wu, "Residential appliance dr energy management with electric privacy protection by online stochastic optimization,"

[75] L. Zhao and B. Zeng, "Vulnerability analysis of power grids with line switching," *Power Systems, IEEE Transactions on*, vol. 28, no. 3, pp. 2727–2736, 2013.

[76] C. Li, S. Tang, Y. Cao, Y. Xu, Y. Li, J. Li, and R. Zhang, "A new stepwise power tariff model and its application for residential consumers in regulated electricity markets," 2013.

[77] P. C. Reiss and M. W. White, "Household electricity demand, revisited," *The Review of Economic Studies*, vol. 72, no. 3, pp. 853–883, 2005.

[78] A. Ben-Tal, A. Goryashko, E. Guslitzer, and A. Nemirovski, "Adjustable robust solutions of uncertain linear programs," *Mathematical Programming*, vol. 99, no. 2, pp. 351–376, 2004.

[79] L. Zhao and B. Zeng, "An exact algorithm for two-stage robust optimization with mixed integer recourse problems," *University of South Florida, available in optimization-online.com, Under Revision*, 2012.

[80] B. Zeng and L. Zhao, "Solving two-stage robust optimization problems using a column-and-constraint generation method," *Operations Research Letters*, vol. 41, no. 5, pp. 457 – 461, 2013.

[81] Ontario Hydro, "Time-of-use pricing." http://www.ontario-hydro.com, 2011.

[82] L. A. Wolsey and G. L. Nemhauser, *Integer and combinatorial optimization*. John Wiley & Sons, 2014.

[83] J. K. Lenstra, *Local search in combinatorial optimization*. Princeton University Press, 2003.

[84] A. H. Land and A. G. Doig, "An automatic method for solving discrete programming problems," in *50 Years of Integer Programming 1958-2008*, pp. 105–132, Springer, 2010.

[85] R. J. Dakin, "A tree-search algorithm for mixed integer programming problems," *The Computer Journal*, vol. 8, no. 3, pp. 250–255, 1965.

[86] J. T. Linderoth and M. W. Savelsbergh, "A computational study of search strategies for mixed integer programming," *INFORMS Journal on Computing*, vol. 11, no. 2, pp. 173–187, 1999.

[87] T. Achterberg, T. Koch, and A. Martin, "Branching rules revisited," *Operations Research Letters*, vol. 33, no. 1, pp. 42–54, 2005.

[88] R. E. Gomory, "Outline of an algorithm for integer solutions to linear programs," pp. 64:275–278, 1958.

[89] G. B. Dantzig, "Note on solving linear programs in integers," *Naval Research Logistics Quarterly*, vol. 6, no. 1, pp. 75–76, 1959.

[90] H. Crowder, E. L. Johnson, and M. Padberg, "Solving large-scale zero-one linear programming problems," *Operations Research*, vol. 31, no. 5, pp. 803–834, 1983.

[91] E. Balas and R. Jeroslow, "Canonical cuts on the unit hypercube," *SIAM Journal on Applied Mathematics*, vol. 23, no. 1, pp. 61–69, 1972.

[92] E. Balas, "Facets of the knapsack polytope," *Mathematical Programming*, vol. 8, no. 1, pp. 146–164, 1975.

[93] E. Balas and E. Zemel, "Facets of the knapsack polytope from minimal covers," *SIAM Journal on Applied Mathematics*, vol. 34, no. 1, pp. 119–148, 1978.

[94] E. A. Boyd, "Fenchel cutting planes for integer programs," *Operations Research*, vol. 42, no. 1, pp. 53–64, 1994.

[95] L. A. Wolsey, "Valid inequalities and superadditivity for 0-1 integer programs," *Mathematics of Operations Research*, vol. 2, no. 1, pp. 66–77, 1977.

[96] P. L. Hammer, E. L. Johnson, and U. N. Peled, "Facet of regular 0–1 polytopes," *Mathematical Programming*, vol. 8, no. 1, pp. 179–206, 1975.

[97] H. D. Sherali and Y. Lee, "Sequential and simultaneous liftings of minimal cover inequalities for generalized upper bound constrained knapsack polytopes," *SIAM Journal on Discrete Mathematics*, vol. 8, no. 1, pp. 133–153, 1995.

[98] Z. Gu, G. L. Nemhauser, and M. W. Savelsbergh, "Sequence independent lifting in mixed integer programming," *Journal of Combinatorial Optimization*, vol. 4, no. 1, pp. 109–129, 2000.

[99] A. Atamtürk, "Sequence independent lifting for mixed-integer programming," *Operations Research*, vol. 52, no. 3, pp. 487–490, 2004.

[100] B. Zeng and J.-P. P. Richard, "A framework to derive multidimensional superadditive lifting functions and its applications," in *Integer Programming and Combinatorial Optimization*, pp. 210–224, Springer, 2007.

[101] A. Angulo, D. Espinoza, and R. Palma, "Sequence independent lifting for mixed knapsack problems with gub constraints," *Mathematical Programming*, pp. 1–26, 2015.

[102] E. I. Gokce and W. E. Wilhelm, "Valid inequalities for the multi-dimensional multiple-choice 0–1 knapsack problem," *Discrete Optimization*, vol. 17, pp. 25–54, 2015.

[103] D. Bertsimas and M. Sim, "Robust discrete optimization and network flows," *Mathematical Programming*, vol. 98, no. 1-3, pp. 49–71, 2003.

[104] O. Klopfenstein and D. Nace, "Cover inequalities for robust knapsack sets, application to the robust bandwidth packing problem," *Networks*, vol. 59, no. 1, pp. 59–72, 2012.

[105] E. Zemel, "Easily computable facets of the knapsack polytope," *Mathematics of Operations Research*, vol. 14, no. 4, pp. 760–764, 1989.

[106] M. Fischetti and M. Monaci, "Cutting plane versus compact formulations for uncertain (integer) linear programs," *Mathematical Programming Computation*, vol. 4, no. 3, pp. 239–273, 2012.

# APPENDICES

# Appendix A Copyright Permissions

## A.1 Permission from IEEE to Reuse [1] in Chapter 4